dnj-14: A new *C. elegans* model for neurodegenerative diseases

Thesis submitted in accordance with the requirements of the University of Liverpool for the degree of Doctor in Philosophy by

Sudhanva Srinivas Kashyap

December 2013

Dedicated to my beloved Ajji - my putsu.

ACKNOWLEDGEMENTS

I would like to thank my supervisor Prof. Alan Morgan for obtaining the grant for this project thus enabling me to work with him and all the other members of Red Block. His help, motivation, accomodative nature, extreme patience and trust in me has been instrumental in the completion of this study. It was a pleasure working for him and I greatly appreciate his support especially when things did not go the way they were supposed to. The motivation he provided me to move forward when I was ill with shingles was something that I will be eternally grateful for.

A special thanks goes out for Dr. James Johnson who constantly dealt with my nagging questions and took time out to answer each one of them patiently. Our discussions on genetics, music and football were great fun and I will miss them. Then there is Matthew Edmonds with whom I could have a discussion on virtually everything under the sun be it history, cricket, tennis or even lowly Wycombe Wanderers! A big thank you to Xi Chen who was always there to take care of my worms whilst I was away. The shared office space brought with it some amazing savoury Chinese delicacies and bitter dark chocolate which one day I might appreciate.

I will be eternally grateful to Prof. Bob Burgoyne, Dr. Jeff Barclay and Dr. Lee Haynes for their guidance and advise. I would also like to thank all the Red Blockers past and present - Dayani Rajamanoharan, Leanne Bloxam, Vicky

Martin, Hannah McCue, Pryank Patel, Mimi Ayala, Joanna Wardyn, Joseph Zeguer, Marie Cawkwell, Ciara Walsh, Margaret Graham and Michèle Riesen for making my time in the lab memorable.

A very special thank you to my lovely wife Swati Lodha without whom I would not have been able to achieve what I have. The long nights in the lab through which she has motivated me to push through and all her help in proof reading this thesis – her support throughout my Ph.D has never dithered. I would also want to thank my parents BS Srinivas and Bhargavi Srinivas for all their support, motivation and letting me pursue my dream. I would like to thank my brother Kshitij for being there when I needed him and my grand parents B Seetharamaiah and Late BS Seethalakshmi for being a great inspiration and a beacon of happiness in my life.

CONTENTS

ABSTRACT

Human neurodegenerative diseases are becoming an increasing burden on society as populations age. However, the underlying mechanisms that cause age-dependent neurodegeneration still remain unclear. Consequently, therapies for these debilitating and eventually fatal disorders are lacking. Simple model organisms have great potential for uncovering conserved mechanisms of neurodegeneration and thus for identifying neuroprotective drugs.

In this study we describe a new *C. elegans* model of age-dependent neurodegeneration caused by mutation of the *dnj-14* gene. DNJ-14 is the worm homologue of cysteine string protein (CSP), a neuronal chaperone protein that prevents the misfolding of presynaptic proteins. Previously it has been shown that CSP knockout mice have a short lifespan and exhibit progressive age-related neurotransmission defects, sensorimotor dysfunction and pre-synaptic neurodegeneration. We show in this study that mutations in *C. elegans dnj-14* also result in a significant reduction of lifespan. In addition, *dnj-14* mutants exhibit age-dependent reductions in locomotion and sensitivity to aldicarb - a behavioural read-out of cholinergic neurotransmission. The above phenotypes correlate to an age-dependent loss of neurons as indicated by the punctate/abnormal expression of the GFP marker in *dnj-14* worms. This loss of neurons in the head region corresponds with a reduced ability of the *dnj-14* mutants to reach a food source or a volatile attractant indicating the loss of

chemosensory neurons. Treatment with resveratrol, a polyphenol with a neuroprotective role in several neurodegenerative disease models, rescues the phenotypes of the *dnj-14* mutant worms. This suggests that the *dnj-14* model can be used to identify generic neuroprotective interventions rather than drug targets that are disease specific.

CSP is thought to prevent neurodegeneration by chaperoning the synaptic SNARE protein, SNAP-25. In this study we have shown that the mutation of *ric-4*, worm SNAP-25 homologue, produced phenotypes similar to those seen in *dnj-14* mutants, suggesting a functional interaction between the two presynaptic proteins. The *dnj-14;ric-4* double mutant showed no further deterioration of lifespan and locomotion phenotype. This suggested genetic epistasis in *C. elegans* similar to CSP knock out mice. Moreover, treatment with resveratrol rescued the lifespan phenotype of the *ric-4* worms and also the *ric-4;dnj*-14 double mutant. Overexpression of *ric-4* in *dnj-14* mutants rescued the lifespan and chemosensory defects as seen in the food race assays. This further suggests that the *dnj-14* model is similar to the CSP knock out model in mice. More importantly, mutations in CSP cause Adult-onset Neuronal Ceroid Lipofuscinosis (ANCL), a human neurodegenerative disease. Hence, characterisation of *dnj-14* mutants could well act as a model to study ANCL.

ABBREVIATIONS

Abbreviation	Description
6-OHDA	6-hydroxydopamine
aak-2	AMP activated kinase-2
abu-11	Activated in Blocked Unfolded protein response-11
AD	Alzheimer's Disease
aex-2	Aboc EXpulsion defective-2
AMP	5'-Adenosine MonoPhosphate
ANCL	Adult-onset Neuronal Ceroid Lipofuscinosis
aph-1	Anterior Pharynx defective-1
apl-1	Amyloid Precursor-Like-1
APOE4	APOlipoprotein E-4
APP	Amyloid Precursor Protein
AR-JR	Autosomal Recessive-Juvenile Parkinsonism
ATP	Adenosine TriPhosphate
Aβ	Amyloid-beta
BACE	Beta-site Amyloid-beta A4 precursor protein Cleaving Enzyme
bec-1	beclin-1
BLAST	Basic Local Alignment Search Tool
cAMP	cyclic Adenosine MonoPhosphate
CEP	CEPhalic
CGC	Caenorhabditis Genetics Centre

CLN	Ceroid-Lipofuscinosis, Neuronal
CSPα	Cysteine String Protein alpha
daf	abnormal DAuer Formation
dat-1	dopamine active transporter 1
DEG-3	DEGeneration of certain neurons-3
DES-2,	DEgeneration Suppressor-2
DNA	Deoxyribonucleic Acid
DNAJC5	DnaJ homolog subfamily C member 5
dnj-14	DNaJ domain
ER	Endoplasmic Reticulum
FOXO	Forkhead Box Class O
FTDP	Frontotemporal Dementia and Parkinsonism
GABA	Gamma-Aminobutyric Acid
GAD	Glutamic Acid Decarboxylase
GBA	Glucosidase, Beta, Acid
GFP	green fluorescent protein
glit-1	GLIoTactin homolog-1
HD	Huntington's Disease
HDAC	Histone deacetylases
hic	Hypersensitivity to inhibition by Cholinesterases
HIP-1	Huntingtin Interacting Protein-1
hipr-1	Huntingtin Interacting Protein Related-1
hop-1	Homolog Of Presenilin-1

Hsc70	Heat Shock Cognate 70
hsf-1	Heat Shock Factor-1
HSP-16	Heat Shock Protein-16
Hsp40	Heat Shock Protein-40
Hsp70	Heat Shock Protein-70
htt	huntingtin
IGF-1	Insulin like Growth Factor-1
IIS	Insulin like Growth Factor-1 like Signalling
IL	Inner Labial
LRRK2	Leucine-rich repeat kinase-2
mec-7	MEChanosensory abnormality-7
mTOR	mammalian Target Of Rapamycin
NAD	Nicotinamide adenine dinucleotide
NCL	Neuronal Ceroid Lipofuscinosis
NFT	Neurofibrillary Tangles
NGM	Nematode Growth Media
NMJ	Neuromuscular Junction
Nrf2	Nuclear factor (erythroid-derived 2)-like-2
OL	Outer Labial
PARK1	Parkinson disease, familial-1
PBS	Phosphate Buffered Saline
PC12	PheoChromocytoma
PCR	Polymerase Chain Reaction

PD	Parkinson's disease
PDE	PhosphoDiEsterase
PEG	Polyethylene Glycol
pen-2	presenilin enhancer-2
PINK1	PTEN induced putative kinase-1
PKA	Protein Kinase A
PKC	Protein Kinase C
PPT-1	palmitoyl protein thioesterase
pqe-1	PolyQ (poly glutamine tract) toxicity Enhancer
PS1/PS2	Presenilin-1/ Presenilin-2
Resv	Resveratrol
Rol	Rolipram
Rex3p	RNA exonuclease
ric	Resistance to Inhibitors of Cholinesterase
RNAi	Ribose Nucleic Acid Interference
Rrs1	Regulator of Ribosome Synthesis-1
SDS	Sodium dodecyl sulphate
sel-12	Suppressor/Enhancer of Lin-12
SEM	Standard Error of the Mean
SGT	small glutamine-rich TPR-containing protein
sir-2.1	Silent Information Regulator-2.1
skn-1	SKiNhead
SNAP-25	Synaptosomal-associated protein 25

SNARE	Soluble NSF Attachment Protein REceptor
snb-1	SyNaptoBrevin related-1
spe-4	defective SPErmatogenesis-4
TOR-2	human TORsin related-2
TPP1	Tripeptidyl peptidase-1
TSA	Trichostatin A
UCH-L1	Ubiquitin carboxy-terminal hydrolase L1
unc-54	UNCoordinated phenotype-54
YFP	Yellow Fluorescent Protein

CHAPTER 1: INTRODUCTION

1.1 INTRODUCTION

1.1.1 NEURODEGENERATIVE DISEASES

Advancements in medical science have increased human life expectancy many fold. Increased life expectancy brings with it a challenge in the form of neurodegenerative diseases that have become a burden to the elderly in our society. Alzheimer's disease (AD), Parkinson's disease (PD), Huntington's disease (HD) and other such diseases affect and claim the lives of millions of people all over the world. AD affects more than 30 million people worldwide (Brookmeyer et al., 2007); PD affects 1-4% of the population over the age of 65 (de Lau and Breteler, 2006) and HD affects 3 to 7 people per 100,000 people of European ancestry. Due to their high prevalence and the associated personal, social and economic costs it is essential to tackle neurodegenerative diseases making the research to develop effective therapies for treatment highly imperative. A major hallmark of these diseases is the progressive loss of neurons or neuronal activity due to the accumulation of protein aggregates within the nervous system (Skovronsky et al., 2006). However, the exact mechanism whereby protein aggregate accumulation in the nervous system leads to neuronal loss is relatively unclear.

1.1.2 PARKINSON'S DISEASE

Parkinson's disease is characterized by symptoms that are movement related and gradually leads to cognitive and behavioural impairment. Pathophysiologically, the formation of large intracellular inclusions called Lewy bodies, containing the protein α-synuclein, cause neurodegeneration predominantly in the dopaminergic neurons in the substantia nigra of the mid brain and in other monoaminergic neurons in the brain stem (Gibb et al., 1987, Spillantini et al., 1997, Forno, 2001). Although Lewy body pathogenesis remains unclear, the discovery that misfolded α-synuclein is a major component of these inclusions and its presence in neuronal processes as Lewy neurites has led to the classification of PD as a synucleinopathy (Dickson et al., 2009) has changed the pathological outlook of the disease.

Familial PD is a result of duplication and triplication or a mutation in the PARK1 locus that encodes α-synuclein (Conway et al., 1998, Singleton et al., 2003). Mutation in this locus results in a very rare form of PD which is excluded in most cases of sporadic or familial PD (Parsian et al., 1998, Vaughan et al., 1998). A second PD gene locus was discovered, aptly named PARK2, which was observed to be a result of mutations in the parkin gene known to cause autosomal recessive juvenile parkinsonism (AR-JR) (Kitada et al., 1998). The discovery of the PARK2 locus led to the detection of at least eight other loci which cause various kinds of familial and sporadic PD (Dawson and Dawson, 2003). However,

the fact that α-synuclein is a major component of Lewy bodies focussed the attention of investigators on this pre-synaptic protein. In vitro studies of the mutated form of α-synuclein have indicated an increased tendency of insoluble aggregate formation (Conway et al., 1998). α-synuclein knockout mice have normal brain structure and exhibit wild-type dopaminergic system and are also viable and fertile which suggests that PD is likely to be caused due to a gain of function mutation in α-synuclein (Jensen et al., 1998). A recent study revealed that loss of all forms of synucleins (3 types namely α, β and γ synuclein) in mice causes age-dependent neuronal dysfunction without the loss of synapses or neurons (Greten-Harrison et al., 2010). This late onset phenotype was rather attributed to the changes in synaptic protein composition and axonal structure. This further strengthens the notion that alterations in the physiological function of synucleins could contribute to the development of PD.

Apart from synucleins, investigation of familial PD has revealed several other autosomal dominant and autosomal recessive gene mutations responsible for different variants of the disease (Houlden and Singleton, 2012). These genes include parkin, ubiquitin carboxyl-terminal hydrolase L1 (UCH-L1), DJ-1, phosphatase and tensin homolog-inducible kinase 1 (PINK1), leucine-rich repeat kinase 2 (LRRK2), and glucocerebrosidase (GBA). Of these, parkin and LRRK2 are the most widely studied as they have been known to have the most common genetic link to young onset and late onset PD respectively (Kitada et al., 1998, Valente et al., 2001, Clark et al., 2006, Tan et al., 2006). LRRK2 (present in the

PARK8 locus) encodes for a protein called dardarin. A heterozygous mutation in LRRK2, G2019S, is commonly described in the majority of familial cases of PD (Dawson and Dawson, 2003). G2019S mutation along with several others (Haugarvoll et al., 2008) has been shown to induce the formation of Lewy bodies and cause neuronal loss in the substantia nigra of the brain. However, the co-localization of LRRK2 with α-synuclein suggests that they are part of the same pathway and also that LRRK2 mutations act upstream of a number of critical pathways and ultimately result in cell death (Bardien et al., 2011). Interestingly, polymorphisms in tau have been identified as a genetic risk factor for PD (Pastor et al., 2001). Also, frontotemporal dementia with parkinsonism (FTDP) is, in part, caused by these mutations (Hutton et al., 1998).

Pathogenesis of neurodegeneration in PD is attributed mainly to the increased expression, aggregation and accumulation of α-synuclein (Eriksen et al., 2003). α-synuclein induced neurodegeneration is associated with abnormal aggregation of detergent insoluble α-synuclein and abnormal proteolytic processing of the protein (Dawson et al., 2010). Studies in Drosophila and mice have indicated that an overexpression of wild type α-synuclein results in a progressive loss of dopaminergic neurons (Masliah et al., 2000, Auluck et al., 2002). Filamentous inclusions of α-synuclein were also seen in *Drosophila* with overexpressed α-synuclein. Overexpression of Hsp70 rescued the transgenic flies expressing mutant and wild-type α-synuclein (Auluck et al., 2002). The mechanism behind α-synuclein mediated neuronal cell loss is not yet known.

Also, it is unclear how mutations in α-synuclein, a ubiquitously expressed protein, lead to the selective loss of dopaminergic neurons.

Mutations in LRRK2 represent the highest risk of familial and sporadic PD (Paisan-Ruiz et al., 2004, Zimprich et al., 2004). Heterozygous mutations in GBA have been associated with PD and Lewy body pathology (Neumann et al., 2009, Sidransky et al., 2009). It has been established that heterozygous loss of function mutation also leads to a higher risk of PD (Mitsui et al., 2009). However, the pathogenic mechanism is unclear (DePaolo et al., 2009) and as GBA is a lysosomal protein, a possible link to lysosomal dysfunction needs to be scrutinized.

Mutations linked to early onset PD account for about 1% of cases of all types of PD. These include recessive loss of function genes encoding parkin, PINK1 and DJ-1. DJ-1 mutations affect a protein involved in redox sensing (Ishikawa et al., 2009) and is the most uncommon cause for PD. PINK1 is a mitochondrial kinase and parkin was originally thought to be a ubiquitin E3-protein ligase (Dawson and Dawson, 2003). However, reports suggest that PINK1 and parkin could be functionally linked as their expression induces mitochondrial fission (Lutz et al., 2009). Another study showed that parkin rescues neurodegeneration in PINK1 null flies by getting recruited to dysfunctional mitochondria and promoting their autophagic degradation (Narendra et al., 2009). However, aged parkin/DJ-1/PINK1 triple mutant mice fail to develop nigral neurodegeneration (Kitada et

al., 2009) and hence the impact of these proteins on the pathology of PD might be low (Brooks et al., 2009). It is important to identify critical pathways which may be affected by these mutations to elucidate the mechanistic process of neurodegeneration in PD.

1.1.3 ALZHEIMER'S DISEASE

Alzheimer's disease, one of the most common neurodegenerative diseases, is an incurable and terminal neurodegenerative disease first described by a German psychologist, Alois Alzheimer. It is characterized by late onset of dementia leading to progressive loss of memory, recognition of people and objects, task performance and various other age-dependent cognitive impairments. The cause and progression of AD is attributed to the formation of extracellular amyloid plaques, hyper-phosphorylated intraneuronal neurofibrillary tangles (NFTs) containing tau and Lewy bodies in the brain (Tiraboschi et al., 2004). Most cases of Alzheimer's are sporadic in nature however, there are some genetic risk factors, the most common being the inheritance of ε4 allele of the apolipoprotein E (APOE4) (Strittmatter et al., 1993). It has been shown that the allele increases the risk of Alzheimer's in heterozygotes by 3 times and as much as 15 times in homozygotes.

A major component of the plaques are β-amyloid peptides Aβ, which are 40-42 amino acids in length and are created as a result of proteolytic cleavage of a larger transmembrane protein of unknown function, amyloid precursor protein (APP) (Kang et al., 1987). APP is cleaved by the enzymes α-, β- and γ-secretase sequentially (Jacobsen and Iverfeldt, 2009) and mutations in this precursor protein are known to promote the formation of Aβ (Citron et al., 1992). Not only do mutations internal to APP increase the self-aggregation of Aβ, the

mutations in presenilin proteins- PS1 and/or PS2, part of the complex that forms γ-secretase (Wolfe et al., 1999) also promote processing of APP to form Aβ (Crook et al., 1998). It has also been shown that APOE4 leads to excess Aβ build up in the brain before AD symptoms arise (Bales et al., 1997).

The cleavage of APP may occur in two different pathways - amyloidogenic and the non-amyloidogenic pathways. The non-amyloidogenic pathway is more prevalent, wherein APP is cleaved initially by α-secretase at a position 83 amino acids from the C-terminus (C83), producing a large N-terminal ectodomain which later gets secreted into the extracellular membrane (Kojro and Fahrenholz, 2005). The resulting C83 fragment is retained in the membrane and is subsequently cleaved by γ-secretase (Haass et al., 1993). Importantly in this pathway, α-secretase cleaves APP within the Aβ region, thereby precluding the formation of Aβ.

The alternative pathway, called the amyloidogenic pathway, leads to the formation of Aβ. Here, the initial cleavage is mediated by β-secretase resulting in a 99 amino acid C-terminal fragment (C99), which is retained within the membrane, and a sAPPβ fragment that is released into the extracellular space. Subsequent cleavage of C99 by γ-secretase enzyme (between residues 38 and 43) frees the intact Aβ peptide. Most of the full-length Aβ peptides are 40 residues in length ($A\beta_{40}$), whereas a small proportion (approx. 10%) is the 42 amino acid variant called $A\beta_{42}$. $A\beta_{42}$ is more hydrophobic and more prone to

fibril formation than $A\beta_{40}$ (Jarrett et al., 1993).

Neurofibrillary tangles (NFTs) contain hyperphosphorylated tau protein and these are considered as a primary marker of AD (Lee et al., 2005). Tau is a microtubule-associated protein that binds to and assists in the formation and stabilization of the microtubules. When hyperphosphorylated, it is unable to bind to the microtubules making them unstable (Lee et al., 2005). The unbound tau clumps together to form the NFTs which are thought to interfere with several neuronal functions (Lee et al., 2005).

The amyloid hypothesis suggests that the accumulation of Aβ is the key event that triggers neurodegeneration. Build up of Aβ inhibits certain enzyme functions in the mitochondria of AD patients and the utilization of glucose by neurons (Chen and Yan, 2006). Several studies suggest that Aβ induces changes in synaptic efficacy in vivo (Selkoe, 2002). It has been shown in primary neuronal culture and mouse models that Aβ acts synergistically with NFTs resulting in neurodegeneration (Lewis et al., 2001, Rapoport et al., 2002). It has also been reported that even the most severe consequences of NFTs are not enough to induce Aβ suggesting that the NFTs seen in AD brains are likely to have been deposited after the metabolic changes due to Aβ, rather than before (Lewis et al., 2001). However, the exact mechanism by which the disease manifests itself into neuronal loss is relatively unknown and this is where research using model organisms becomes increasingly important.

1.1.4 POLYGLUTAMINE DISORDERS AND HUNTINGTON'S DIESASE

Polyglutamine diseases are a class of genetic disorders that are characterized by tri-nucleotide repeats (CAG) in typically coding regions of otherwise unrelated proteins. There are currently nine neurological diseases attributed to CAG repeats, Huntington's Disease (HD) being one among them, all of which display an extremely selective pattern of neurodegeneration. Autosomal dominant mode of inheritance is a common trait among most of these disorders. During protein synthesis, the expanded CAG repeats are translated into a series of glutamine residues forming Poly-Q tracts, which are prone to forming aggregates. It has also been observed that these disorders have a midlife onset, a progressive course and a correlation of the number of CAG repeats with the severity of the disease as well as the age of onset (Walker, 2007). These diseases have also been shown to exhibit genetic anticipation wherein the severity increases with each successive generation that inherits the disease (Ridley et al., 1988).

HD is the most common of all the polyglutamine diseases and has higher prevalence among people with western European rather than Asian or African ancestry. It is caused due to an autosomal dominant mutation in the gene huntingtin (htt), present on the short arm of chromosome 4 (Huntington's Disease Collaborative Research Group, 1993). HTT is a ubiquitously expressed protein and the highest concentrations can be found in the brain and testes (Schilling et al., 1995, Sharp et al., 1995). This is one of the reasons why patients

have neurological symptoms along with symptoms like muscular atrophy, weight loss, cardiac failure, glucose intolerance, etc. The mutation usually results in the expansion of poly-Q tract of HTT with the addition of more than 36 glutamines on the N-terminus having the capacity to increase the decay rate in certain types of neurons. It has also been observed that mutations leading to addition of longer repeats result in an earlier onset of symptoms (Hahn-Barma et al., 1998). There are studies that suggest a correlation between the threshold of aggregation in vitro and the threshold for human disease, which is consistent with the idea of aggregation being directly linked to pathogenicity (Davies et al., 1997, Scherzinger et al., 1999).

The function of HTT is relatively unclear but recent studies suggest an interaction with proteins involved in transcription, cellular transport and signalling (Harjes and Wanker, 2003, Walker, 2007). Studies using animal models have revealed several functions of HTT like embryonic development, use as an anti-apoptotic agent, neurogenesis, vesicle transport, synaptic transmission and neuronal gene transcription. It was shown that is primarily associated with vesicles and microtubules (DiFiglia et al., 1995, Hoffner et al., 2002). It is also thought to be involved in vesicle trafficking as it interacts with HIP-1, a clathrin-binding protein, to mediate endocytosis (Velier et al., 1998, Waelter et al., 2001). However, its exact function is still yet unclear and it has been shown that loss of function of huntingtin is lethal in mice (Nasir et al., 1995). The fact that the disruption of the wild type htt gene, in humans, does

not cause the disease (Housman, 1995) indicates that HD is a result of gain of toxic function of mHTT protein.

At a cellular level, the toxicity of mHTT can manifest itself in many ways to produce HD pathology. As a result of post-translational modifications, mHTT cleavage may leave behind several shorter fragments made up of parts of the poly-Q tract toxic to the cell (Rubinsztein and Carmichael, 2003). There is increasingly clear evidence that a number of transcriptional pathways are impaired in HD, however, the relevance of these interactions and how they affect disease pathogenesis still remains unclear (Landles and Bates, 2004). Alternatively, reports suggest that HTT interacts with Hsp70 and Hsp40 family of chaperones and its co-localization with the aggregates in both animal models of poly-Q and patient tissue samples suggests that an impairment of protein folding may cause HD pathology (Sakahira et al., 2002). RNAi studies revealed that only two Hsp70s and one member of the DnaJ family of chaperones affected poly-Q protein aggregation and toxicity (Nollen et al., 2004). A common feature of HD and all other neurodegenerative diseases is that the inclusions are ubiquitinated and also associated with several subunits of the proteasome, which strongly indicates a failure of the degradation machinery of the cell (Ciechanover and Brundin, 2003). Also, the mammalian target of rapamycin (mTOR) was shown to be isolated in HTT aggregates, thereby decreasing the kinase activity of the cell and eventually leading to the induction of autophagy (Ravikumar et al., 2004).HD pathogenesis is also likely to induce

impairments in intracellular transport, mitochondrial function and synaptic transmission (Landles and Bates, 2004).

1.2 *C. ELEGANS* AS A MODEL FOR NEURODEGENERATIVE DISEASES

Most of the neurodegenerative models in mice are highly advantageous as they closely resemble the phenotypes seen in humans. This makes drug screening more relevant to human diseases. However, they do have their own share of problems. Not only are high throughput screens in rodents very expensive and time consuming, invariably, they are only limited to a small number of animals per treatment. Also, monitoring *in vivo* conditions in these mammals becomes very difficult. Thus invertebrate models like *Caenorhabditis elegans* become very important as they offer much greater experimental flexibility and control in a better defined physiological and genetic background.

C. elegans is a free living nematode that is less than a millimetre in size with a very short lifespan (about 3 weeks), short generation cycle (about 3 days) and a transparent body that aids in visualisation of all cell types at all stages of development (Brenner, 1974). This makes in vivo screening of degenerative changes in all or discrete subsets of neurons straightforward. Also, because of its short lifespan, screening of neurons and any age-dependent behavioural assays become simple to perform.

Additionally, *C. elegans* have a simple nervous system of 302 neurons in the adult hermaphrodite, in which each neuron has a unique position and an identity that is reproducible from animal to animal. Furthermore, the synaptic

and gap connections between these neurons are also reproducible based on nervous system reconstruction at the electron microscope level of analysis. The majority of neurotransmitter systems are conserved in *C. elegans* contributing to the appeal of the nematode for neuroscientists. At least 42% of human disease related genes have a *C. elegans* ortholog (Culetto and Sattelle, 2000), suggesting that most biochemical pathways are conserved across evolution. Arguably, the most attractive characteristic of the nematode is its suitability for experimental approaches which is not possible in mammalian models. Thus, *C. elegans* has emerged as an attractive and powerful in vivo model system for studying pathological mechanisms in several major neurodegenerative disorders.

1.2.1 *C. ELEGANS* AS A MODEL FOR PARKINSON'S DISEASE

C. elegans has 6 PD genes that are orthologs of human PD genes, however, it lacks an endogenous gene for α-synuclein (Harrington et al., 2010). Despite this, there have been several PD models in worms characterised to study α-synuclein toxicity. *C. elegans* has 8 dopaminergic neurons. There is selective and progressive loss of these neurons in a worm model that overexpresses human wild type and mutant α-synuclein with GFP driven by pan-neuronal (*aex-2*) and/or dopaminergic (*dat-1*) promoters (Lakso et al., 2003). This was subsequently confirmed by another study which also suggests a link between α-synuclein toxicity and ER-Golgi vesicular trafficking (Cao et al., 2005).

A second model found accumulation of α-synuclein in the cell bodies and neurites of dopaminergic neurons overexpressing the wild type or mutant protein, but no significant loss of CEP neurons (Dawson et al., 2010). Interestingly a subset of wild-type and mutant transgenic worms was immuno-reactant to phosphorylated α-synuclein (at Ser-129) which is a characteristic feature of human Lewy bodies (Fujiwara et al., 2002). Classically, slowing down of worms in response to food is controlled by dopaminergic neurons and worms expressing α-synuclein fail to modulate their locomotion in response to food.

Screens in yeast have made use of this model for synucleinopathy to validate findings in a multicellular context. α-synuclein when overexpressed, leads to a

blockage in ER-Golgi trafficking which is relieved when members of exocytotic machinery are co-expressed. For example, *rab-1* expression with α-synuclein in worms' dopaminergic neurons led to an increase in neuronal health compared to α-synuclein alone (Cooper et al., 2006).

A *C. elegans* model which expressed a fusion protein, α-synuclein::GFP, in the body wall muscles with the *unc-54* promoter was used to screen 868 genes by RNAi and 20 genes that enhanced the aggregation of the fusion protein were identified. (Hamamichi et al., 2008). TOR-2 (the worm ortholog of TorsinA) was also co-expressed with α-synuclein to maintain a threshold for the expression of the fusion protein. The above study was later extended to neurons and 5 genes that provided significant neuroprotection in dopaminergic neurons were identified (Hamamichi et al., 2008).

A pharmacological model was also established where in a neurotoxin called 6-hydroxydopamine (6-OHDA) was used to selectively induce degeneration of dopaminergic neurons in worms (Nass et al., 2002). These could be monitored by illuminating the *dat-1* neurons with GFP. This was shown to be rescued by the treatment of acetaminophen (Locke et al., 2008), suggesting that this model could be used to screen drugs that ameliorate neurodegeneration in PD. All these studies suggest that *C. elegans* can be used as a powerful tool to study neurodegeneration in PD.

1.2.2 *C. ELEGANS* MODELS OF ALZHEIMER'S DISEASE

C. elegans has an APP-related gene, *apl-1*, but the APL-1 protein lacks the Aβ peptide (Daigle and Li, 1993). The *C. elegans* genome encodes three presenilin orthologs (*sel-12*, *hop-2* and *spe-4*) and additionally, *aph-1*, *pen-2*, and *aph-2* (nicastrin) whose genes products combine to form the canonical functional γ-secretase complex. Yet, the *C. elegans* genome does not encode a β-secretase (BACE ortholog).

Due to the absence of an endogenously expressed Aβ peptide, transgenic lines expressing human Aβ peptide had to be constructed to study AD in worms. Three engineered *C. elegans* AD models have been described to date, all of which express the longest and most toxic Aβ peptide ($A\beta_{42}$) (Link, 2006, Wu et al., 2006, Chiang et al., 2009). Transgenic animals expressing the $A\beta_{42}$ fragment, under the constitutive *unc-54* body-wall muscle promoter, show intracellular cytoplasmic Aβ deposits leading to progressive paralysis. Expressing a temperature inducible Aβ transcript, carefully constructed using a mini-gene, resulted in a fully penetrant paralysis phenotype. However, when the Aβ fragment was expressed in the neuronal cells (driven by the pan-neuronal*snb-1* promoter) intra-neuronal deposition of Aβ was observed in the transgenic animals with defects in chemotaxis and hypersensitivity to serotonin but no overt locomotive defects (Wu et al., 2006).

Examination of the role of a IGF-1 like signalling (IIS) pathway in *C. elegans* by expressing $A\beta_{42}$ using the unc-54 promoter, demonstrated the dependence of Aβ toxicity on genes previously implicated in longevity studies. It was observed from previous studies that a knockdown of the IGF-1 receptor, DAF-2, reduced Aβ toxicity in the *C. elegans* body-wall muscles through downstream transcription factors, DAF-16 and heat shock factor-1 (HSF-1) (Cohen et al., 2006). Down-regulation of *daf-16* or *hsf-1* had an opposing effect on the $A\beta_{42}$ aggregation. The amount of high-molecular weight Aβ species linked to toxicity increased on *hsf-1*(RNAi) knockdown and decreased on daf-16 knockdown (Cohen et al., 2006).

A number of studies have researched the role of chaperones in Aβ toxicity using the *unc-54*/$A\beta_{42}$ *C. elegans* model and have identified several proteins with chaperone-like function that interact with Aβ (Wu et al., 2010). HSP-16 was found to co-localize with intracellular Aβ (Fonte et al., 2002) and HSP-16.2 overexpression partially suppressed the Aβ-induced paralysis phenotype. All these studies are suggestive of protein turnover being a critical determinant in Aβ toxicity.

1.2.3 *C. ELEGANS* MODELS OF HUNTINGTON'S AND POLY-Q TOXICITY

C. elegans do not have an endogenous huntingtin protein, thus an expression of human mutant huntingtin (mHTT) in the nervous system is an obvious approach to model HD in worms. Similar to mammalian models, expression of mHTT in the *C. elegans*' ASH (chemosensory) neurons leads to neurodegeneration. Studies to identify the worm proteins involved have shown that the mutation of the *pqe-1* gene worsens the neuronal loss. Not surprisingly, overexpression of the *pqe-1* gene protects animals from mHTT aggregation (Faber et al., 2002). Although no clear *pqe-1* ortholog has been found in humans, a loss of a similar exonuclease, Rex3p, causes synthetic lethality in yeast lacking Rrs1, the mammalian ortholog of which has been implicated in HD toxicity; suggesting a conserved mechanism may be at work (Nariai et al., 2005, Carnemolla et al., 2009). Age-dependent accumulation of aggregates was also seen when poly-Q expanded YFP was expressed in the worm muscles. 186 genes which affect protein aggregation were identified in an RNAi screen (Nollen et al., 2004). Many of these were associated with protein synthesis and proteasome degradation indicating the need to study these proteins and their mutations in greater detail.

An independent neuronal HD model was developed using the *mec-7* β-tubulin gene promoter and human huntingtin with normal and expanded poly-Q tracts fused to GFP and was expressed in the six touch receptor neurons of the worm

body (Parker et al., 2001). The correlation between the consequent mechanosensory defects and the increased poly-Q expansion was significant. Analysis of the touch receptor neurons in the tail (PLM) revealed aggregate formation and various morphological abnormalities, but no apoptotic features (Parker et al., 2001). However, this model was later pivotal in the demonstration of a neuroprotective role of *hipr-1*, the worm ortholog of the huntingtin-interacting protein 1 (Parker et al., 2007).

The two HD models (ASH and touch cells) have been used to examine the role of histone deacetylases (HDACs) in poly-Q induced neurodegeneration. In touch cells, overexpression of the worm homologue of*sir-2 (sir-2.1)*, a class III HDAC, resulted in a daf-16 dependent rescue of the above-mentioned mechanosensory phenotype (Parker et al., 2005). The same model showed evidence of neuroprotection when treated with resveratrol, a chemical activator of sirtuins (Parker et al., 2005). Interestingly, loss of HDACs exacerbated poly-Q neurodegeneration, whereas reducing *sir-2.3* had no effect (Bates et al., 2006). Increasing acetylation globally by treatment with trichostatin-A (TSA), a HDAC inhibitor, also reduced poly-Q toxicity (Bates et al., 2006). However contrary to this study, studies have revealed that decreasing acetylation by overexpressing sirtuins using resveratrol treatment suppressed poly-Q toxicity (Parker et al., 2005), suggesting that the role of HDACs in poly-Q toxicity is complex.

Several other pan neuronal (Brignull et al., 2006), muscle-specific (Yamanaka et al., 2004, Nishikori et al., 2008) models have been described in studies all of which recapitulate the critical aspects of human HD which are age and poly-Q length dependent.

1.3 NEURONAL CEROID LIPOFUSCINOSIS

Neuronal ceroid lipofuscinosis (NCL) is the general term given for a family of at least eight genetically separate neurodegenerative disorders which are characteristic of an excess accumulation of an autofluorescent lipid, lipofuscin in the body's tissues including neurons (Jalanko and Braulke, 2009). NCLs are characterised as lysosomal storage disorders as they are caused due to the malfunction of lysosomes.

NCLs are classified as early infantile, late infantile, juvenile, and adult depending on the age of onset of symptoms. The symptoms in the infantile form of NCL start as early visual loss leading to complete retinal blindness by the age of two years. This is the first indicator of the disease. By three years, a vegetative state is reached and the infant dies usually by the age of four. Late infantile NCL usually manifests between two and four years of age. The symptoms include seizures and deterioration of vision leading to mortality by the age of 10-12 years. Symptoms of juvenile NCL includes considerable vision loss along with seizures and psychological degeneration starting between ages four and ten. Patients usually die during mid- to late-20s. Adult onset NCL (ANCL or Kuf's Disease) is less severe and the symptoms appear around age 30 leading to mortality about ten years later.

The genes affected in different NCLs have been characterized and have been predominantly found to encode lysosomal proteins (Jalanko and Braulke, 2009). Mutations in PPT-1, a member of the palmitoyl protein thioesterase family, leads to infantile NCL (Vesa et al., 1995). PPT-1 is a small glycoprotein involved in the catabolism of lipid-modified proteins during lysosomal degradation. Its function is to remove thioester-linked fatty acyl groups like palmitate from cysteine residues in proteins. A mis-sense transversion of an A to T at position 364 is a known to cause infantile NCL. This mutation results in the substitution of tryptophan with arginine in position 122, close to a lipase consensus sequence containing the putative active site of PPT-1 (Vesa et al., 1995). This could affect the depalmitoylation of the cysteine residues during lysosomal degradation and thereby leading to infantile NCL.

Late infantile NCL is caused due to mutations in the protein, TPP1 (Tripeptidyl peptidase-1) which is a serine protease. To date, 26 mutations and 14 polymorphisms have been reported in TPP1 gene locus (Mole et al., 1999). These include three small deletions, a small insertion, 12 mis-sense mutations, 3 nonsense mutations, a large deletion and 6 splice-site mutations. These mutations resulted in a failure to degrade specific neuropeptides and a subunit of ATP synthase in the lysosome (Jalanko and Braulke, 2009).

Juvenile NCL is caused due to mutations in the gene CLN3 (encoding battenin)

located on chromosome 16 of the human genome. Mitochondrial, golgi and lysosomal functions have been reported for CLN3 but the exact function of the translated battenin protein is unclear. Similar to TPP1, many mutations and polymorphisms have been reported in patients suffering from juvenile NCL. The most common of these is the 1kb deletion, which removes most of the exons 7 and 8, found in more than 85% of victims (Mole et al., 1999).

Adult onset NCL or ANCL is the late-onset and the rarest form, comprising 1.3%-10% of all NCLs. It has sporadic and autosomal dominant and recessive forms. The autosomal dominant and recessive forms are also known as Parry's and Kuf's disease. It was thought that CLN4 was responsible for ANCL however much information relating to the disease manifestation and the mutations in CLN4 was unavailable. It was also found that, mutations in PPT1 gene, implicated in infantile NCL, also caused a rare form of ANCL (Ramadan et al., 2007). A recent study has shown that mutations in CLN6, associated with a variant form of late infantile NCL, could also lead to autosomal recessive ANCL (Arsov et al., 2011). However, the genetic and molecular basis of ANCL with dominant inheritance (Parry's disease) was not known until recently. A recent study has implicated mutations in the gene DNAJC5, which encodes for Cysteine String Protein alpha (CSPα), cause ANCL (Benitez et al., 2011, Noskova et al., 2011, Velinov et al., 2012). These three studies identified this mutation to be in the di-leucine motif of CSPα where leucine 115 was substituted by arginine or leucine 116 was

deleted. These mutations seem to affect palmitoylation dependent sorting to vesicles and the amount of CSPα in neuronal cells (Noskova et al., 2011). There is also evidence from recent studies that in CSPα mutant cells that cause ANCL, there is increased aggregation of mutated CSPα aggregates that are palmitoylated (Greaves et al. 2012).

1.4 CYSTEINE STRING PROTEIN

1.4.1 STRUCTURE

Cysteine string protein alpha was first identified as neuronal-specific antigens recognised by a monoclonal antibody raised against Drosophila heads (Zinsmaier et al., 1990). The importance of CSPα was then illustrated by genetic experiments in Drosophila which revealed a semi-lethal and neurodegenerative phenotype (Umbach et al., 1994, Zinsmaier et al., 1994). This led to the cloning of mammalian CSP and the recognition of its structural domains. CSP was shown to contain a cysteine string – an approximately 20 amino acid motif toward the C-terminus, containing 14 cysteine residues. These residues are heavily palmitoylated and are responsible for the localisation of CSP to secretory vesicles (Gundersen et al., 1994, Mastrogiacomo et al., 1994, Chamberlain and Burgoyne, 1998b). At the N-terminus, there exists a J-domain which mediates CSP binding and activation of the ubiquitous chaperone Hsc70 forming a chaperone complex at the presynapse (Braun et al., 1996, Chamberlain and Burgoyne, 1997a). This region also contains the HPD motif which when mutated prevents the activation of Hsc70 by CSPα (Zhang et al., 1999). This facilitated binding stimulates the ATPase activity of Hsc70 12-14 fold (Braun et al., 1996, Chamberlain and Burgoyne, 1997a, Zhang et al., 1999). The enzymatically active CSP/Hsc70 chaperone complex requires association with small glutamine-rich TPR-containing protein (SGT) forming a trimeric complex on synaptic vesicles (Tobaben et al., 2001, Tobaben et al., 2003). mRNA expression patterns of CSPα, Hsc70 and SGT in the rat brain show a high degree

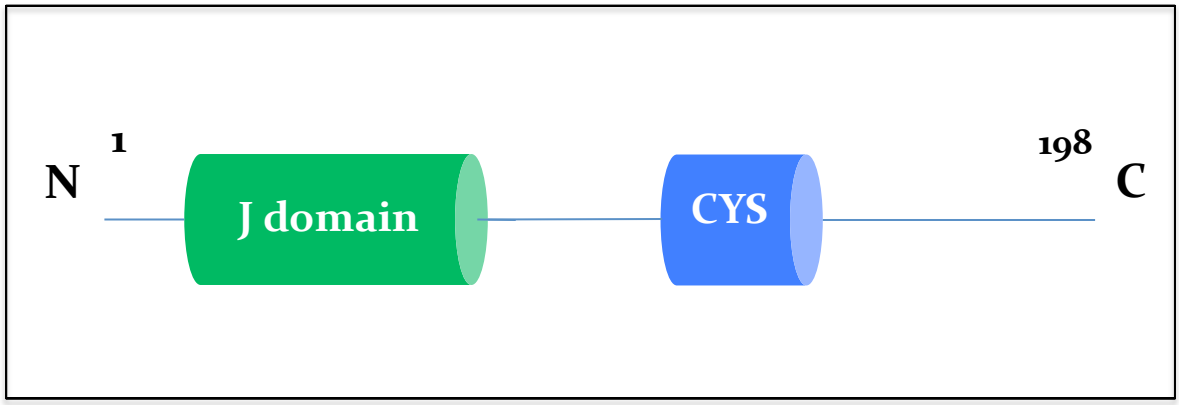

Figure 1.1: Structure of Cysteine String Protein. Shows the structural domains of Cysteine String Protein. The J-domain, involved in Hsc70 binding and activation is present at the N terminus. The cysteine string domain consists of 14 cysteine residues and is involved in targeting the protein to the membranes.

of overlap, with the highest levels in the cerebellum and hippocampus and lower levels in the cortex, olfactory bulb, thalamus, and striatum (Tobaben et al., 2003). The case for the formation of a chaperone complex by the association of CSP, SGT and Hsc70 has been strengthened by several biochemical factors (Tobaben et al., 2001, Tobaben et al., 2003):

1. The complex undergoes an ATP-dependent association-dissociation cycle driven by ATP hydrolysis.

2. Simultaneous binding of CSP and SGT to Hsc70 maximizes the stimulation of the ATPase activity of Hsc70.

3. The trimeric complex exhibits an ATP-dependent strong protein refolding activity as measured with a denatured model substrate. These findings suggest that CSPα recruits Hsc70 and SGT to synaptic vesicles to refold misfolded proteins.

Genetic studies also support a critical and cooperative role of CSP and Hsc70 at Drosophila synapses (Bronk et al., 2001, Bronk et al., 2005) but the significance of SGT's interaction with CSP and Hsc70 at synapses remains less clear. Overexpression of SGT in cultured hippocampal neurons reduces the release probability and the readily releasable vesicle pool size thereby impairing neurotransmitter release (Tobaben et al., 2001).

CSPα has two isoforms in mammals namely CSPβ and CSPγ. These are encoded by separate genes on different chromosomes in both mice and humans. This is in contrast to the findings in Drosophila as the fly CSP only has three isoforms which are splice variants derived from the same gene. A high level of homology exists between CSPα and CSPβ at the N terminus but there is a lack of homology in the C-terminus. A degree of conservation is seen in the above mentioned J domain among both the isoforms and the fly CSP. However, CSPα expression is enriched in the neurons and also in other non-neuronal cell types (Chamberlain and Burgoyne, 2000). However, the expression of CSPβ is enriched in testis and not in neuronal cell types (Gorleku and Chamberlain, 2010). It was also shown that CSPβ had a reduced palmitoylation efficiency compared to CSPα (Gorleku and Chamberlain, 2010).

1.4.2 FUNCTION

Critical insights into the synaptic role of CSPα came from genetic studies of flies and mice. In Drosophila, loss of CSP causes a semi-lethal phenotype causing most mutants to not survive to adulthood (Zinsmaier et al., 1994). The adult survivors progressively exhibit sluggishness, uncoordinated locomotion ending in paralysis and premature death (Zinsmaier et al., 1994, Eberle et al., 1998). CSP knockout flies paralyse within minutes and exhibit a complete loss of evoked neurotransmitter release at higher temperatures (Umbach et al., 1994, Zinsmaier et al., 1994). The progressively developing neurological deficits of adult deletion mutants are mostly due to synaptic failure and subsequent neurodegeneration. Interestingly, overexpression of individual fly CSP isoforms also causes temperature sensitive lethality, severely reduced lifespan and developmental defects (Nie et al., 1999).

In mice, the phenotype of the CSPα knock out mutant is less severe as compared to that of the fly. Mutant mice are indistinguishable from wild-type littermates for the first few weeks but later develop progressive motor and sensorimotor defects with neurodegeneration and a shortened lifespan (Fernandez-Chacon et al., 2004). In contrast to CSP mutant flies, evoked neurotransmitter release is normal in young CSPα knockout mice and thereafter becomes asynchronous and deteriorates progressively with age (Fernandez-Chacon et al., 2004, Ruiz et al., 2008). By P30, the reduction in the evoked

neurotransmitter release at mice CSPα mutant neuromuscular junctions (NMJ) and the calyx of Held is quantitatively similar to that seen at fly NMJs (Umbach et al., 1994, Zinsmaier et al., 1994, Dawson-Scully et al., 2000, Fernandez-Chacon et al., 2004, Ruiz et al., 2008).

1.4.3 NEUROPROTECTIVE ROLE OF CSP

The biochemical and genetic analysis of CSP function in various systems produced compelling evidence that CSP provides an essential chaperone activity that maintains synaptic function and structure. This is supported by the following findings:

1. CSP can act as a 'classical chaperone' along with Hsc70 and/or SGT and prevent protein misfolding at the presynapse (Braun et al., 1996, Chamberlain and Burgoyne, 1997a, b, Zhang et al., 1999).

2. Deletion of CSP in flies and mice causes progressive neurodegeneration that leads to neurological deficits and early death (Zinsmaier et al., 1994, Fernandez-Chacon et al., 2004, Bronk et al., 2005, Chandra et al., 2005).

Although there was little doubt that CSP constituted a synaptic chaperone system, the targeted molecules and the way CSP prevented neurodegeneration was not well understood. It was thought that CSP could prevent neurodegeneration by preventing a general accumulation of misfolded proteins or by preventing an accumulation of a few specific proteins which could have a high neurotoxic potential. Studies in flies showed that CSP is required for facilitating evoked release before the onset of neurodegeneration implying that a defect in facilitation of release by CSP triggers neurodegeneration (Umbach et al., 1994, Ranjan et al., 1998, Dawson-Scully et al., 2000, Bronk et al., 2005). However, the phenotype of CSPα knockout mice argued against this idea as

new-born mutant mice show no behavioural or functional synaptic deficits during the first few weeks and structural deficits consistent with degeneration becomes apparent when synaptic function is impaired (Fernandez-Chacon et al., 2004, Chandra et al., 2005, Ruiz et al., 2008). Hence, CSPα knockout model supports a general chaperone function that maintains synaptic integrity during stress (Fernandez-Chacon et al., 2004). However, this can be only true as long as there is no closely related protein that compensates for the loss of CSPα activity. The surprising discovery that overexpression of α-synuclein in CSPα knockout mice rescues the phenotypes of the mutants animals altered this notion (Chandra et al., 2005).

Overexpression of α-synuclein in CSPα knockout mice reversed their weight loss, locomotion defects and the neurodegenerative phenotypes. It was also shown that the deletion of endogenous synucleins accelerated the lethality and neurodegeneration in CSPα knockout mice (Chandra et al., 2005). The loss of CSPα in mice also resulted in a decline in the levels of SNAP-25. There was also a defect in the formation of the SNARE complex (Fernandez-Chacon et al., 2004). Interestingly, overexpression of α-synuclein rescues the defective SNARE complex association but fails to rescue the decline of SNAP-25 levels in CSPα knockout mice (Chandra et al., 2005) suggesting an alternate pathway to the formation of SNARE complex. Also, loss of all three α, β, and γ synucleins in mice resulted in a phenotype similar to CSP knockout mice (Greten-Harrison et

al., 2010). These results suggest that CSP controls specific protein activity such as SNARE complex assembly and also contributes to the chaperone activity by the proper folding of a number of synaptic proteins.

In vitro and cell culture studies have revealed that overexpression of CSPα in PC12 cells enhanced exocytosis (Chamberlain and Burgoyne, 1998a) but inhibited exocytosis in insulin secreting cells (Brown et al., 1998, Zhang et al., 1999). Overexpression of CSPα in adrenal chromaffin cells impaired catecholamine exocytosis by reducing the number of release events and slowing their release kinetics, suggesting that CSP modulates proteins that are involved at a step close to membrane fusion (Graham and Burgoyne, 2000).

There is evidence of a direct interaction of CSP with syntaxin, another key member of the SNARE complex in neurons, in both Drosophila and mammalian cells (Magga et al., 2000, Chamberlain et al., 2001, Evans et al., 2001). In addition, CSPα was shown to interact with the SNARE synaptobrevin and the calcium sensor synaptotagmin (Leveque et al., 1998, Evans and Morgan, 2002, Boal et al., 2004) . This interaction with syntaxin and synaptotagmin was found to be controlled by cAMP dependent protein kinase A (PKA) and protein kinase B/Akt which could fine-tune the release kinetics of neurotransmission (Evans et al., 2006). Phosphorylation of CSPα at Ser10 reduces binding to syntaxin 10 fold and abolishes the slowing of release kinetics effects induced by CSP

overexpression (Evans et al., 2001, Evans and Morgan, 2002, Evans et al., 2006).

More recently, a study suggested that CSPα interacts with SNAP-25 by chaperoning it into the SNARE complex (Sharma et al., 2011). This interaction was shown to enhance synaptic activity. In vivo studies in the CSPα knockout mice suggested that a heterozygous loss of SNAP-25 resulted in the worsening of the neurodegeneration phenotype in CSPα knockout mice (Sharma et al., 2012). There was also a decrease in the SNARE complex assembly and a further reduction in the lifespan of the mutant mice. These defects were not seen with a knock down of SNAP-25 alone suggesting an interaction between CSPα and SNAP-25. Large decreases in SNAP-25 levels by themselves did not cause a major impairment in synaptic transmission. Also shown in the same study was the rescue of the neurodegeneration phenotype of the CSPα knockout mutants by the overexpression of SNAP-25 (Sharma et al., 2012). This suggests that the key substrate of CSPα in mice is SNAP-25 and its key function is to chaperone SNAP-25 into the SNARE complex. Also, the CSPα knockout phenotype is largely if not completely caused by the loss of CSPα dependent chaperoning of SNAP-25 which leads to impaired SNARE complex assembly which in turn causes neurodegeneration. These studies suggest that SNARE complex assembly does not cause neurodegeneration through a decrease in neurotransmitter release but because the impairment in SNARE complex assembly leads to an excess of reactive SNARE proteins that do not participate in the SNARE complexes. The

loss of SNAP-25 in CSPα knockout mice results in an excess build up of syntaxin-1 and synaptobrevin-2 which are highly reactive. They may engage themselves in inappropriate protein interaction that damage the nerve terminals resulting in neurodegeneration. The fact that α-synuclein overexpression does not restore SNAP-25 levels, but directly enhances SNARE complex assembly, suggests that it acts through a pathway that is independent of CSPα (Burre et al., 2010). It was shown that α-synuclein was directly bound to synaptobrevin and thus promoted SNARE complex assembly (Burre et al., 2010). The same study also showed that the loss of all three synucleins resulted in age dependent neurodegeneration and premature death. This suggests that α-synuclein plays a major role in sustaining normal SNARE complex assembly independent of CSPα.

These findings beg the question - does the neurodegenerative mechanism explained above potentially apply to other forms of neurodegeneration, and is this mechanism relevant for human disease? There are several studies which suggest that neurodegeneration in some cases of Alzheimer's and Parkinson's disease point to a presynaptic locus (Wishart et al., 2006, Kramer and Schulz-Schaeffer, 2007, Scheff et al., 2007). In poly-Q disorders, the activity of CSP may be compromised as expanded poly-Q tracts form huntingtin protein sequester CSP and block its activity (Miller et al., 2003). The recent discovery that mutations in CSPα causes ANCL (Benitez et al., 2011, Noskova et al., 2011,

Velinov et al., 2012) further strengthens the claim that CSPα could be a key player in neuroprotection against several if not one neurodegenerative disease.

1.5 AIMS AND OBJECTIVES

Caenorhabditis elegans has been used to model various neurodegenerative diseases, mainly by overexpressing human genes with disease causing mutations. In these models the affected underlying mechanisms are disease specific despite the shared feature of protein misfolding and/or aggregation (van Ham et al., 2009, Chen and Burgoyne, 2012). Several studies have shown that neurodegeneration in these disease specific models can be rescued by the treatment with several drugs. Studies in mice have shown that the loss of an endogenous factor (CSPα) leads to neurodegeneration (Burre et al., 2010, Chandra et al., 2005, Fernandez-Chacon et al., 2004, Sharma et al., 2011). Identifying the compounds that compensate for the loss of an endogenous physiological neuroprotective factor such as CSPα may help in identifying generic neuroprotective interventions (Sleigh et al., 2011). This needs a more robust and high throughput model as compared to mice. As CSP mutants in *Drosophila* are more sick than mutant mice, it is important to characterize a model that is more reflective of the phenotypes observed in mice. The CSPα of the model organism *Caenorhabditis elegans* is yet to be characterised. *C. elegans* is a robust model and high throughput drug screens can be performed easily. It has a simple and well characterised nervous system and hence neurodegeneration can be characterised with ease. Therefore, characterisation of a *C. elegans* model that lacks CSPα could help in the identification of novel therapeutic drug targets. Hence the specific aims of this study are:

1. To characterise the endogenous CSPα in *C. elegans–dnj-14* and elucidate

its phenotypic similarity to the CSPα knockout mice

2. To identify compounds that compensate the loss of *dnj*-14 in *C. elegans* and elucidate the mechanism of rescue.
3. To analyse the interaction of CSPα and SNAP-25 in *C. elegans*.

CHAPTER 2: METHODS

2.1 NEMATODE METHODS

2.1.1 NEMATODE STRAINS

Caenorhabditis elegans strains Bristol N2, *dnj-14(ok237), ric-4(md1088)*, *sir-2.1(ok434)* were obtained from the *Caenorhabditis* Genetics Center (University of Minnesota, Twin Cities, MN, USA). Nematode strain *dnj-14(tm3223)* was obtained from the National Bioresource Project for the Experimental Animal "Nematode *C. elegans"* based in the lab of Dr. Shohei Mitani (Tokyo Women's Hospital, Tokyo, Japan). The transgenic strain CZ1200 was obtained from the lab of Dr. Brian Kraemer (University of Washington, Seattle, USA). The other wild-type transgenic strains were obtained using microinjection performed by Dr. James Johnson and Dr. Hannah McCue. Mutant transgenic strains, outcrossed strains and double mutants were obtained by performing genetic crosses.

2.1.2 GENERAL METHODS AND *C. ELEGANS* STOCK MAINTENANCE

All *C. elegans* strains for maintenance were grown on 60mm tissue culture plates containing 8mL nematode growth media agar [NGM: 2% (w/v) agar, 0.3% (w/v) NaCl, 0.25% (w/v) peptone, 1mM $CaCl_2$, 1mM $MgSO_4$, 25mM KH_2PO_4, 5µg/mL cholesterol] at 20°C seeded with 30µL of OP50 strain of *E. coli* to form a bacterial lawn which served as food source according to standard culture techniques (Brenner, 1974). Stocks were maintained either by transferring 5-10 gravid adult worms periodically to fresh plates or by cutting a section of agar from one plate and inverting it onto a fresh plate (chunking). A worm pick made of platinum wire was used to transfer the worms to the plates. The end of the

pick was covered in *E. coli* from the bacterial lawn each time the worms were lifted off the agar.

2.1.3 FREEZING WORMS

C. elegans stocks were frozen in a cryoprotectant for long term storage. Starved plates containing several L1 and L2 larvae were washed in 3mL M9 buffer (5g/L NaCl, 3g/L KH_2PO_4, 6g/L Na_2HPO_4, 1mM $MgSO_4$) and equal volume of freezing solution (100mM NaCL, 50mM KH_2PO_4, 5.5mM NaOH, 3mM $MgSO_4$ and 30% (w.v) glycerol) added and mixed well. Ten cryovials were filled with 0.6mL of this mixture packed in a polystyrene box and stored in a -80°C freezer. The aliquots were tested the following day by thawing out one vial to check for viable worms.

2.1.4 LIFESPAN ASSAY

Lifespan was tested to analyse the effects of genetic mutation and/or the effect of pharmaceutical drugs on the worms. The worms were age-synchronized using the following procedure. Initially 5 gravid adult worms were allowed to lay eggs overnight and removed onto an NGM plate. The progeny were monitored and 25-30 L4 hermaphrodites were placed on to a fresh plate. The worms were checked for survival every two days by prodding them twice with a worm pick. Absence of response to prodding was scored as a death and the number of deaths were recorded. Worms were transferred onto fresh plates every two days in the first two weeks to prevent progeny formation. Whenever FUdR (5-

fluoro-2'-deoxyuridine) was used to prevent progeny formation, the animals were transferred onto fresh plates on nearing exhaustion of food.

2.1.5 MAINTENANCE OF MALE WORMS

The male worms used during this study were obtained from Dr. Michèle Riesen, University College London, UK. Young adult hermaphrodites were picked onto a plate and left for 4 hours to rid them of eggs. They were then transferred to another plate containing young male worms The ratio of male to hermaphrodite worms maintained at 3:1. The worms were allowed to mate for 3 days to develop the F1 progeny with approximately 50% males. Repeating the above steps with the F1 males resulted in a sizeable male worm population. To increase the percentage of male worms on the plate, the hermaphrodites for crossing were picked from an old mating plate with the assumption that they would carry eggs from a prior mating event.

2.1.6 GENETIC CROSSES

Three young mutant hermaphrodites with no eggs were picked on to a plate with nine wild type males and allowed to mate for three days. The resulting F1 males would be heterozygous mutant. These males were picked and washed in M9 buffer to rid them of any eggs or larvae stuck to their bodies. The worms were then placed onto a plate with hermaphrodites of the second mutant with male to hermaphrodite ratio again maintained at 3:1. After three days, hermaphrodites from the plate (heterozygous in nature) were segregated such

that each 35mm plate had a single worm. They were then allowed to self-fertilize and the F1 segregated into F2 worms on individual plates. The F2 were then genotyped for the double mutant using single worm PCR. According to Mendelian genetics, if the mutations were on different chromosomes, about 1/16th of the F2 progeny would be double mutant.

2.1.7 DRUG TREATMENT

Individual compounds were dissolved in appropriate vehicles and added directly to molten NGM before pouring plates. Control NGM plates were poured by adding the appropriate dilution of vehicle. On drying overnight, the plates were seeded with 30µL of OP50 bacteria. Age synchronized worms at day 1 of adulthood were then placed on these drug plates and the assays were performed. Worms were transferred on to fresh drug plates every two days. Whenever FUdR was used, the worms were transferred on to fresh plates with the exhaustion of OP50 or upon infection due to other bacteria and/or fungi.

2.1.8 NEURODEGENERATION ASSAY

Transgenic strains expressing *gfp* in all or a subset of neurons were imaged to assay neurodegeneration. The worms were age synchronized as explained before and categorized into three groups - young (<Day 7), mid-age (Days 9-12) and old (>Day 12). The worms were then placed on slides with 3µl of 20:20 PEG:glycerol suspension and left for a minute to immobilize the worm. A cover slip was placed on top of the suspension and the worm imaged under a

fluorescent microscope using NIS-Elements Microscope Imaging Software (Nikon Instruments Europe B.V.) or using a NikonD90 camera plugged into the microscope.

2.1.9 BEHAVIOURAL ASSAYS

2.1.9.1 LOCOMOTION ASSAY

Worms were age synchronized as mentioned above and assayed on reaching adulthood. The locomotory ability of worms in solution was quantified by thrashing assays (Johnson et al., 2009). A thrash was defined as one complete sinusoidal movement of the worm. A worm was placed in a drop of Dent's Ringer solution (10mM D-glucose, 10mM HEPES, 140mM NaCl, 6mM KCl, 1mM $MgCl_2$ and 3mM $CaCl_2$), allowed to acclimatize for 5 minutes and the number of times the worm thrashed per minute was recorded. For age-dependent locomotion, worms were picked from a lifespan plate and thrashing assay was performed at days 1, 3, 6, 9 and 12 of adulthood. The worms were returned to their plates on completion of the assay.

2.1.9.2 PHARYNGEAL PUMPING

Feeding in *C. elegans* is regulated by pharyngeal pumping. The pharynx is the organ that sits in the head of the worm at the entry into the gut cavity. Pumping is a process wherein the liquid from the bacteria containing plate is sucked into the worm and through a cycle of contraction and relaxation, the liquid is expelled out transporting the bacteria into the intestine. For pharyngeal pumping assays, feeding worms were observed under high magnification (8x objective) using a stereo microscope. The number of contraction relaxation cycles or pumps were counted per thirty seconds.

2.2.9.3 ALDICARB ASSAY

Aldicarb assays were performed by assessing the sensitivity of the worms to an acetylcholinesterase inhibitor, aldicarb (Mahoney et al., 2006, Graham et al., 2011). 25-30 worms were picked on to an unseeded NGM plate containing 1mM aldicarb (Sigma-Aldrich®) and observed at the start of the assay (time=0) to ensure that the worms were not dead and/or paralyzed. Paralysis was defined as a worm showing no movement and no pharyngeal pumping, spontaneously or after prodding on the head three times by the worm pick. The number of paralyzed worms were recorded every ten minutes.

2.1.9.4 FOOD RACE ASSAY

A food race assay, which is a measure of the time taken for the worms to move to a bacterial food source (*E. coli*), were performed (Mitchell et al., 2010). 60mm NGM plates were poured three days before use and seeded with 30µL OP50 10mm from the edge of the plate. 20-30 age-synchronized worms were washed twice in M9 buffer and placed 10mm from the edge opposite the food. The number of worms reaching the food was recorded every 10 minutes for two hours and after which the worms on the food were removed.

2.1.9.5 CHEMOTAXIS

Chemotaxis is a measure of the attraction coefficient of the worms to a volatile compound. The experiments were performed as explained in Bargmann et al., 1993. Chemotaxis index was calculated as number of worms at

attractant/repellent minus number of worms at control divided by the total number of worms. Chemotaxis plates were made three days before use on 100mm tissue culture plates (containing 2% (w/v) agar, 5mM KH_2PO_4, 1mM$CaCl_2$, 1mM $MgSO_4$). The worms were washed in M9 buffer and placed in the centre of the plate. One micro litre of the attractant/repellent and the diluent (ethanol) were pipetted onto the opposite ends of the plate and the number of worms on either side of the plate were counted after 90 minutes. Chemotaxis index of 0.11 was considered as baseline for false positives

2.1.9.6 MECHANOSENSATION

Mechanosensory assays were performed as explained in Chalfie and Sulston, 1981. A male eyelash was plucked and the root end of this was glued to a toothpick, leaving the tapered end free. Before assaying, this was sterilized by dipping in 70% ethanol and subsequently air-dried. The worms were then transferred on to an unseeded 35mm plate and left for five minutes to acclimatise. Anterior touch response was tested by touching the worm gently on the pharynx. Nose touch assay was performed by gently placing the eyelash such that the worm hits it at a perpendicular angle. Each worm was assayed ten times and the number of times the worm either stopped or reversed its direction of movement was recorded.

2.1.10 STATISTICAL ANALYSIS

Student's t-test was performed to directly compare two data sets using

Microsoft Office® Excel® 2012. Lifespan analyses were performed using the online tool OASIS (Online Application for the Survival Analysis of Lifespan Assays; http://sbi.postech.ac.kr/oasis/introduction/) (Yang et al., 2011). The software used log-rank test to compare survival of two different data sets and Fischer's exact test to compare survival at specific time points.

2.2 MOLECULAR BIOLOGY

2.2.1 GENOMIC DNA EXTRACTION

Ten adult gravid worms were dissolved in 50µL of 1X Phusion® High Fidelity PCR buffer (New England BioLabs®) containing 1mg/mL proteinase K and were spun down to the bottom of a PCR tube. This was then placed in a thermocycler and heated at 65°C for 90 minutes and then again at 95°C for a further 15 minutes to heat inactivate the proteinase K.

2.2.2 SINGLE WORM PCR

Single worm PCR was carried out to genotype the organism. Genomic DNA from a single worm was extracted by dissolving a single adult gravid worm in 10µL of 1X Phusion® High Fidelity PCR buffer (New England BioLabs®) buffer containing 1mg/mL proteinase K and lysed by heating as, mentioned above. 2µL of genomic DNA was added to 1X One*Taq*® Master Mix with Standard Buffer (New England BioLabs®). 2µL each of sense and anti-sense primers were added and the total volume of the PCR reaction was set to 50µL by adding Ambion® Nuclease Free Water (Life Technologies™). The mixture was then spun down to the bottom of a PCR tube and placed inside a thermocycler. The program used to run the amplification was:

Step	Temperature (°C)	Time
Initial Denaturation	95	10 minutes
	95	30 seconds
30 Cycles	45-68	30 seconds
	68	30 seconds/kb
Final Elongation	68	5 minutes
Hold	4	Infinity

2.2.3 GEL EXTRACTION AND SEQUENCING

To analyse mutations in worm strains, primers were constructed along two regions of a gene and the DNA was amplified. This amplified DNA was then run on an agarose gel for visualisation. The bands were then excised, extracted and purified using GenElute™ Gene Extraction Kit (Sigma-Aldrich®). 3.2µM of the sense and anti-sense primers were added to two tubes containing 10µL each of the purified DNA and the final volume was made up to 32µL by adding Ambion® Nuclease Free Water (Life Technologies™). This was then sent for sequencing to The DNA Sequencing & Services at the University of Dundee, UK.

2.2.4 AGAROSE GEL ELECTROPHORESIS

0.4% (w/v) agarose (SigmaAldrich®) was dissolved in 1X TAE buffer (2mM Tris HCl, 50mM EDTA, pH 8.0) and microwaved for a minute. 1X SYBR® Safe (Life Technologies®) was added to the molten agarose which was then cast into a

mould with wells in one corner to load DNA samples. On setting, the gel was immmersed in 1X TAE buffer and the DNA samples were loaded onto it. The gel was run at 80V for 40 minutes and the samples were then visualised using Gel Doc XR System (Bio-Rad®).

2.2.5 SOFTWARE FOR ANALYSIS

VectorNTI® (Invitrogen; v11.0) was used to annotate genes and construct primers used for PCR. DNABaser® Sequence Assembly Software (Heracle BioSoft) was used to visualize DNA chromatogram data from the sequencing results. BLAST searches were performed to verify the accuracy of the sequencing results.

CHAPTER 3: PHENOTYPIC ANALYSIS OF CSP IN *C. ELEGANS*

3.1 INTRODUCTION

3.1.1 CYSTEINE STRING PROTEIN GENETICS

Cysteine String Protein (CSP) is a presynaptic protein involved in the folding of misfolded proteins in the pre-synapse (Fernandez-Chacon et al., 2004). CSP forms a co-chaperone complex by associating with Heat shock cognate 70 (Hsc70) and a small glutamine-rich tetratricopeptide repeat protein (SGT) (Chamberlain and Burgoyne, 1997, Tobaben et al., 2001). Structurally CSP consists of two domains: a J domain at the N terminus involved in Hsc70 binding and activation (Chamberlain and Burgoyne, 1997) and a central chain of 14 heavily palmitoylated cysteine residues involved in targeting synaptic vesicles (Chamberlain and Burgoyne, 1998). Loss of function of CSP in *Drosophila* results in a semi-lethal phenotype and the flies that survive show synaptic failure and pre-synaptic morphological abnormalities resulting in premature death (Umbach et al., 1994).

CSP knockout mice grow normally for the first 2-3 weeks but start exhibiting progressive sensorimotor disorders and neurodegeneration leading to reduced lifespan (Fernandez-Chacon et al., 2004). Interestingly, the phenotype of CSP knock out mice was shown to be rescued by the overexpression of α-synuclein, a protein with the ability to potentiate the SNARE complex (Chandra et al., 2005) but not γ-synuclein (Ninkina et al., 2012), suggesting a specific interaction between CSP and α-synuclein. Also, loss of all three α, β, and γ synucleins in

mice resulted in a phenotype similar to CSP knock out mice (Greten-Harrison et al., 2010). As α-synuclein is implicated in neurodegenerative disease, CSP might be a key player in neuroprotection at the pre-synapse. CSP has also been shown to promote SNARE complex activity by chaperoning SNAP-25 (Sharma et al., 2011). In CSP knockout mice a heterozygous loss of SNAP-25 leads to worsening of the neurodegeneration phenotype which was shown to be rescued by the overexpression of SNAP-25 (Sharma et al., 2012). The above studies reiterate the fact that CSP is a key neuroprotective protein and facilitates neuroprotection by regulating the SNARE complex. More recently, mutations in the di-leucine motif (L115R and ΔL116) of CSP has been implicated in a human neurodegenerative disease called adult-onset neuronal ceroid lipofuscinosis (ANCL) (Benitez et al., 2011, Velinov et al., 2012). A recent cell culture study also shows that as a result of these mutations, CSP is mis-targeted and forms SDS resistant aggregates concordant to other mutant proteins linked to neurodegenerative diseases (Greaves et al., 2012). This clear implication of CSP in human neurodegenerative disease strengthens our case to characterise a *C. elegans* model with loss of CSP to screen drugs that alleviate neurodegeneration and identify novel targets for therapeutic use.

3.1.2 CSP IN NEMATODES

As previously mentioned, knockdown of CSP in flies results in a semi-lethal phenotype with only less than 10% of the animals surviving on to adulthood (Zinsmaier et al., 1994). The flies that did manage to survive were severely ill and died prematurely (Zinsmaier et al., 1994). However, the phenotype of the CSP knockout mice was less severe and the animals developed into adults similar to the wild-type (Fernandez-Chacon et al., 2004). It was only after postnatal days 40-60 did these mice exhibit progressive motor and sensory impairments leading to neurodegeneration (Fernandez-Chacon et al., 2004, Chandra et al., 2005).

In *C. elegans,* the *dnj-14* gene is the closest homologue to CSP and consists of three exons (Figure 3.1A). As shown in Figure 3.1B, DNJ-14 has a homologous DnaJ domain and a cysteine string domain with 13 cysteines, one less than CSP. It contains the HPD domain involved in Hsc70 binding and activation (Chamberlain and Burgoyne, 1997) and the di-leucine motif which is mutated in Adult-onset Neuronal Ceroid Lipofuscinosis (Benitez et al., 2011, Velinov et al., 2012). It has 54% sequence homology towards human CSP and the level of conservation is high in the important structural domains (Figure 3.1B).

DNJ-14 in *C. elegans* had not been previously characterised and therefore it was important to characterise a model for CSP in *C. elegans*. Although some phenotypic similarities exist between the mouse and the fly models for CSP

(Umbach et al., 1994, Zinsmaier et al., 1994, Eberle et al., 1998, Fernandez-Chacon et al., 2004), the two models are not very similar. The phenotypes seen in *Drosophila* are not progressive and the loss of CSP leads to a semi lethal phenotype in flies (Umbach et al., 1994, Zinsmaier et al., 1994). As explained before, this is not the case with the mice (Fernandez-Chacon et al., 2004). Hence the investigation of *dnj-14* knock out in nematode *C. elegans,* would give much insight into the conservation of CSP function. Moreover, the characterisation of the *dnj-14* mutant in worms would enable us to perform more high-throughput drug screens which would enable us to find neuroprotective drug targets.

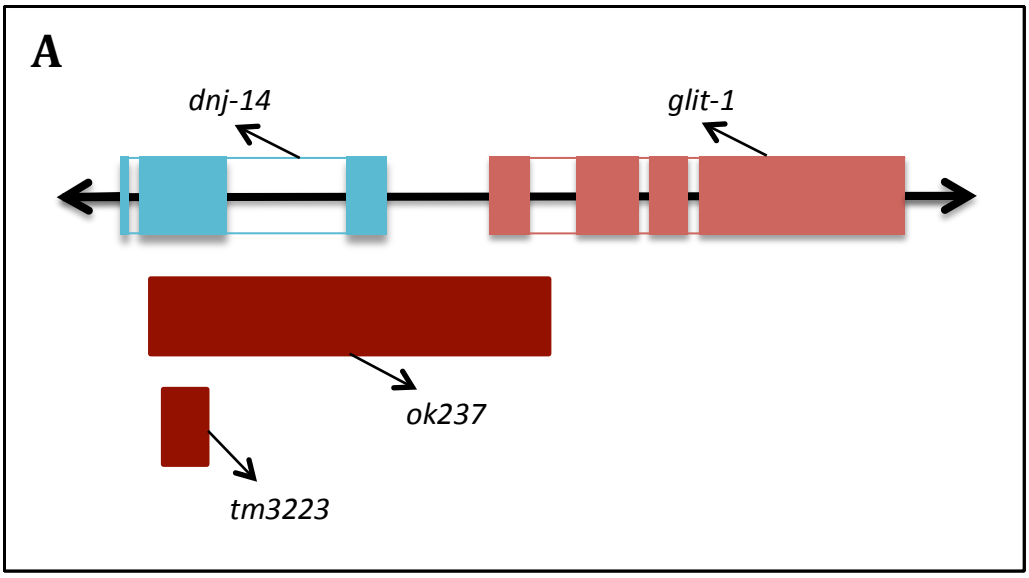

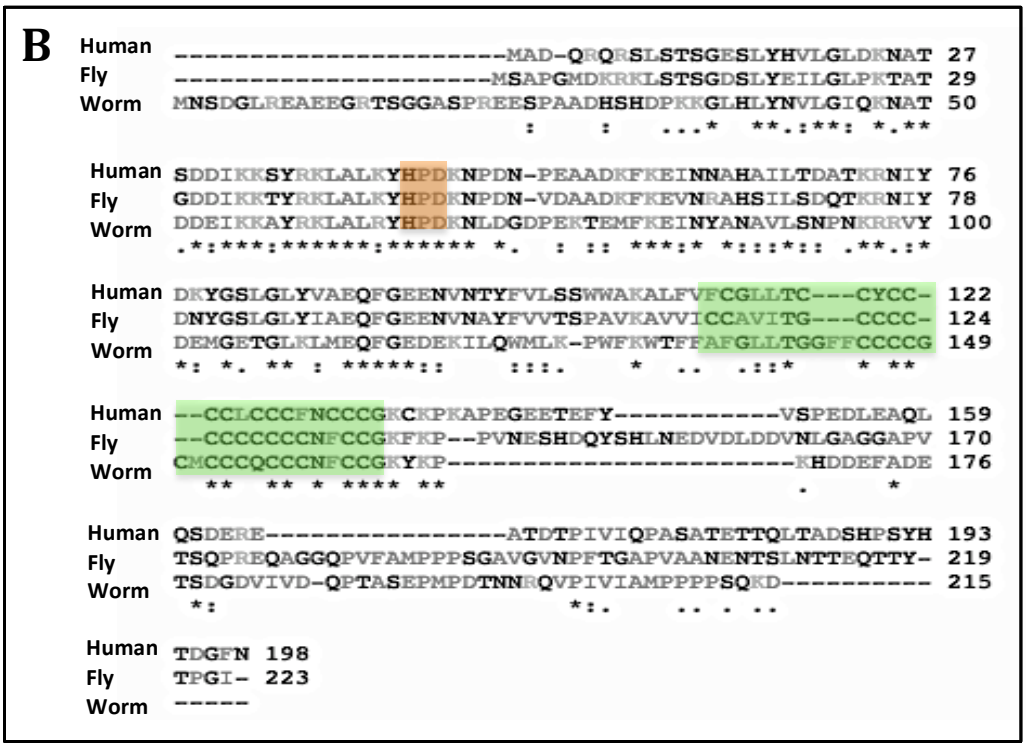

Figure 3.1: Genetic analysis and homology of *dnj-14* gene: A) Shows the gene structure of *dnj-14.* The gene is composed of three exons with the N-terminal first exon separated from the second exon by a large intron. The second exon comprises of the cysteine string domain and much of the unstructured C-terminal region. The figure also shows the different alleles of *dnj-14*, namely, *ok237* and *tm3223.* As it can be seen, the *ok237* mutation extends upstream from the N-terminal region and also deletes much of the first exon of the adjacent gene, *glit-1.* B) Shows the multiple sequence alignment of *dnj-14* gene with its fly and human CSP counterparts. Highlighted are the HPD domain that is involved in Hsc70 activation (orange) and the cysteine string domain (green). It can be seen that *dnj-14* has 13 cysteine residues as compared to 14 in the fly and human CSPs.

3.2 METHODS

3.2.1 NEMATODE HUSBANDRY

3.2.1.1 NEMATODE STRAINS

The *C. elegans* strains used in this chapter Bristol N2 and *dnj-14(ok237)* were obtained from the *Caenorhabditis* Genetics Centre (CGC; University of Minnesota, Twin Cities, MN, USA) and the strain *dnj-14(tm3223)* was obtained from the National Bioresource Project for the Experimental Animal 'Nematode *C. elegans'* (Tokyo Women's Hospital, Tokyo, Japan). *Escherichia coli* strain OP50 used as a food source for the worms was also obtained from CGC. The outcrossed strains were obtained by crossing the mutants back on to the wild-type Bristol N2s multiple times.

3.2.1.2 CULTURE

The *C. elegans* strains were grown on 60mm cell culture plates (except for segregated lines from crosses which were cultured in 40mm plates) on nematode growth media as explained before in chapter 2 according to standard growth conditions *(Brenner, 1974)*.

3.2.2 NEMATODE TECHNIQUES

3.2.2.1 OUTCROSSING STRAINS

Most of the mutant strains obtained from CGC may have mutations elsewhere in their genome because these mutants are obtained by treatment with chemicals or electromagnetic spectra. So there is a need to rid the animals of these mutations and this is obtained by crossing the mutants with the wild type worms multiple times. Hermaphrodite *dnj-14* mutants were first crossed with the wild-type N2 male worms and of the resulting progeny, half of them would be *dnj-14* males. These males were crossed again with N2 hermaphrodites and the resulting hermaphrodites would all be heterozygous for *dnj-14* mutation. These heterozygous hermaphrodites were segregated on 40mm NGM plates such that each plate contains a single worm. Once the worm self-fertilises and lays eggs, the parent worm was genotyped for homozygosity by single worm PCR. According to Mendelian genetics, one in four of the segregated lines would be homozygous. The resulting homozygous mutant would thus be outcrossed twice. These steps were repeated thrice to obtain six times outcrossed worms. All the N2 males and hermaphrodites used in crossing were transgenic lines containing an extra chromosomal array expressing *gfp* driven by a *rab-3* promoter (Ex(P*rab-3*::*gfp*)). The progeny from the cross were screened for this *gfp* marker to obtain transgenic mutants. The extra chromosomal marker was, in some experiments, selectively lost to obtain non-transgenic outcrossed mutants.

3.2.2.2 AGE SYNCHRONISATION

Worms were age synchronised for several experiments so all the worms assayed would be of the same age. To achieve this, ten adult worms were washed in M9 buffer (5g/L NaCl, 3g/L KH_2PO_4, 6g/L Na_2HPO_4, 1mM $MgSO_4$) and placed onto a plate overnight to lay eggs. The next day, these worms were sacrificed and the resulting progeny, all of which would be age synchronised, was allowed to develop. Once these worms reached the L4 stage, they were transferred on to a clean plate for assaying.

3.2.3 MOLECULAR BIOLOGY

3.2.3.1 GENOMIC DNA EXTRACTION

Genomic DNA extraction was carried out as explained in chapter 2. Stocks of wild type N2 and *dnj-14* mutants were prepared by dissolving ten adult gravid worms in 50µL of Phusion® High Fidelity PCR buffer (New England BioLabs®) containing 1mg/mL proteinase K and spun down to the bottom of a PCR tube. This was then placed in a thermocycler and heated at 65°C for 90 minutes and heated again at 95°C for a further 15 minutes to heat inactivate the proteinase K. For single worm PCR analysis, each segregated parent worm was dissolved in 10µL of the above buffer and lysed as mentioned above in the thermo cycler.

3.2.3.2 SINGLE WORM PCR

Single worm Polymerase Chain Reaction was performed to genotype mutant strains. The reaction was performed as mentioned in chapter 2. 2µL of genomic DNA was added to the polymerase mix along with custom-made primers, the reaction mixture made up to 50µL using nuclease free water and the reaction was performed in a thermocycler as explained before. The resulting amplified DNA was then visualised using agarose gel electrophoresis. Primers used for PCR analysis includes: a) dnj-14 del rev - 5'-TGCTCTCAACAGACCCATAC-3', b) tm3223 del full fwd: 5'-GCTTGTCTTACCTTATGTCGTCG-3', c) dnj-14 del full fwd: 5'-CAGATAGTTCATACTGAAAATCT-3', d) dnj-14 del mid fwd: 5'-ATTCGCACGATCCGAAAAAG-3'.

3.2.3.3 TRANSGENIC CONSTRUCTS

For transgenic rescue experiments, a construct comprising of the genomic coding region of *dnj-14* plus 560 bp of upstream flanking sequence was inserted into a pPD117.01 plasmid with the GFP-coding region removed.

3.2.3.4 SOFTWARE ANALYSIS

For PCR, the optimal annealing temperature was calculated using 'Tm Calculator' (New England Biolabs®). Primers for the study were designed using VectorNTI® (Invitrogen; v11.0). Analysis of the DNA chomatogram was performed using DNABaser® Sequence Assembly Software (Heracle BioSoft). The accuracy of the sequencing results were verified by performing BLAST searches.

3.2.4 NEMATODE ASSAYS

3.2.4.1 LIFESPAN

Worms were age synchronized as explained above and the assay was performed as explained in chapter 2. Twenty-five of these worms were transferred on to 60mm NGM plates on their first day of adulthood. The worms were monitored every two days for survival by gently prodding them thrice using a worm pick till all worms were dead. To prevent the progeny from crowding the plate, the worms were transferred on to fresh plates every two days and/or on exhaustion of food. All the experiments were repeated at least twice to check for reproducibility.

3.2.4.2 NEURODEGENERATION ASSAY

Transgenic wild type lines expressing *gfp* driven by a pan-neuronal promoter *rab-3* were obtained from Dr. James Johnson and wild type worms expressing *gfp* in the GABA neurons (*unc-25* promoter) were obtained from Dr. Brian Kraemer, University of Washington, Seattle, USA. These were crossed with the *dnj-14* mutants to obtain mutant transgenic lines. Worms were immobilized in PEG 20000: Glycerol as explained before and imaged using a fluorescent microscope using NIS-Elements Microscope Imaging Software (Nikon Instruments Europe B.V.) or a NikonD90 camera plugged into the microscope.

3.2.4.3 ALDICARB ASSAY

NGM plates containing 1mM aldicarb were poured and dried overnight.

Aldicarb assays were performed as explained before on 25-30 worms and compared to the wild type N2 worms as control. The experiments were repeated several times to check for reproducibility. All experiments were performed on the worms at day 5 of adulthood.

3.2.4.4 LOCOMOTION

Locomotion assays were performed in Dent's Ringer solution as explained in chapter 2. Assays were performed on the outcrossed and non-outcrossed strains of both *dnj-14* mutants using wild type N2 animals as control.

3.2.4.5 FOOD RACE ASSAY

Food race assays were performed as explained in chapter 2. All the experiments were performed on outcrossed *dnj-14* mutants except for the transgenic rescue of *dnj-14(ok237)* worms. Wild type N2 worms were used as control. Worms were assayed on days 3, 6 and 9 of adulthood.

3.2.4.6 CHEMOTAXIS

Chemotaxis assays were performed using the compounds 2,3-buteine-di-one (10^{-4}X), nonenone (10^{-3}X) and isoamyl alcohol (10^{-3}X), all of which were diluted in ethanol. The experiments were performed as explained in chapter 2 and experiments were performed at days 3, 6 and 9 of adulthood.

3.2.4.7 MECHANOSENSATION

Nose touch assay was performed on both *dnj-14* mutants using a male eyelash sterilized in 70% ethanol as explained earlier in chapter 2. The experiments were carried out on worms which were at day 6 of adulthood and each worm was assayed ten times.

3.2.4.8 STATISTICAL ANALYSIS

Student's t-test was performed to compare two data sets using Microsoft Office® Excel® 2012. Lifespan analyses were performed using the online tool OASIS (Online Application for the Survival Analysis of Lifespan Assays; http://sbi.postech.ac.kr/oasis/introduction/) (Yang et al., 2011). The software used log-rank test to compare survival of two different data sets and Fischer's exact test to compare survival at specific time points.

3.3 RESULTS

3.3.1 PRELIMINARY PHENOTYPIC ANALYSIS OF *ok237* ALLELE

The worm has a single CSP homologue called *dnj-14*. A deletion in *dnj-14* is characteristic of the worm strain *dnj-14*(*ok237*) used in our study. The deletion starts at the beginning of the second exon and extends all the way across the gene, effectively knocking out the expression of the DNJ-14 protein completely. Hence, this makes our model similar to the CSP KO mice and *Drosophila*. Behavioural and phenotypic assays were performed on this mutant strain.

CSP knockout mutants in mice and flies exhibit lethargy and show irregular locomotion (Zinsmaier et al., 1994, Fernandez-Chacon et al., 2004). This could be analyzed in worms in two ways:

(i) body bends on agar - number of times the worm makes a sinusoidal movement on agar plates per minute,

(ii) thrashing - similar to body bends but performed in solution. Both these assays give an accurate read out of the locomotion rates of worms.

Thrashing assays were performed on the *dnj-14(ok237)* worms and it was shown to have a significantly ($P<0.01$) reduced locomotion rate as compared to the wild-type N2 (Figure 3.2A). This was similar to what was seen in CSP knockouts in mice suggesting conservation in CSP function.

CSP knockout flies and mice also exhibited defects in neurotransmitter release (Umbach et al., 1994, Zinsmaier et al., 1994, Fernandez-Chacon et al., 2004, Chandra et al., 2005). Although this can be analysed in worms by performing electrophysiological experiments using patch-clamp, this is a very difficult technique. However an indirect method exists where in pre-synaptic neurotransmission can be analysed in worms using an acetylcholinesterase inhibitor called aldicarb (Mahoney et al., 2006). This assay is based on the paralyzing effects of aldicarb. The regulatory cholinesterase is blocked at the synapse and hence in wild-type worms, there is an increased calcium influx in the post synaptic regions leading to paralysis. Worms exhibiting defects in neurotransmission show increased resistance to aldicarb and hence paralyze later compared to the wild-type and are known to exhibit a 'Ric' (resistance to inhibition by cholinesterase) phenotype. Worms with elevated levels of neurotransmission paralyze quickly and exhibit a 'Hic' (hypersensitive to inhibition by cholinesterase) phenotype. In order to ascertain whether the *dnj-14* mutants have a neurotransmission phenotype similar to flies and mice, aldicarb assay was performed. It was observed that the *dnj-14(ok237)* mutants had a defect in the release of acetylcholine as shown in Figure 3.2B. The *dnj-14(ok237)* mutants had a 'Ric' phenotype that was found to be significant ($P<0.05$).

In flies and mice, the locomotion and the neurotransmission defect

corresponded to an eventual increase in mortality and the animals died prematurely. Hence, the survival of the *dnj-14(ok237)* mutants was then analysed (Figure 3.3A) to check if it replicated the fly and the mouse models. The *dnj-14(ok237)* worms showed a significant decrease in the lifespan compared to the wild type N2 (mean lifespan in days of adulthood with SEM: N2=19.28 ± 0.34, *dnj-14(ok237)*: 15.60 ± 0.35).

Mutations in *C. elegans* are usually obtained by the use of either chemical reagents or radiation. Due to this there could be background mutations elsewhere in the mutant worms' genome which could interfere with the phenotypes observed. To eliminate these, the worms have to be outcrossed against the wild-type several times. The *dnj-14(ok237)* strain was then outcrossed six times using the wild-type male worms. Once the strain was outcrossed, lifespan assays were performed and it was found that the reduction in the lifespan of the *dnj-14(ok237)* mutants still persisted (Mean lifespan in days of adulthood with SEM: N2=18.99 ± 0.54; *dnj-14(ok237)* OC=15.19 ± 0.56) (Figure 3.3B). All further experiments were performed using these outcrossed strain unless otherwise mentioned.

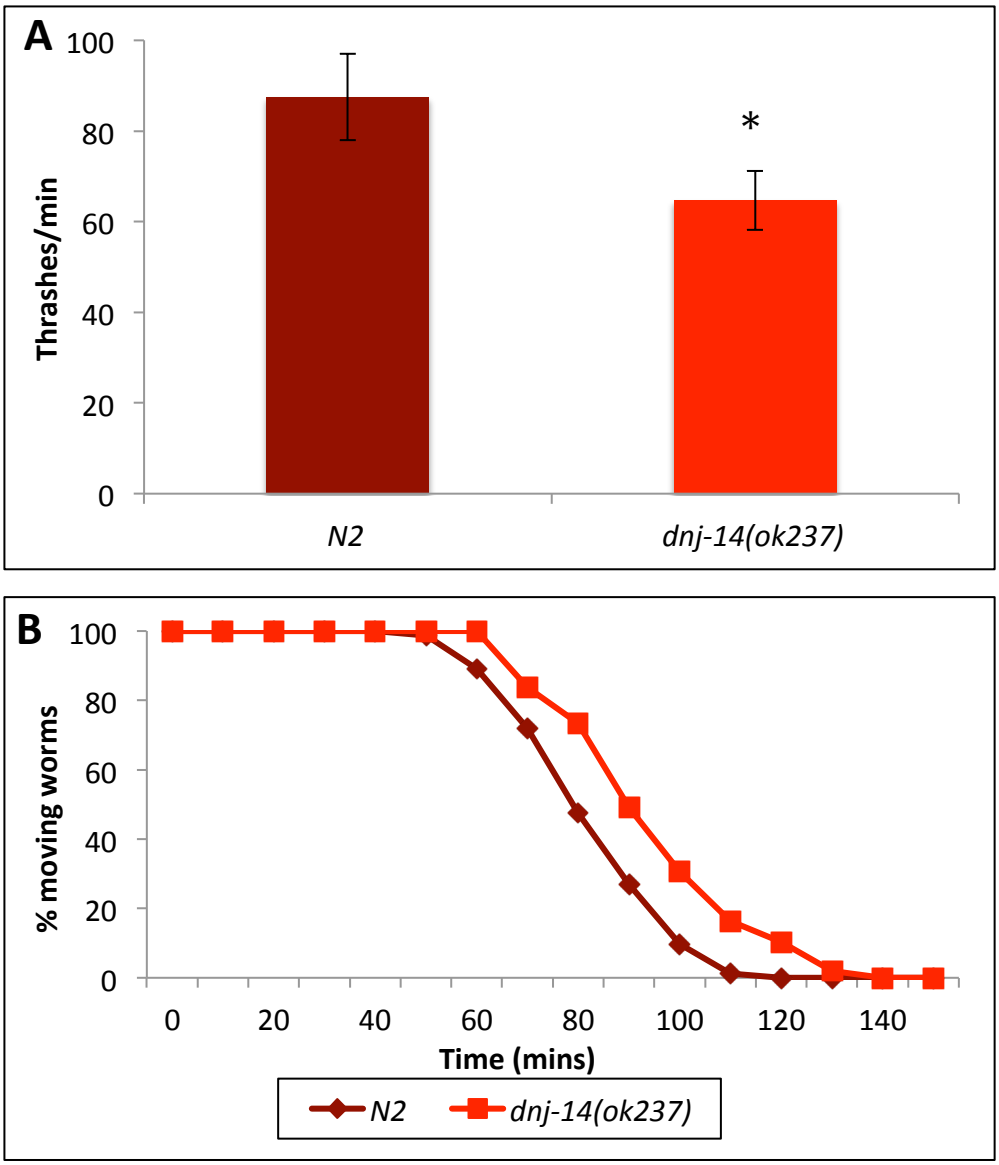

Figure 3.2: The *dnj-14(ok237)* mutant has lower locomotion and neurotransmission defect: A) Shows thrashing assays performed on the *dnj-14(ok237)* mutants with the wild-type N2 as control. Worms were age synchronized to day 5 of adulthood and placed in a drop of Dent's Ringer solution. The number of times the worm makes a complete sinusoidal movement per minute was counted. It can be seen that the *dnj-14(ok237)* mutant has a significantly lower thrashing rate compared to the wild-type N2. Above represented are pooled data from three independent biological replicate studies. Mean thrashing rate: N2=87.52 ± 9.54; *dnj-14(ok237)*=64.65 ± 6.49. n=55 for both strains. Student's t-test was used to calculate significance and $P<0.01$ was considered to be significant (*). B) Shows aldicarb assay performed on the *dnj-14(ok237)* mutant with wild-type N2 as control. Aldicarb assay is an indirect read-out of neurotransmission in worms. 20-25 worms were age synchronized to day 5 of adulthood and placed on plates containing 1mM aldicarb. The worms paralyze over time and the number of worms moving after every ten minutes are noted till all of the worms paralyze. As it can be seen, the *dnj-14(ok237)* worms are significantly resistant compared to the wild-type N2. Mean paralysis times: N2=84.51 ± 1.61 (n=82); *dnj-14(ok237)*=96.53 ± 1.88 (n=98). Above represented are pooled data from four independent biological replicate studies. Log-Rank test was used to calculate significance and $P<0.05$ was considered to be significant.

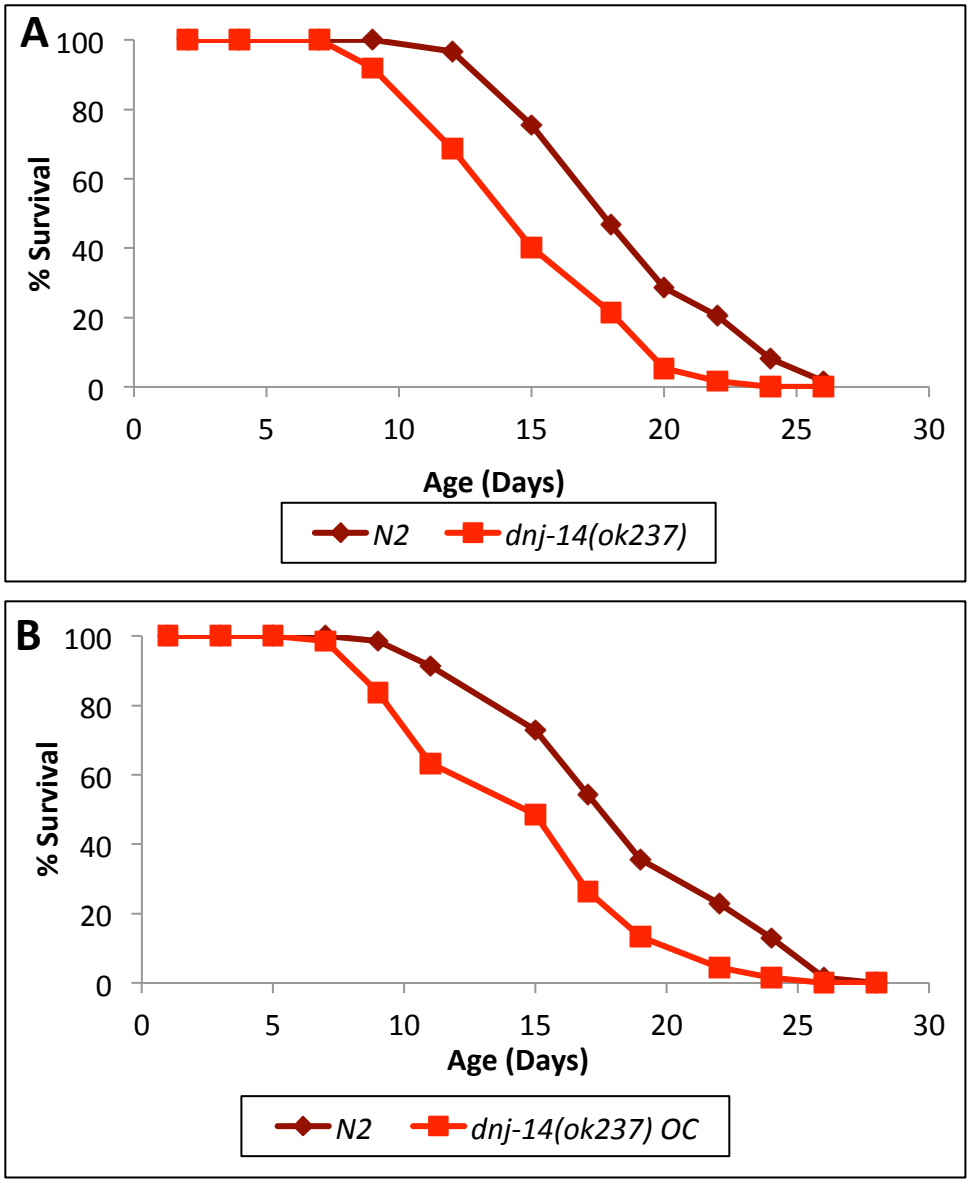

Figure 3.3: *dnj-14(ok237)* mutants have a shorter lifespan: A) Shows lifespan of *dnj-14(ok237)* mutants with wild-type N2 as control. Worms were age synchronized by letting ten worms lay eggs overnight and 25 of the progeny were transferred on to seeded NGM plates. Worms were monitored every alternate day and transferred to fresh plates to prevent progeny formation. It can be seen that the lifespan of *dnj-14(ok237)* mutants is significantly lower than the wild-type N2. Above represented are pooled data from five independent biological replicate studies. Mean lifespan in days of adulthood: N2=19.28 ± 0.34 (n=122); *dnj-14(ok237)*=15.60 ± 0.35 (n=112). Log Rank test was used to calculate significance and $P<0.05$ was considered to be significant. B) Shows lifespan of six times outcrossed *dnj-14(ok237)* mutants compared with the wild-type N2 as control. Similar to the non-outcrossed strain, the outcrossed *dnj-14(ok237)* mutants also have a significant reduction in survival. Above represented are pooled data from five independent biological replicate studies. Mean lifespan in days of adulthood: N2= 18.99± 0.54 (n=70); *dnj-14(ok237)*= 15.19 ± 0.56 (n=68). Log Rank test was used to calculate significance and $P<0.05$ was considered to be significant.

3.3.2 ANALYSIS OF THE SECOND ALLELE

The *dnj-14(ok237)* worms showed a phenotype that was similar to the CSP KO mice as observed from earlier studies. There was a reduction in mean lifespan of the animals and a reduction in locomotion. A reduction of neurotransmitter release was also seen in the presence of an acetylcholinesterase inhibitor, aldicarb. However, in the *ok237* allele mentioned above, the deletion in *dnj-14* extended up to the adjacent *glit-1* gene (Figure 3.1A), which encodes a carboxyesterase. The *glit-1* gene is known to maintain a blood-nerve barrier in *Drosophila* (Auld et al., 1995), however, knowledge about the nematode protein is very limited. Hence, a second mutant where the mutation was specific to *dnj-14* alone was obtained from the Mitani Lab, Tokyo. The *tm3223* mutation was analysed prior to the performance of phenotypic assays. The mutation was sequenced using PCR amplification and it was found that the deletion in the *tm3223* allele began immediately after the J-domain of DNJ-14 (Figure 3.4A and C) leading to an early truncation. Thus as shown in Figure 3.4C, the truncated protein, if actively expressed in the worm, would only contain the J-domain. Hence, not only can this mutant be used to determine the specificity of the previously mentioned phenotypes to *dnj-14* but might also be used for structure-function assays.

To ascertain whether the phenotype in the *dnj-14(ok237)* strain is specific to the deletion in *dnj-14* or an artefact of concomitant loss of *glit-1*, phenotypic assays were performed on the *dnj-14(tm3223)* strain. It was found that the *dnj-*

14(tm3223) mutants show a reduction in locomotion and reduction in neurotransmitter release on inhibition by aldicarb (Figure 3.5A and B).

Lifespan assays were then performed on the *dnj-14(tm3223)* worms (Figure 3.6A) and it was found that similar to the *dnj-14(ok237)* mutants, the *dnj-14(tm3223)* mutants also had a significant reduction in lifespan (Mean lifespan in days of adulthood with SEM: N2=18.44 ± 0.5; *dnj-14(tm3223)*=15.02 ± 0.5). These mutants were then outcrossed five times by successively crossing them with wild-type N2 males to eliminate background mutations. Subsequently, lifespan assay was performed (Figure 3.6B) and it was found that the *dnj-14(tm3223)* mutants still exhibited a significant higher mortality compared to the wild-type N2 and this was comparable to the non-outcrossed mutants (Mean lifespan in days of adulthood with SEM: N2=19.68 ± 0.41; *dnj-14(tm3223)* OC=15.59 ± 0.44). All these results suggest that the *dnj-14(tm3223)* mutants are a phenocopy of *dnj-14(ok237)* mutants. Hence, it can be concluded that the phenotype of the knockout (*dnj-14(ok237)*) mutant is specific to the lack of DNJ-14 and not GLIT-1.

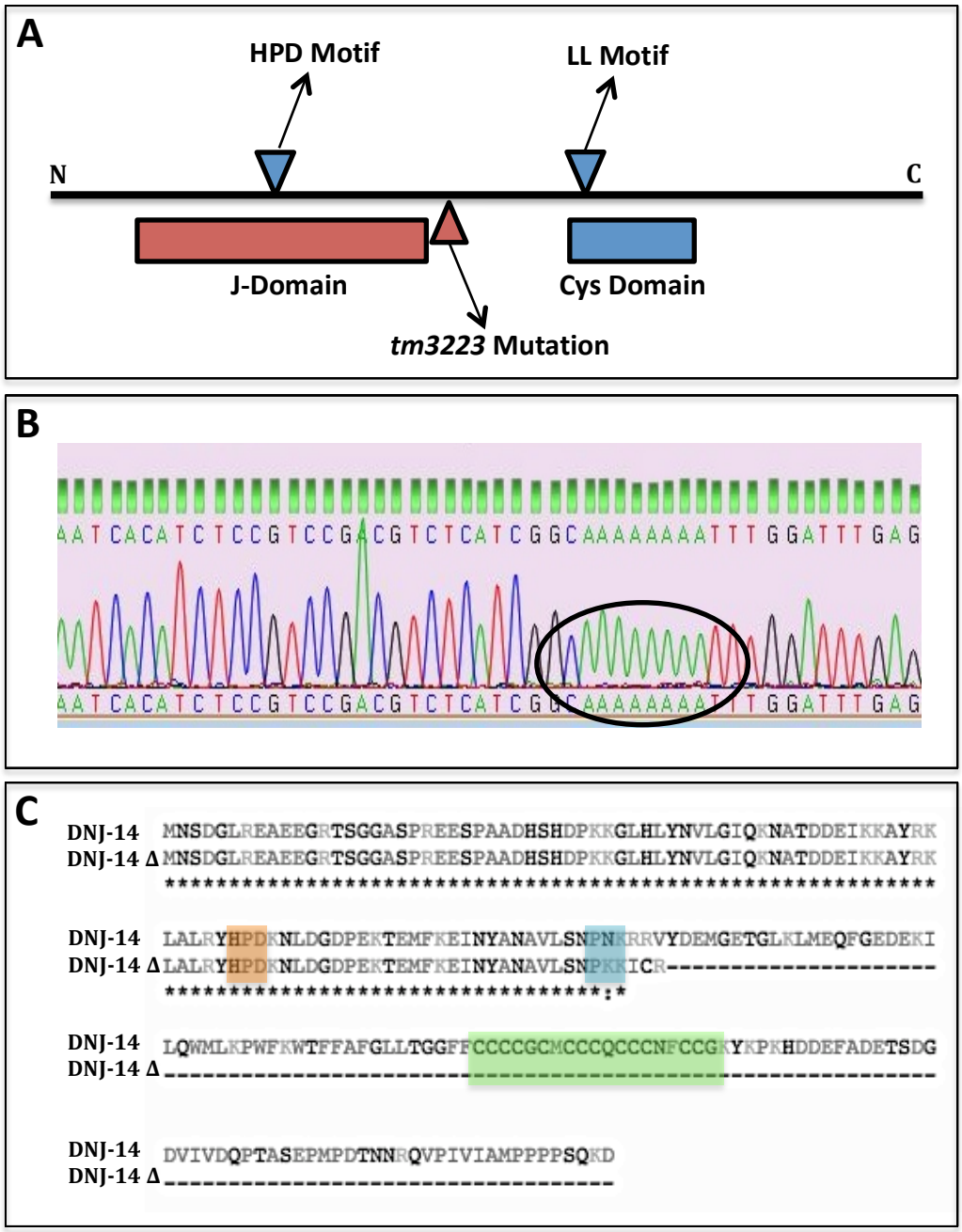

Figure 3.4: Analysis of the *tm3223* mutation: A) Shows the secondary structure of DNJ-14 with the positions of the conserved motifs along with the mutation site in the *tm3223* allele. B) Shows the DNA chromatogram of the mutation site in *tm3223* allele confirming the addition of 5 adenine residues instead of the 3 adenine residues mentioned in wormbase. C) Shows the alignment of the putative sequence of the truncated protein against the wild-type DNJ-14 protein. As shown in the figure, the protein gets truncated just after the J-domain.

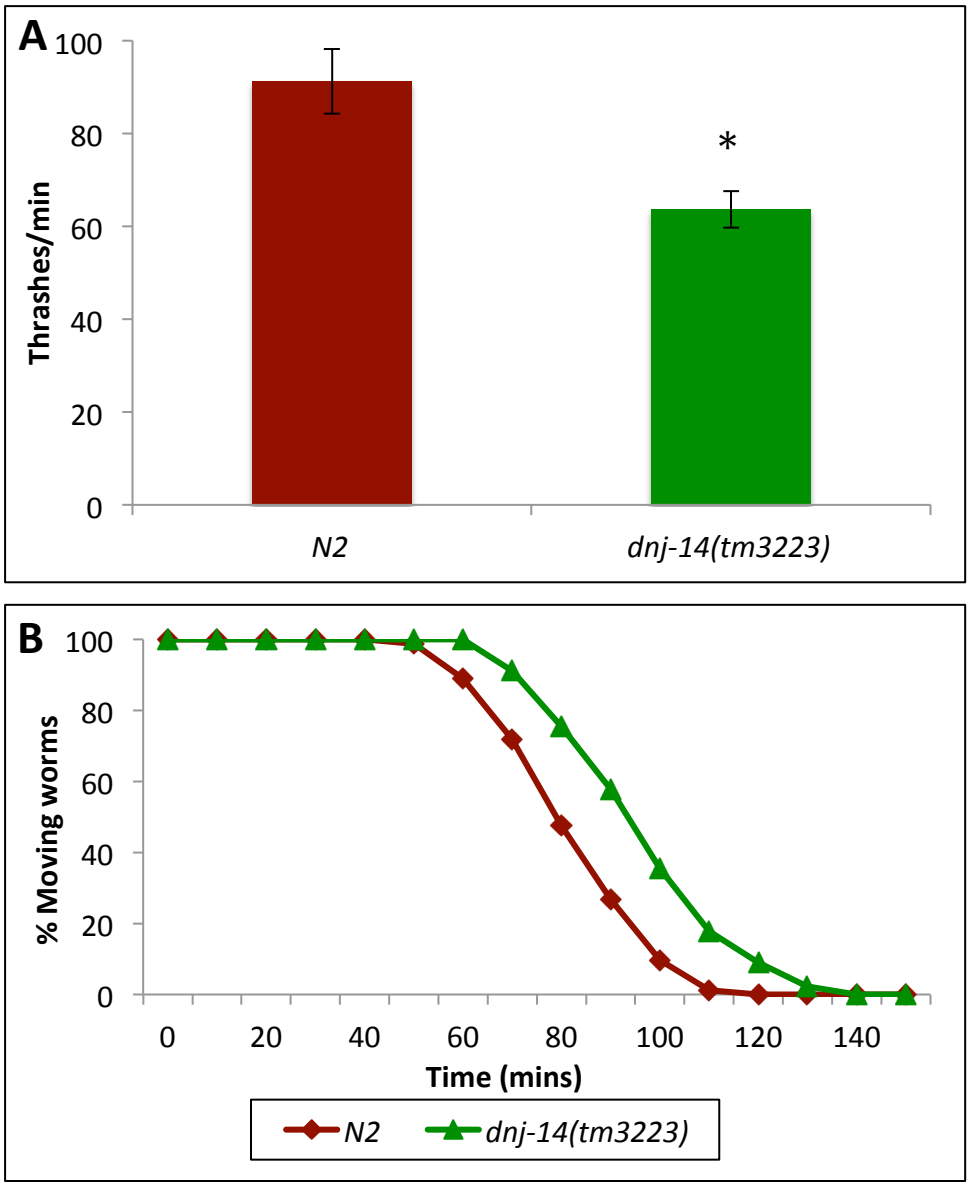

Figure 3.5: The *dnj-14(tm3223)* mutant has reduced locomotion and neurotransmission: A) Shows thrashing assays performed on the *dnj-14(ok237)* mutants with the wild-type N2 as control. The experiment was performed as explained earlier. It can be seen that the *dnj-14(tm3223)* mutant has a significantly lower thrashing rate compared to the wild-type N2. Above represented are pooled data from two independent biological replicate studies. Mean thrashing rate: N2=91.24 ± 7.01; *dnj-14(ok237)*=63.64 ± 3.96. n=35 for both strains. Student's t-test was used to calculate significance and P<0.01 was considered to be significant (*). B) Shows aldicarb assay performed on the *dnj-14(ok237)* mutant with wild-type N2 as control. The experiment was performed as explained before. As can be seen, the *dnj-14(tm3223)* worms are significantly resistant compared to the wild-type N2. Mean paralysis times: N2=84.51 ± 1.61 (n=82); *dnj-14(ok237)*=98.89 ± 1.85 (n=90). Above represented are pooled data from four independent biological replicate studies. Log-Rank test was used to calculate significance and P<0.05 was considered to be significant.

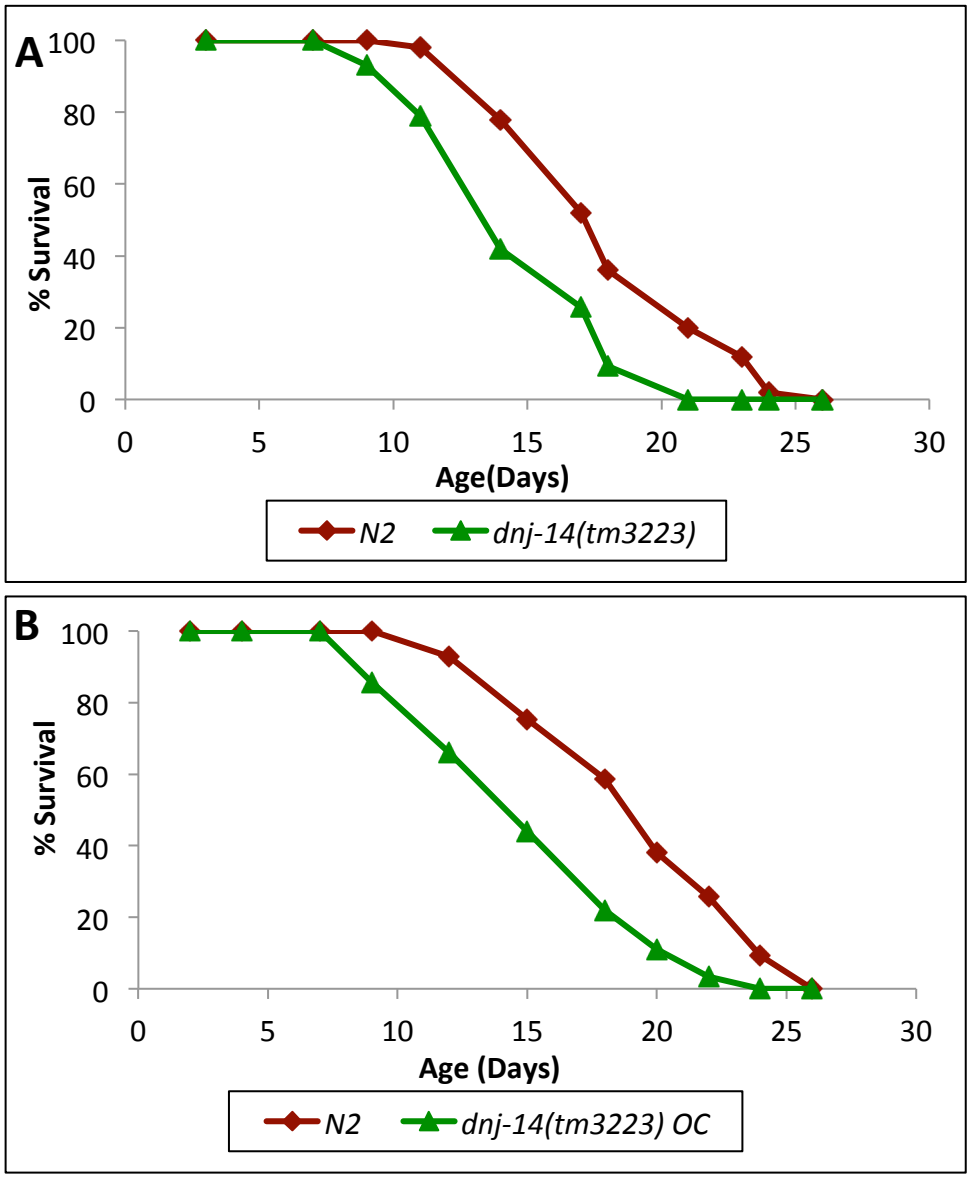

Figure 3.6: *dnj-14(tm3223)* mutants have a shorter lifespan: A) Shows lifespan of *dnj-14(tm3223)* mutants with wild-type N2 as control. The experiment was performed as explained before. It can be seen that the lifespan of *dnj-14(tm3223)* mutants is significantly lower than the wild-type N2. Above represented are pooled data from two independent biological replicate studies. Mean lifespan in days of adulthood: N2=18.44 ± 0.5 (n=50); *dnj-14(tm3223)*=15.02 ± 0.5 (n=43). Log Rank test was used to calculate significance and $P<0.05$ was considered to be significant. B) Shows lifespan of five times outcrossed *dnj-14(tm3223)* mutants compared with the wild-type N2 as control. Similar to the non-outcrossed strain, the outcrossed *dnj-14(tm3223)* mutants also have a significant reduction in survival. Above represented are pooled data from five independent biological replicate studies. Mean lifespan in days of adulthood: N2= 19.68 ± 0.41 (n=97); *dnj-14(tm3223)*= 15.59 ± 0.44 (n=91). Log Rank test was used to calculate significance and $P<0.05$ was considered to be significant.

3.3.3 NEURODEGENERATION

The *dnj-14(ok237)* mutants were next examined to see if they exhibited age-dependent presynaptic neurodegeneration as seen in CSP KO mice and flies. The worms were injected with an extra chromosomal array containing *gfp* driven by a *rab-3* promoter. RAB-3 is a pan neuronal protein and hence all neurons expressing RAB-3 would also express EGFP and emit fluorescence observable using a fluorescent microscope. It has been shown in previous studies that loss of GFP signal or even abnormal GFP expression in neurons could be considered as signs of neurodegeneration (Nass et al., 2002, Locke et al., 2008). Neurons were scored to be degenerating when at least one of the degenerating changes such as dendrite blebbing, loss of cell body, cell body rounding and/or loss of processes was seen (Locke et al., 2008). The results are shown in Figure 3.7 A and quantified in Figure 3.7 B. The mutant worms had clear punctate appearance on the nerve cords (65.9%) as a result of either blebbing of dendrites or rounding of cell bodies or both. In the wild-type, a relatively lower number of worms showed punctate appearance (28.57%). This phenotype was termed as puncta phenotype.

However, the *dnj-14* mutants showed unusual expression of EGFP (70.54%). These worms showed morphological differences in the expression of EGFP in the head. There were loss of cell bodies and processes along the head. There was also an overall reduction in the intensity of GFP observed in the head (not

quantified). A smaller snout was also observed in the mutants compared to the wild-type. In the control, however, only about 8% had this unusual phenotype. This phenotype was termed as the abnormal snout phenotype. However, due to the pan-neuronal expression of GFP, it would be very difficult to identify which neurons were affected. Thus, the assay needs to be repeated using promoters specific to the different neurons in the head to give a clear indication as to where when the neurons in the head are being degenerated.

UNC-25 is the *C. elegans* homologue of the GABA neurotransmitter biosynthetic enzyme, glutamic acid decarboxylase (GAD). *unc-25* activity is essential for GABA synthesis and thus is expressed in all GABAergic neurons (Jin et al., 1999). More importantly, the *unc-25* promoter driven GFP marker was found to be a very efficient in observing neurodegeneration at the nerve cord. Hence the *dnj-14(tm3223)* worms were crossed into a CZ1200 strain, which has *gfp* expressed in the GABA neurons, to obtain *dnj-14(tm3223)* worms expressing GABAergic *gfp*. This expression helped in the observation of neurodegeneration in the nerve cords as gaps which were wide enough to quantify (Liachko et al., 2010). The worms were imaged at day 15 of adulthood and surprisingly, no loss of GFP was observed in the *dnj-14* mutants compared to the CZ1200 strain as control (Figure 3.8). This would suggest that the GABA system in the *dnj-14* worms remains unaffected and so the neurodegeneration in these mutants could be attributed to the loss of a different set of neurons but not GABAergic.

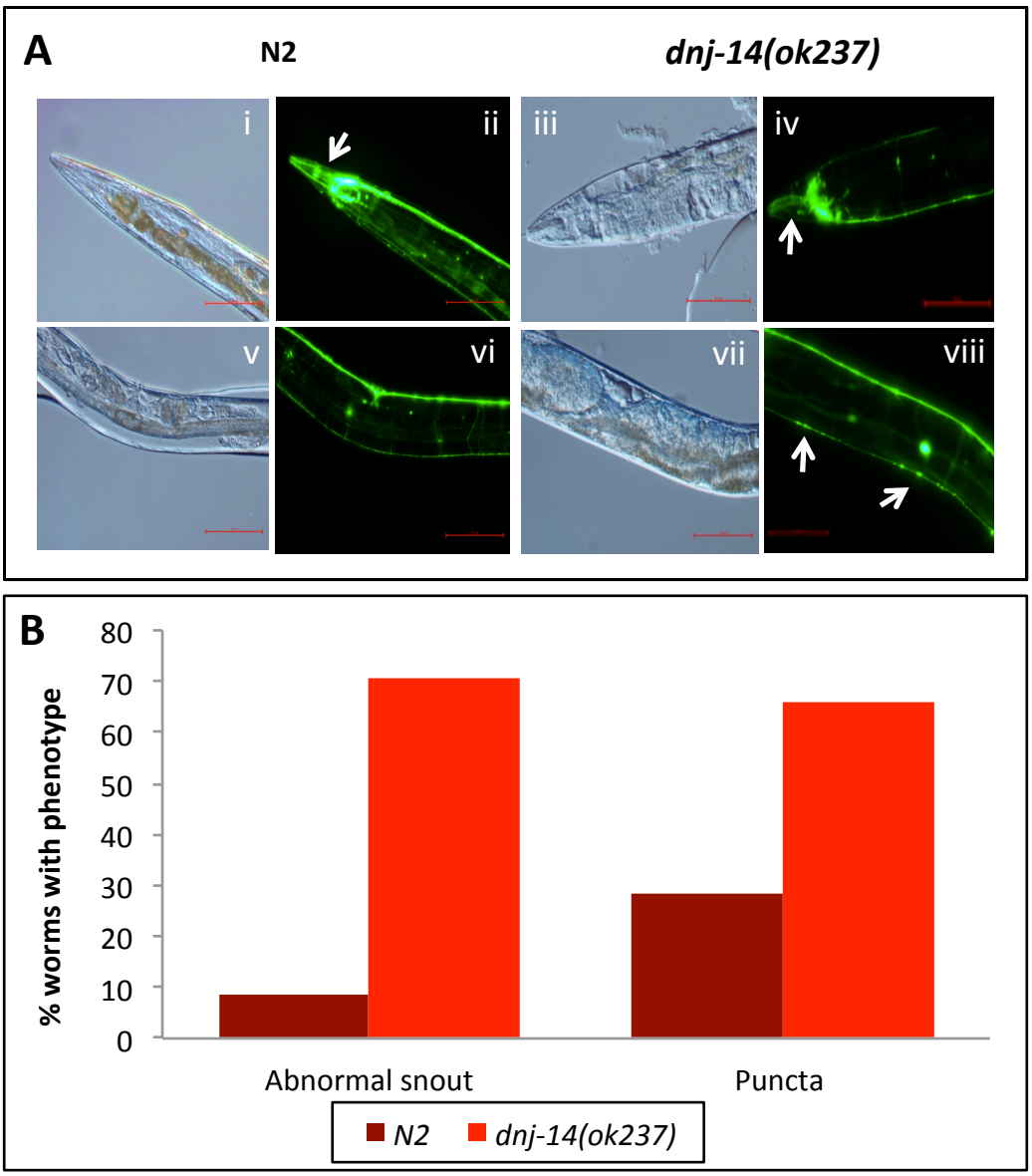

Figure 3.7: Neurodegeneration in *dnj-14(ok237)* mutants and quantification: A) N2 worms were injected with a plasmid construct expressing GFP driven by a pan-neuronal *rab-3* promoter. GFP expressing *dnj-14(ok237)* were obtained by crossing them with the transgenic N2. All worms were age synchronized and imaged at days 3, 9 and 15 of adulthood. The images shown are of 15 day old worms. All worms were immobilized in 20:20 PEG20,000:Glycerol in PBS and the images were captured using a fluorescent microscope. Images were processed using the software NIS Elements. As it is clearly seen, the *dnj-14* mutants show loss of neurons in the head (arrow heads in iv) and punctae along its nerve cords (viii). This is absent in the wild-type N2 as shown in panels (ii) and (vi). B) Shows quantification of the above mentioned data. N2: n=35, worms showing neurodegeneration=3; *dnj-14(ok237)*: n=44, worms showing neurodegeneration: 31. Scale= 50µm.

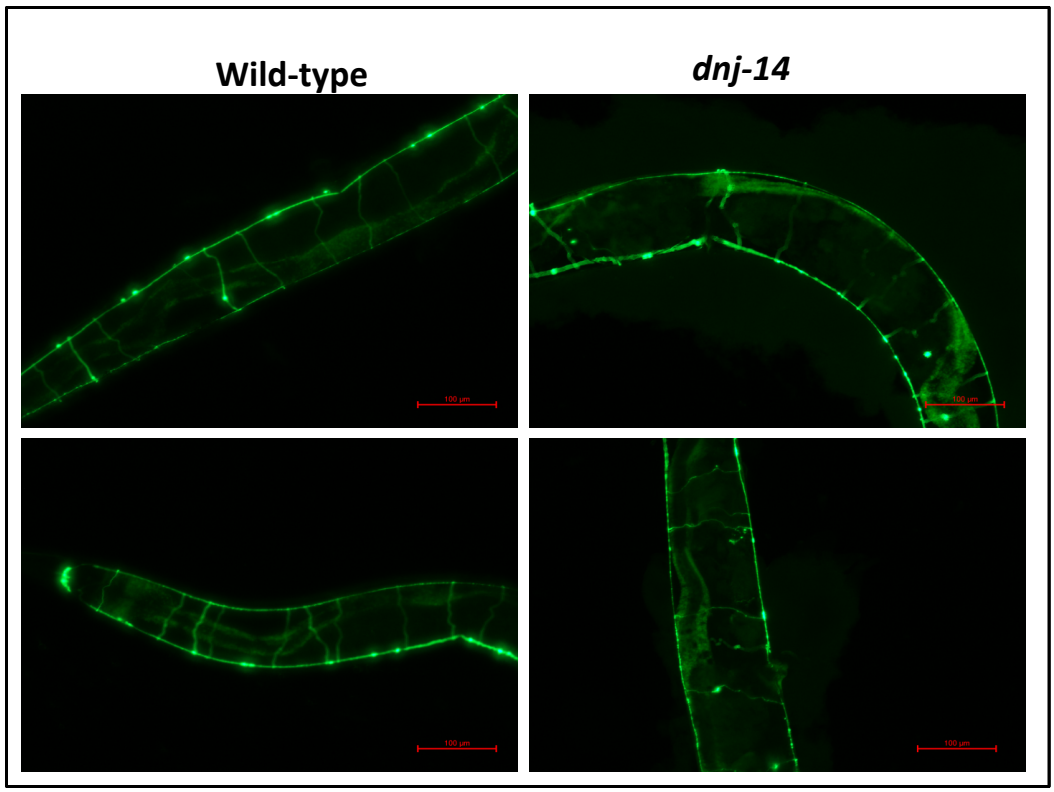

Figure 3.8: GABAergic neurons remain unaffected in *dnj-14* mutants: Shows the GABAergic *gfp* expression in the wild-type N2 and *dnj-14(ok237)* worms. CZ1200 strain of worms having wild-type *unc-25* expression were crossed with the *dnj-14(ok237)* mutants and the resulting homozygous progeny was age synchronized and imaged as explained before. The representative images shown are of worms aged day 15 of adulthood. It can be seen that there is no difference in the expression pattern of *gfp* in between the wild-type N2 and the *dnj-14(ok237)* mutants. Hence it can be inferred that there is no loss of GABAergic neurons in *dnj-14* mutants. N=10 for both strains.

3.3.4 NEURODEGENERATION CORRESPONDS TO CHEMOSENSORY DEFECTS

With the possibility of degeneration of GABAergic neurons ruled out, the *gfp* expression pattern in the head of the *dnj-14 worms* was observed more closely. In Figures 3.7, it can be seen clearly that the loss of neurons in the head appears to be concentrated towards the inner and outer labial regions of the worm pharynx. Therefore, these affected neurons could be the ones involved in pharyngeal pumping. Hence, pharyngeal pumping assays were performed on mutant worms aged day 6 of adulthood. Experiments could be performed at a later age, but the mutant worms would become more lethargic when old making the results incomparable with the wild type, which moves without signs of lethargy even at a later age. On performing the pharyngeal pumping assay (Figure 3.9 A), it was found that the mutant worms pump in a manner similar to that of the wild-type N2 and these results were deemed insignificant. Hence, proving that the neurons degenerating in the worms were not the ones involved in normal pharyngeal pumping.

The other possible set of neurons in the region where abnormal *gfp* expression was seen included the OLL, OLQ, IL1 and IL2 neurons as shown in the cartoon (Figure 3.10). OLL, OLQ and IL1 neurons are mechanosensory in nature (Kaplan and Horvitz, 1993, Hart et al., 1995, Goodman, 2006) thus nose touch assays were performed on worms at day 6 of adulthood (Figure 3.9 B). As before, we saw no significant change in the response of the mutant as compared to the

wild type. This suggested that at day 6, the mechanosensory apparatus functions normally. However, the possibility that the mechanosensory neurons might degenerate in the later stages of life still exists. This degeneration could not be examined as the *dnj-14* mutants exhibit uncoordinated movement in the later stages of their lifespan. With the mechanosensory neurons namely, OLL, OLQ and IL1, ruled out, IL2 neurons were the only other potential neuronal type that could be degenerating. IL2 neurons are known to be chemosensory in nature (Bargmann et al., 1993, Shaham, 2010) and are 6 in number. They are present in the inner labial region of the anterior pharyngeal bulb. Due to the involvement of these neurons in chemosensation, chemosensory assays like food race and chemotaxis assays were performed on the *dnj-14* worms again at day 6 of adulthood. It was found that both the *dnj-14* mutants were defective in sensing the food and hence took a longer time as compared to the wild-type N2 to reach the food on an NGM plate (Figure 3.11 A and B). This phenotype was also found to be age dependent with worms aged 3 days reaching the food in a more effective way compared to the worms aged 6 and 9 days. Wild type worms of all ages reached the food with insignificant or no time lag (Figure 3.12).

Similarly, chemotaxis assays were performed and *dnj-14* mutants were chemotaxis variant for three drugs namely, 2,3-buteine-di-one, nonenone and isoamyl alcohol (Figure 3.13 A). The effect of isoamyl alcohol was mild but

significant and also consistent with successive repeats. Hence this drug was used for further experiments (Figure 3.13 B). The effect of isoamyl alcohol was observed over different ages and as in the case of food race assays this effect was observed to be dependent on age (Figure 3.14). The worms aged 3 days had very little or insignificant difference in the chemotaxis index as compared to the wild-type. However, the worms aged 6 and 9 days had significantly reduced chemotaxis indices compared to the wild type. Again, the wild-type N2 showed very little difference in chemotaxis index over age. These experiments suggested a direct correlation between the neurodegeneration seen before and the chemosensory defects explained above. This would mean that in the *dnj-14*, the chemosensory defects seen at day 6 of adulthood, manifests itself as neurodegeneration once the worm reaches ages beyond day 11.

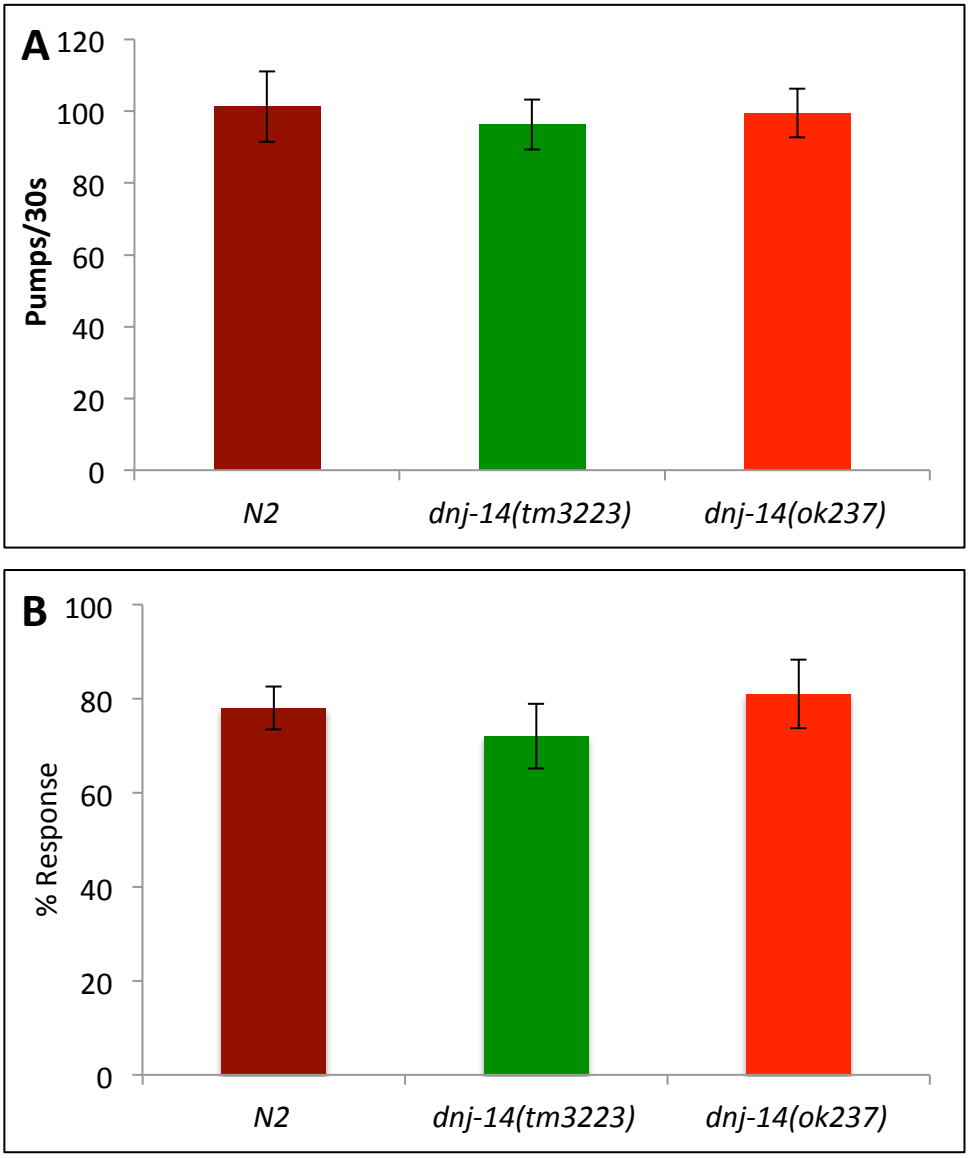

Figure 3.9: Normal pharyngeal pumping and nose touch response in *dnj-14*: A) Shows a pilot screen for pharyngeal pumping in *dnj-14* mutants. Worms were aged to day six of adulthood and placed on a fresh NGM plate and viewed under 80X magnification. The number of times the worms' pharyngeal girder made a complete to and fro motion was counted for 30 seconds. As it can be seen from the figure, the pharyngeal pumping rate for both the *dnj-14* mutants are similar to the wild-type N2. Mean pumping rate per 30 seconds: N2=101.3; *dnj-14(tm3223)*=96.3; *dnj-14(ok237)*=99.5. B) Shows nose touch response of day six animals. Age synchronized worms were placed on an unseeded NGM plate and its movement was obstructed by placing an eyelash perpendicular to the worms' movement. Normal response would be to retract back. Each worm was analyzed ten times and it can be seen that the *dnj-14* mutants respond in a similar manner to the wild-type N2. Mean response rate in percentage: N2=78; *dnj-14(tm3223)*=72; *dnj-14(ok237)*=81. n=15 for both experiments.

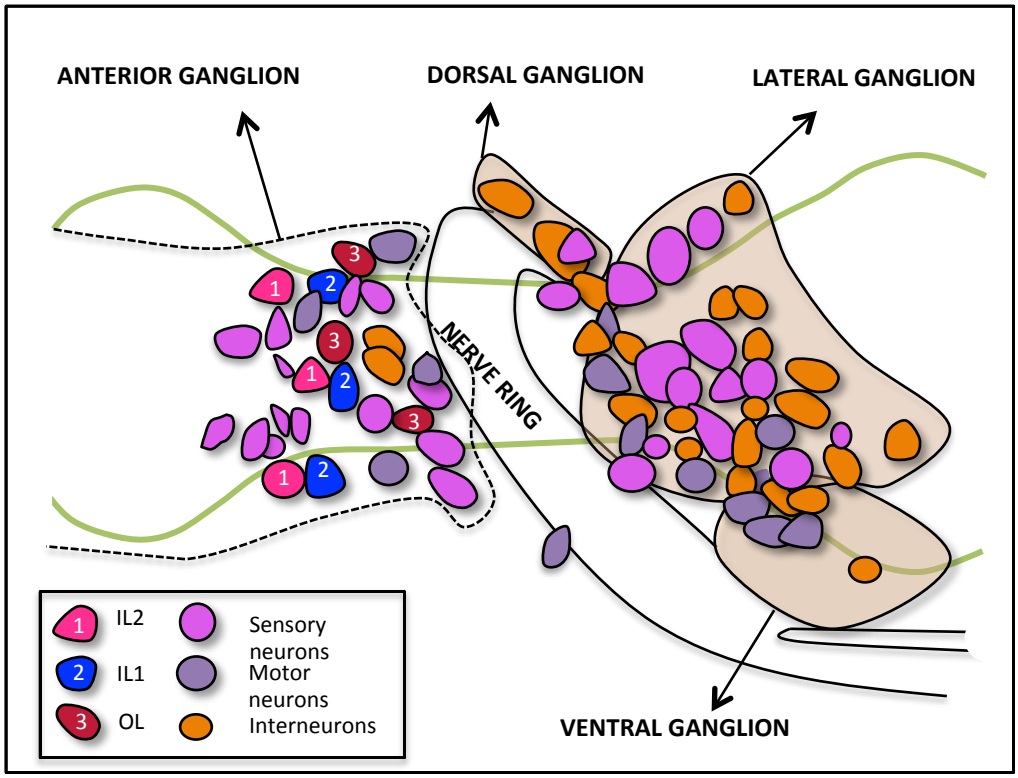

Figure 3.10: Lateral section showing the neuronal cell bodies in the worm's head: Shows the distribution of neuronal cell bodies in the head region of *C. elegans.* Highlighted in pink, blue and red are the IL2, IL1 and the OL neurons which could potentially be the degenerating neurons in *dnj-14* mutants. These are six in number and only three are seen in the lateral section shown in the figure. IL2 neurons are known to be chemosensory while the IL1 and the OL neurons are known to be mechanosensory.

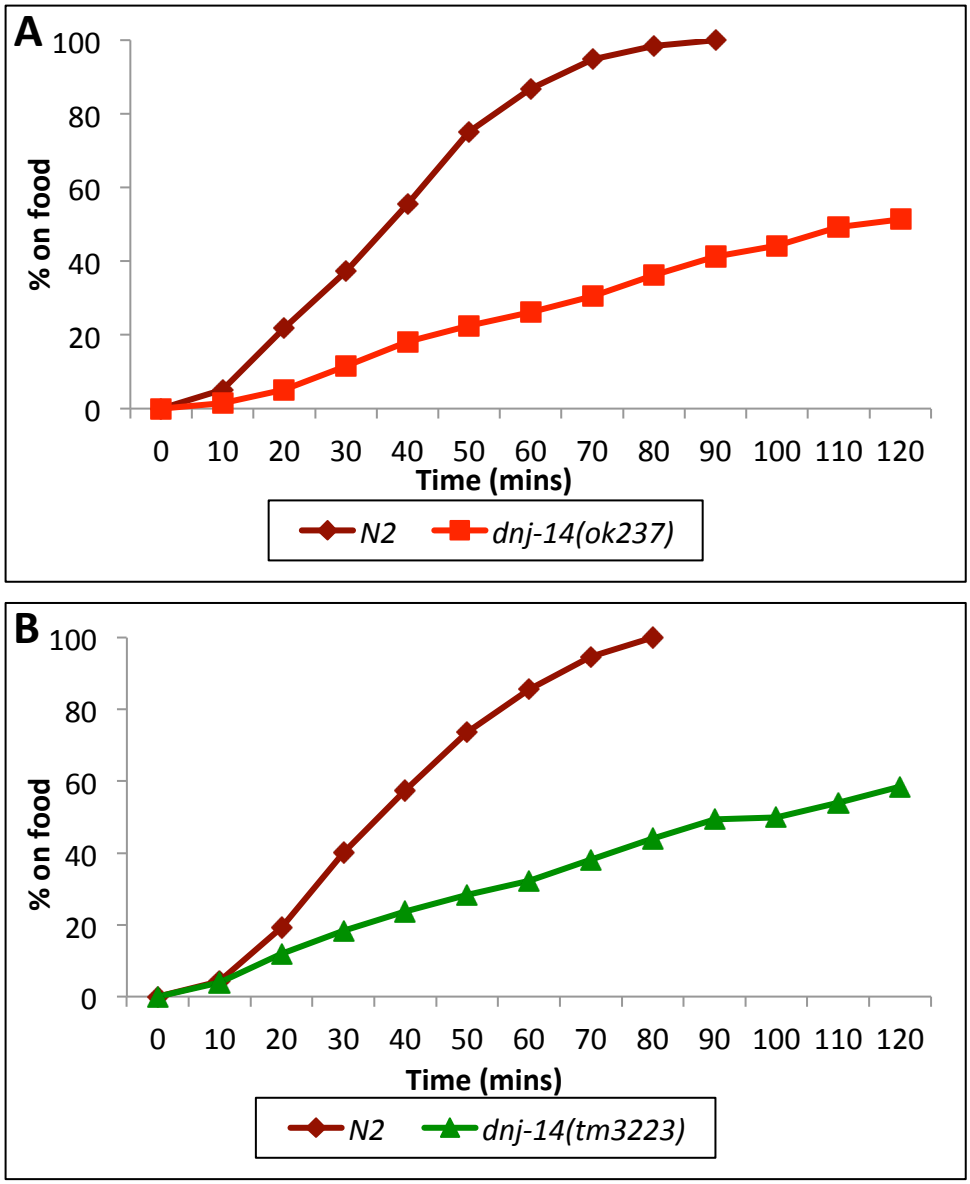

Figure 3.11: Both the *dnj-14* mutants exhibit food sensing defects: A) and B) Shows food race assay performed individually on both the *dnj-14* mutants with wild-type N2 as control. 20-25 worms were washed in M9 buffer and placed on the corner of an NGM plate with 30µL of OP50 on the opposite corner. Worms reaching the food every 10 minutes were noted down till 120 minutes. It can be seen that both the *dnj-14* mutants have an inability in reaching the food source compared to the wild-type N2. This was found to be significantly different from the wild-type N2. Above represented are pooled data from five and six independent biological replicate studies for A) and B) respectively. Mean time taken to reach food (mins): A) N2: 42.48 ± 1.61 (n=137); *dnj-14(ok237)*=91.38 ± 3.04 (n=138); B) N2=42.51 ± 1.43 (n=167); *dnj-14(tm3223)*=84.61 ± 3.19 (n=152). Log-Rank test was used to calculate significance and $P<0.05$ was considered to be significant.

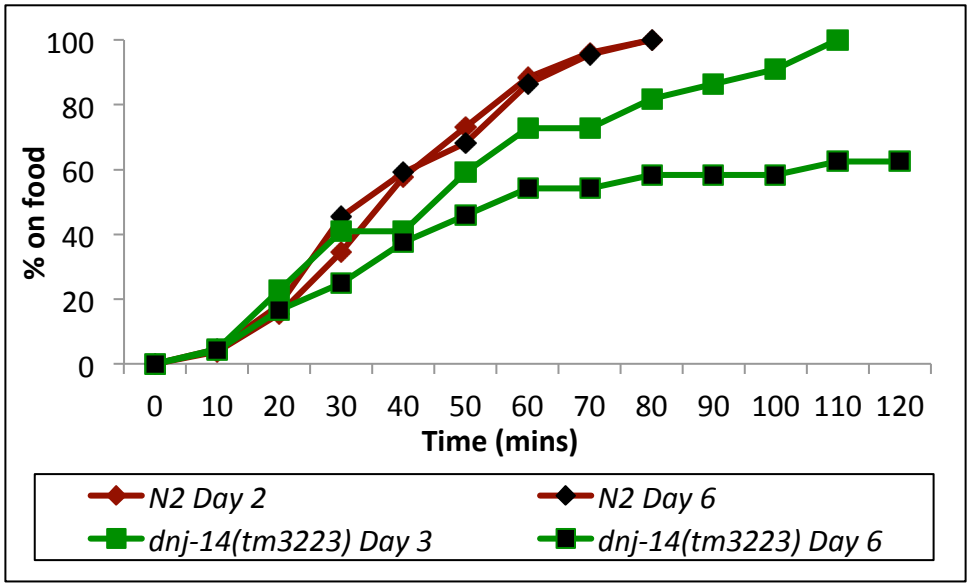

Figure 3.12: Age-dependent decline in food sensing ability of *dnj-14:* Shows age-dependency of *dnj-14(tm3223)* in sensing food in a food race assay. The experiment was performed as explained earlier. It can be seen that at day 3 of adulthood, *dnj-14(tm3223)* worms are superficially wild-type and its food sensing ability is comparable to the wild-type N2 ($P>0.05$). As the mutants reach day 6 of adulthood, a significant decrease in the ability to sense food is observed. This however is not seen in the wild-type N2. Mean time taken to reach food (mins): N2: Day 2= 43.08 ± 3.39 (n=26), Day 6=42.27 ± 4.01 (n=22); *dnj-14(tm3223)*=52.73 ± 6.43 (n=22), Day 6=72.50 ± 8.54 (n=24). Above represented is data from a single biological study. Log-rank test was used to calculate significance and $P<0.05$ was considered to be significant.

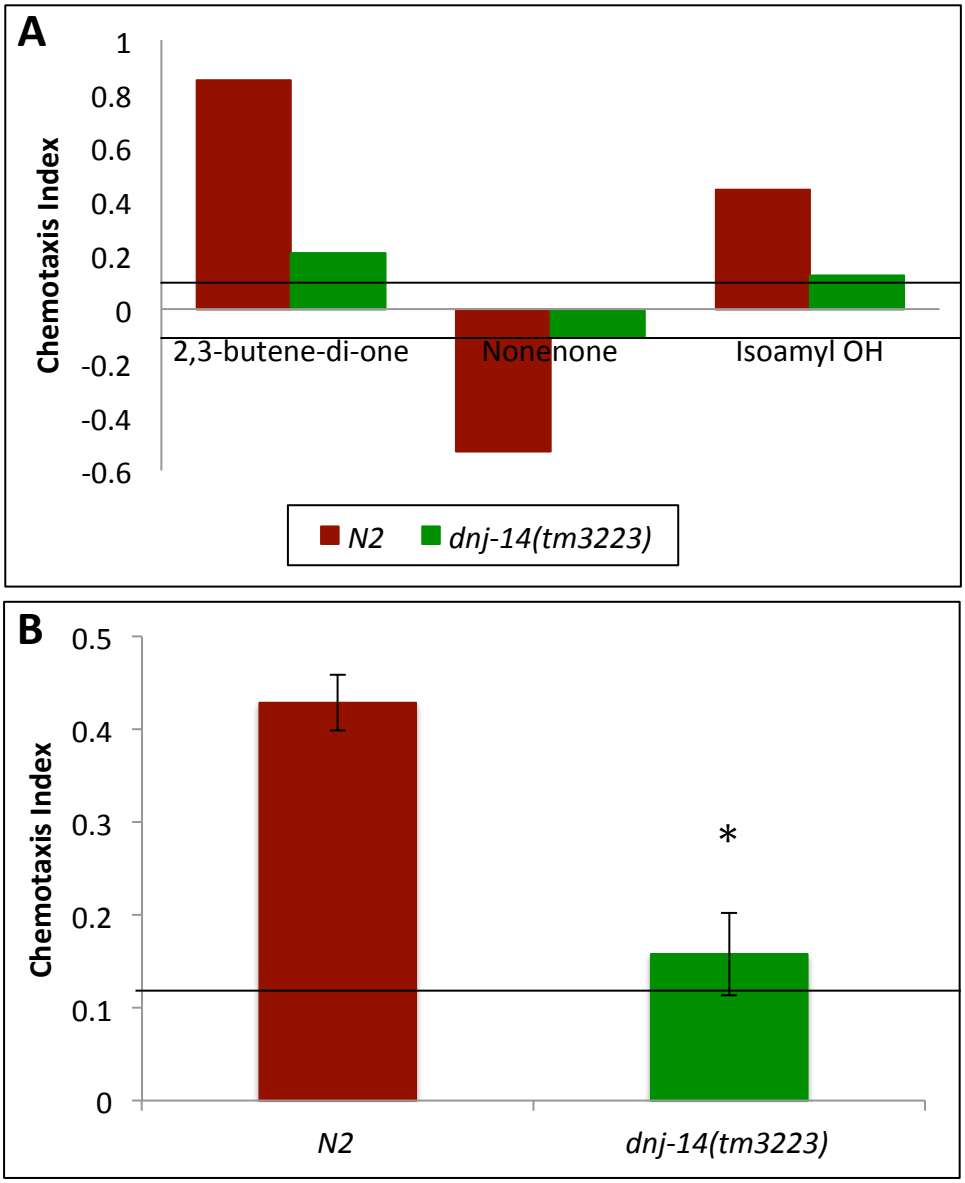

Figure 3.13: *dnj-14* mutants are chemotaxis variant to volatile solvents: A) Shows chemotaxis assays performed with 2,3-butene-di-one, nonenone and isoamyl alcohol on six day old worms. Worms were washed in M9 buffer and placed on the centre of a chemotaxis plate with 1µL of the solvent and ethanol on either side of the plate. After 90 minutes, chemotaxis index was calculated as (number of worms on drug-number of worms on control)/total number of worms. It can be seen that the *dnj-14(tm3223)* mutants are severely variant to volatile compounds. Dilutions used: 2,3-butene-di-one:10^{-4}; Nonenone: 10^{-3}; Isoamyl alcohol: 10^{-4}. Chemotaxis indices: N2: 2,3-butene-di-one=0.85 (n=20), nonenone=-0.53 (n=24), isoamyl alcohol=0.44 (n=27); *dnj-14(tm3223):* 2,3-butene-di-one=0.208 (n=24), nonenone=-0.1 (n=21), isoamyl alcohol=0.125 (n=24). B) Shows pooled chemotaxis data from five independent biological replicate studies performed with isoamyl alcohol. The experiments were performed as explained before. The mean chemotaxis index of *dnj-14(tm3223)* mutants are significantly lower than the wild-type N2. Mean chemotaxis indices: N2= 0.417 (n=148); *dnj-14(tm3223)*=0.157 (n=171). Student's t-test was performed to calculate significance and $P<0.01$ was considered to be significant (*). Chemotaxis index of 0.11 was considered baseline for false positives for both studies.

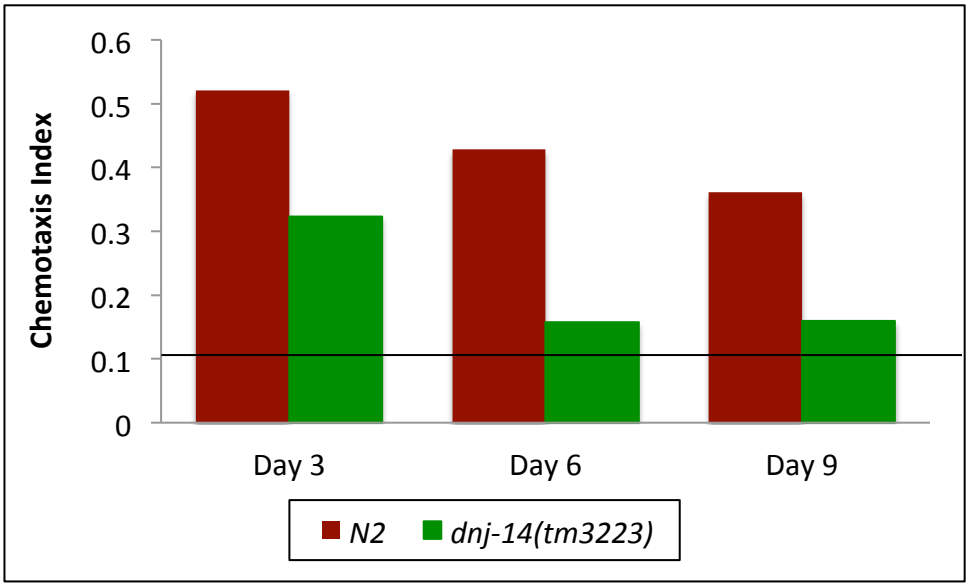

Figure 3.14: *dnj-14(tm3223)* mutants show age dependency in chemotaxis to isoamyl alcohol: Shows chemotaxis performed with isoamyl alcohol on *dnj-14(tm3223)* worms age synchronized to days 3, 6 and 9 of adulthood. It can be seen that at day 3, the *dnj-14(tm3223)* mutants have a higher chemotaxis index and this falls down with age. This indicates that the *dnj-14(tm3223)* show an age dependent decline in sensing volatile compounds. Chemotaxis indices: N2: Day 3=0.52 (n=48), Day 6=0.42 (n=35), Day 9=0.361 (n=36); *dnj-14(tm3223):* Day 3=0.323 (n=65), Day 6=0.157 (n=38), Day 9=0.159 (n=44). Chemotaxis index of 0.11 was considered baseline for false positives for both studies.

3.3.5 GENETIC RESCUE OF *dnj-14*

The above results show that the *dnj-14* mutants have age-dependent phenotypes characteristic of a neurodegenerative disease model. The next obvious step would be to rescue these phenotypes genetically by injecting the *dnj-14* gene back in to the mutants. The *dnj-14(ok237)* strain was rescued by injecting the *dnj-14* gene driven by its endogenous promoter. Pan neuronal GFP driven by *rab-3* promoter was used as a control (injections were made by Dr. James Johnson).

These worms were analysed first for lifespan and we found a significant increase in lifespan compared to the *dnj-14(ok237)* mutants and insignificant compared to the wild-type N2 (Figure 3.15A). The locomotion was also analysed by performing thrashing assays and it was found that the rescue animals thrashed less frequently than the *dnj-14(ok237)* mutant (Figure 3.15B). This could be explained since there is overexpression of *dnj-14* in the rescue animals and in flies overexpression of CSP is known to be deleterious to the animal (Nie et al., 1999). The lifespan and the locomotion experiments were performed my Mimi Ayala under my supervision.

Chemosensory assays were also performed on these animals. It was observed that the rescue animals sense the food significantly better than the mutants in a food race assay (Figure 3.16 A). Also, in chemotaxis to isoamyl alcohol, the rescue animals show a significant increase in the chemotaxis index compared to

the mutant. However, the chemotaxis index was still reduced compared to the wild-type N2 (Figure 3.16 B). This suggested that although some of the phenotypes of the rescue animals are not comparable to wild-type levels, it still shows an improvement in the lifespan and chemosensory assays. It also implies overexpression of *dnj-14* in *C. elegans* could be deleterious to the animal just like in flies (Nie et al., 1999). Hence a more refined approach by constructing a single copy inserted rescue would be the way to move forward.

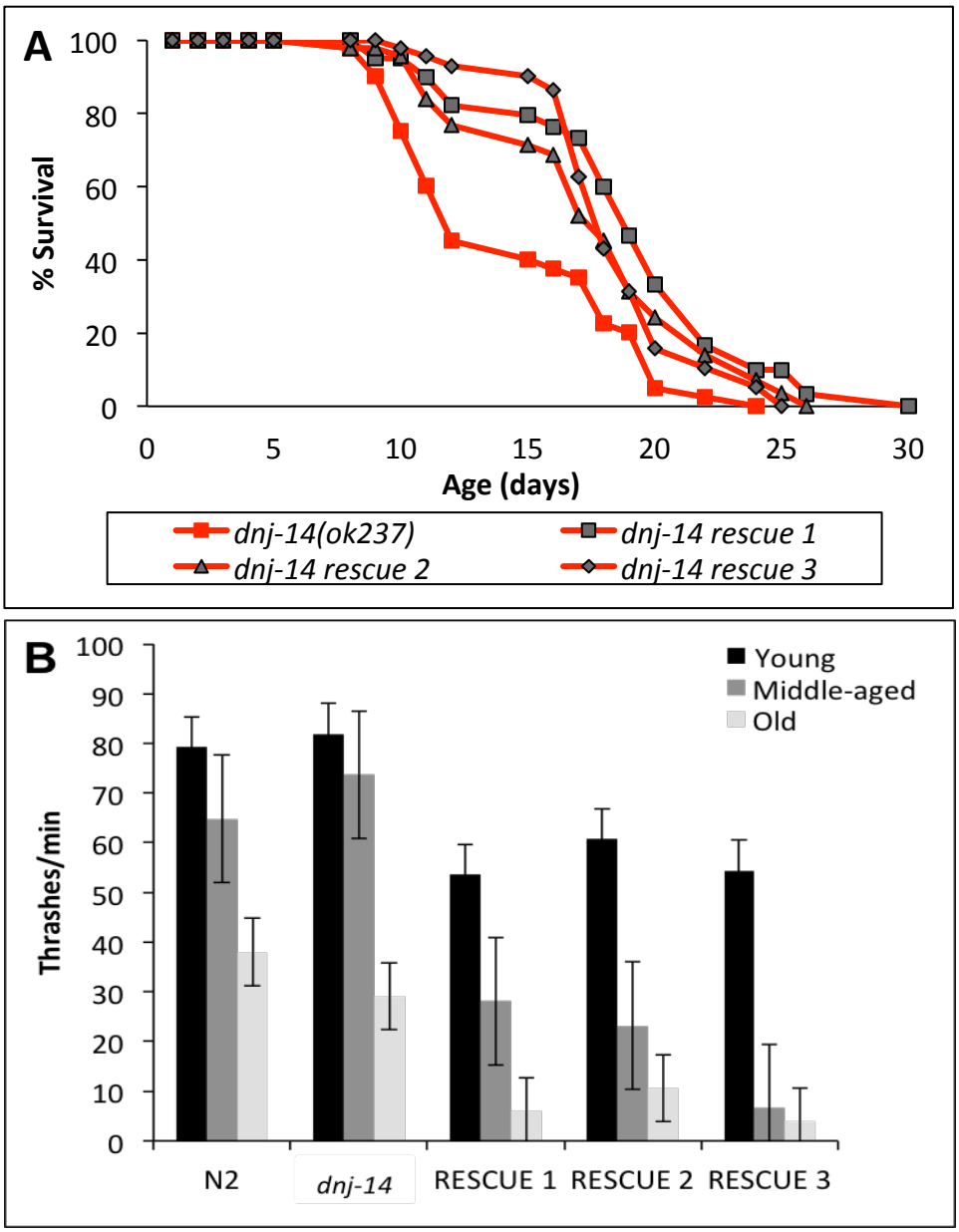

Figure 3.15: Lifespan and thrashing of *dnj-14* rescue lines: A) Shows lifespan of *dnj-14* Rescue lines mutants with *dnj-14(ok237)* mutants as control. The experiment was performed as explained before. It can be seen that the lifespan of all three rescue lines are significantly increased compared to the mutant.. Above represented are pooled data from two independent biological replicate studies and n=50 for all strains. Mean lifespan in days of adulthood with SEM: *dnj-14(ok237)*=14.29 ± 0.35; Rescue1= 18.95 ± 0.65; Rescue2=17.61 ± 0.45; Rescue3=18.44 ± 0.79. B) Shows thrashing assays performed on the transgenic rescue lines of *dnj-14(ok237)* mutants with the wild-type N2 as control. The experiment was performed as explained earlier. Worms between ages 3-5 days of adulthood were considered young, 7-10 days considered middle aged and more than 11 days considered old. It can be seen that the rescue lines have significantly lower ($P<0.01$) thrashing rates at all three age groups compared to the mutants. Above represented are pooled data from two independent biological replicate studies. N=20 for all strains. Student's t-test was performed to calculate significance and $P<0.1$ was considered significant

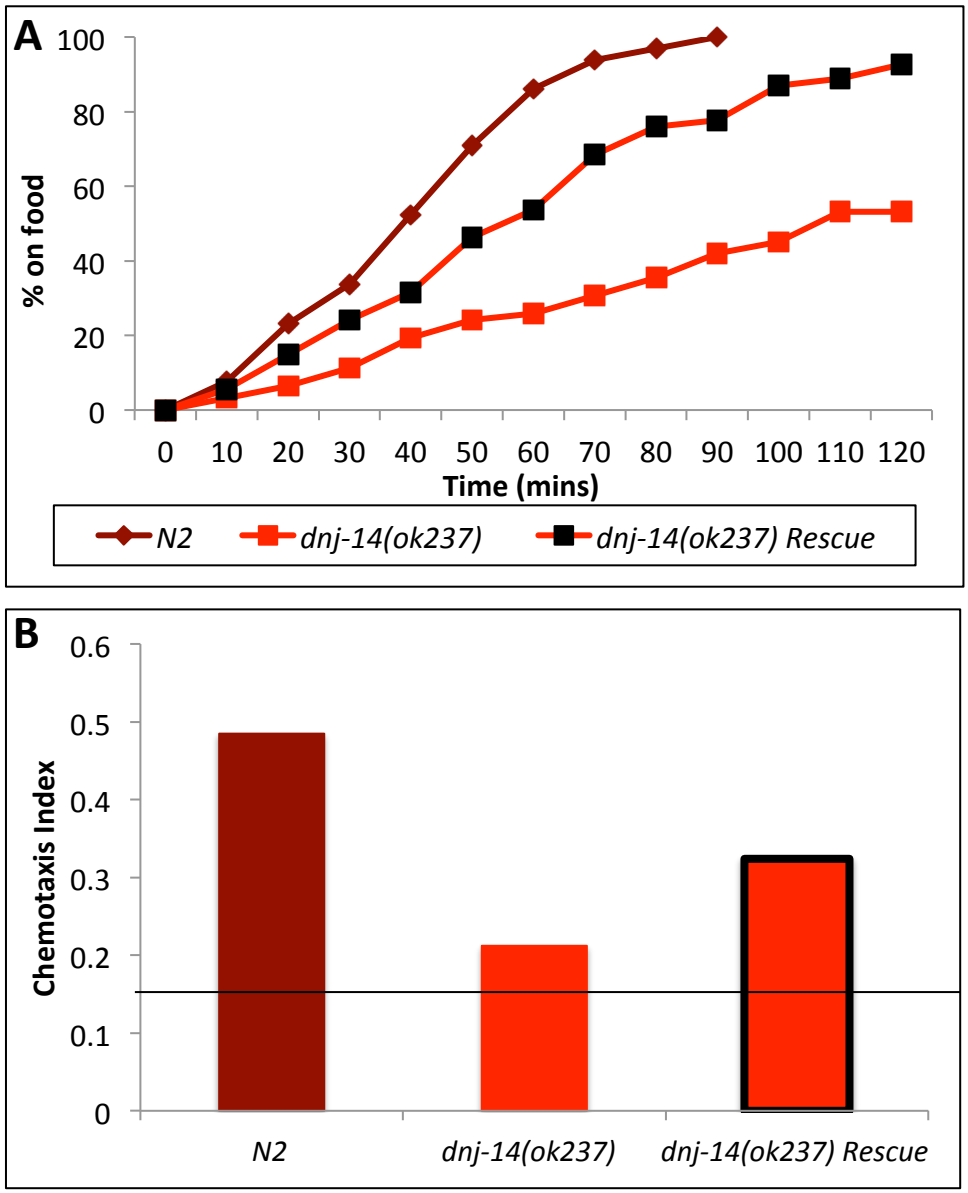

Figure 3.16: Transgenic rescue of *dnj-14(ok237)* rescues food race and chemotaxis: A) Shows food race assay performed on the transgenic *dnj-14* rescue worms with wild-type N2 and *dnj-14(ok237)* mutants as control. The experiment was performed as explained earlier. It can be seen that the transgenic *dnj-14* rescue worms show an improvement in its ability to reach the food source compared to the wild-type N2. This was found to be a statistically significant improvement. Above represented are pooled data from two independent biological replicate studies. Mean time taken to reach food (mins): N2: 45.59 ± 2.65 (n=65); *dnj-14(ok237)*=90.32 ± 4.60 (n=62); *dnj-14(ok237)* Rescue= 62.59 ± 4.44 (n=54). Log-Rank test was used to calculate significance and $P<0.05$ was considered to be significant. B) Shows chemotaxis performed on the above mentioned strains with isoamyl alcohol. It can be seen that although the transgenic rescue of *dnj-14* hasn't completely rescued the phenotype, there is however an increase in chemotaxis index compared to the *dnj-14(ok237)* mutants. Mean chemotaxis indices: N2= 0.485 (n=66); *dnj-14(ok237)*=0.212 (n=66); *dnj-14(ok237)* Rescue=0.324 (n=71). Chemotaxis index of 0.11 was considered baseline for false positives for both studies.

3.4 DISCUSSION

In this chapter, the *C. elegans* gene, *dnj-14*, has been shown to be a key neuroprotective gene like its mammalian homologue, CSP. Two mutant alleles of *dnj-14*, *ok237* and *tm3223* have been characterised phenotypically and these alleles have been shown to be phenotypically similar to CSP knockout mice. They have also exhibited some features of CSP knockout in *Drosophila.*

It has been shown that like the CSP knockouts in mice and *Drosophila* (Zinsmaier et al., 1994, Zinsmaier and Bronk, 2001, Fernandez-Chacon et al., 2004), both the *dnj-14* mutant alleles show a reduced lifespan and significantly lower locomotive capability than the wild type N2. However, the *Drosophila* mutants exhibit a much more severe phenotype compared to the mice with 5% of the fly mutants surviving to adulthood before showing sensorimotor defects and neurodegeneration (Zinsmaier et al., 1994, Zinsmaier and Bronk, 2001). This could be explained by the presence of a highly homologous CSPβ, absent in *Drosophila*, which could potentially compensate for the loss of CSP in the mutant mice (Gundersen et al., 2010). This has been debated in several studies as CSPβ was shown to be expressed only in testes in mice and not in the brain (Gorleku and Chamberlain, 2010). It was also shown that palmitoylation efficiency of CSPβ is greatly reduced compared to the other isoforms (Boal et al., 2007, Gorleku and Chamberlain, 2010). The reason for the severity of phenotype of the fly model is clearly not well understood. The worm genome has a single CSP homologue and hence the mild phenotype seen in worms could

indicate that the worm model is more similar to the mouse model.

Our experiments also showed that both the *dnj-14* mutants exhibited a 'Ric' phenotype when subjected to an acetylcholinesterase inhibitor, aldicarb. This suggests that *dnj-14* mutants have a neurotransmission defect similar to its mammalian counterpart (Fernandez-Chacon et al., 2004). In *Drosophila,* the neurotransmission defect persists even whilst the CSP mutant fly is in its larval stage (Umbach et al., 1994, Dawson-Scully et al., 2000). It was also shown that in *Drosophila* at high concentrations of external calcium, neurotransmitter release in CSP mutants were enhanced (Dawson-Scully et al., 2000). Similarly, rescue of neurotransmitter release by external calcium was shown in mice as well by a second group (Ruiz et al., 2008). Unpublished work from our lab also suggests that locomotion of *dnj-14* mutants, as seen in thrashing assay, was rescued by 10mM external calcium. This suggests that although there is some overlap between the worm *dnj-14* and the fly CSP models, the *dnj-14* mutants are more similar to the CSPα knock out in mice.

Furthermore, to eliminate the effect of background mutations in *dnj-14* mutants, both strains were outcrossed (*ok237* - six times; *tm3223* - five times) repeatedly. The phenotypes persisted despite repeated outcrossing indicating that all the observed phenotypes were an effect of the deletion in *dnj-14* rather than background mutations.

Neurodegeneration assays on the *dnj-14* mutants revealed several interesting results. There was a clear indication of degenerating neurons, but the individual neurons which were degenerating could not be identified in the pan-neuronal *rab-3* reporter construct used in the *dnj-14* mutants. Also, CSP knockout mice showed selective vulnerability of certain classes of neurons, in that hippocampal GABAergic neurons degenerate while the glutamatergic neurons remain unaffected (Garcia-Junco-Clemente et al., 2010). *unc-25* (*C. elegans'* GAD) marker used in other studies of Alzheimer's disease models in *C. elegans* (Liachko et al., 2010) proved to be a robust marker. However, in the *dnj-14* model, no loss of *unc-25::gfp* signal was observed. This indicated that the GABAergic neurons remained unaffected. Even though the GABAergic transmission is unaffected, there could be loss of other sets of neurons like the cholinergic, glutamatergic and dopaminergic neurons which remains to be investigated. There was selective loss of a particular set of sensory neurons in the *dnj-14* mutants similar to the selectivity shown in mice. It could be speculated that in worms, the most active set of neurons would be the first ones to degenerate. As worms are filter feeders, their feeding mechanism is active at all times and in *dnj*-14 experiments indicated that the neurons involved in chemosensation degenerate first, hence, it would be fair to suggest these neurons to be most active. Through neurodegeneration assays, it was clear that one of the possible set of chemosensory neurons which degenerate in the *dnj-14* mutants were the IL2 neurons involved in several pathways. A previous study suggested the involvement of IL2 neurons in nictation, a

dispersal behaviour of worms seen in dauer stage, and the requirement of cholinergic neurotransmission (Lee et al., 2012). Studies have also shown that IL2 neurons express a nicotinic acetylcholine receptor - DEG-3/DES-2 and mutation of this receptor causes neurodegeneration (Yassin et al., 2001). The above studies clearly tie IL2 neurons to cholinergic neurotransmission and neurodegeneration. Another protein, KLP-6 expressed only in the IL2 neurons, is involved in maintaining mitochondrial morphology (Tanaka et al., 2011). A GFP reporter construct driven by *klp-6* promoter was therefore constructed. Tests similar to those conducted on the IL2 neurons could be carried out to test for neurodegeneration. However, due to time constraints this could not be analysed for neurodegeneration.

The chemotaxis assays revealed that the *dnj-14* mutants are chemotaxis variants for isoamyl alcohol. Previous studies have shown that nematodes lacking AWC and AWA neurons (amphid neurons present in the neuronal ganglia near the posterior pharyngeal bulb of the animal) exhibit defective chemotaxis to volatile odourants like isoamyl alcohol (Bargmann et al., 1993). This could mean that in the *dnj-14* mutants the AWC and AWA neurons could also possibly be degenerated along with IL2 neurons. Due to the presence of several other neurons in the neuronal ganglia, the degeneration of AWC and AWA neurons may not be picked out using the *rab-3* promoter driven GFP construct. Hence a reporter construct expressing GFP only in amphid neurons might be useful in further analysis.

It was also shown that the *dnj-14(ok237)* mutants could be rescued by injecting the gene driven by its endogenous promoter in an extrachromosomal array. Whilst the lifespan of *dnj-14(ok237)* was rescued completely, other assays, food race and chemotaxis, showed that a complete rescue was not possible. Interestingly, thrashing assays with the transgenic rescue lines suggested a further decline in the phenotype. This could be explained as it was found that in *Drosophila*, overexpression of CSP was deleterious and the animals were sicker than the wild-type (Nie et al., 1999). It is also important to note that in Figure 3.15B, the *dnj-14(ok237)* mutants thrash similar to wild-type levels. This assay was performed by a Masters student under my supervision and has not been reproduced.

Although there is scope for more work in the area of characterisation of the neurodegeneration phenotype, data gathered from our experiments suggest that *dnj-14* mutants are similar to CSP knockout mice and exhibit neurodegeneration with increased mortality making it a more efficient model to screen drugs and identify novel therapeutic targets.

CHAPTER 4: EFFECTS OF RESVERATROL ON *DNJ-14* MUTANTS

4.1 INTRODUCTION

4.1.1 DRUGS TO RESCUE NEURODEGENERATIVE DISEASES

In 2005, neurodegenerative diseases worldwide affected about 35 million people and are likely to affect 70 million people in the next twenty years (Jellinger, 2011). Alzheimer's, Parkinson's and Huntington's are the most common neurodegenerative diseases and are characterized by acute, gradual and progressive neurodegeneration leading to premature death. All these diseases are characterized by the aggregation of misfolded protein aggregates that are possibly neurotoxic. β-amyloid and tau/phosphorylated tau in Alzheimer's disease, α-synuclein in Parkinson's disease, mutant huntingtin in Huntington's disease (Hung et al., 2010) are the key protein aggregates involved. However the causative mechanism of neurodegeneration is yet to be elucidated. Hence, it is essential to first understand and uncover the mechanism involved in neurodegeneration and then identify new drug targets which in the future could rescue neurodegeneration and improve both the lifespan and the healthspan of patients.

Several drugs like lithium chloride, trichostatin A, mithramycin, etc have been screened in *C. elegans* which have shown neuroprotective properties in models for Huntington's disease (Voisine et al., 2007). Drugs like acetaminophen and valproic acid have been shown to ameliorate neurodegeneration in *C. elegans* models for Parkinson's disease (Locke et al., 2008, Kautu et al., 2013). Plant

extracts from the leaves of gingko biloba have also shown to be neuroprotective in worm models for Alzheimer's disease (Luo, 2006).

4.1.2 RESVERATROL AS A THERAPEUTIC DRUG

Resveratrol, shown to have several therapeutic properties, is a polyphenol and phytoalexin plant product produced as a response to attack by pathogenic bacteria and fungi. A study in 1997 showed that resveratrol prevented skin cancer development in carcinogen treated mice (Jang et al., 1997). High doses of resveratrol were also shown to reduce the number and size of oesophageal tumours in carcinogen treated rats (Li et al., 2002). Interestingly, resveratrol given orally was shown to have no effect on leukaemia and lung cancer (Gao et al., 2002, Athar et al., 2007); but slowed the growth of metastatic Lewis lung carcinomas in mice when injected intraperitoneally (Kimura and Okuda, 2001, Athar et al., 2007). It was initially shown to extend lifespan in *Saccharomyces cerevisiae, Drosophila* and *C. elegans* (Howitz et al., 2003, Wood et al., 2004, Viswanathan et al., 2005) but later reports failed to reproduce these results (Kaeberlein et al., 2005, Bass et al., 2007). In cell culture studies, resveratrol has shown a beneficial effect against the accumulation of β-amyloid (Marambaud et al., 2005). Dietary supplementation of resveratrol was shown to significantly reduce plaque formation (involved in Alzheimer's disease pathogenesis) in mice brains (Karuppagounder et al., 2009). There have been several other studies which elucidate the neuroprotective effects of resveratrol including rat models of stroke (Sinha et al., 2002), spinal cord injuries (Yang and Piao, 2003), etc. It has also been shown to improve drug induced cognitive impairment and oxidative stress in rats (Sharma and Gupta, 2002).

In *C. elegans,* resveratrol has been shown to attenuate radiation damage against cells and neurons by preventing oxidative stress (Ye et al., 2010). More importantly, resveratrol has been shown to rescue the early signs of neuronal dysfunction induced by mutant polyglutamines in a Huntington's disease model in *C. elegans* (Parker et al., 2005). Resveratrol in worms has also been shown to promote autophagy through its activation of sirtuins (Morselli, 2010) and as autophagy acts as a key regulator of neurodegeneration in neurodegenerative diseases (Wong and Cuervo, 2010), resveratrol may have a important role in neuroprotection. Resveratrol has a huge potential therapeutic importance in the treatment of neurodegenerative diseases. In this chapter, the effects of resveratrol on the phenotypes seen in the *dnj-14* mutants in the previous chapter were investigated.

4.2 METHODS

The methodology remains similar to that mentioned in the earlier sections with the exception of the key points mentioned below.

4.2.1 *C. ELEGANS* STRAINS

Apart from the wild type N2, *dnj-14(ok237)* and *dnj-14(tm3223)* which were used in the previous chapter, the *sir-2.1(ok434)* strain obtained from the *Caenorhabditis* Genetics Center (University of Minnesota, Twin Cities, MN, USA) was used for experiments that are the focus of this chapter. Outcrossed *dnj-14* strains were used in most assays. *dnj-14(ok237)* was outcrossed six times whereas *dnj-14(tm3223)* was outcrossed five times.

4.2.2 DRUG TREATMENT

Individual compounds were dissolved in appropriate vehicles and added directly to molten NGM before pouring plates to prepare the control and test plates. On drying overnight, the plates were seeded with 30µL of OP50 bacteria. Age synchronised worms at day 1 of adulthood were then placed on these drug plates and the assays performed. Worms were transferred on to fresh drug plates every two days. The drugs used include resveratrol (Sigma-Aldrich®), rolipram (Sigma-Aldrich®), p-propenylanisole (Resv 1; Ambinter, Orléans, France) and 2-propenylphenol (Resv 4; Tim Tec, Newark, DE, USA). All the drugs were dissolved in ethanol and 100mM stocks were made for each drug before

use. While pouring plates, these stocks were added to molten agar in a 1:1000 dilution to ensure final concentration of 100µM.

4.2.3 WORM CROSSING

The *dnj-14(tm3223);sir-2.1(ok434)* double mutant was made by first crossing *dnj-14(tm3223)* mutants with wild-type N2 male worms. The *dnj-14(tm3223)* male progeny obtained from the cross were then allowed to mate with *sir-2.1(ok434)* hermaphrodites. The resulting F1 hermaphrodite progeny was heterozygous to both alleles. These worms were then picked onto replica NGM plates (40mm) such that each plate had a single worm on it. One-sixteenth of the resulting F2 progeny should be double mutants. The double mutants were genotyped using PCR analysis and agarose gel electrophoresis.

4.2.4 PCR ANALYSIS AND STRAIN VERIFICATION

DNA was extracted from the segregated F2 progeny obtained from the cross and amplified by a PCR as explained before. Four primers were used to amplify the DNA:

a) dnj-14 del rev - 5'-TGCTCTCAACAGACCCATAC-3',

b) tm3223 del full fwd - 5'-GCTTGTCTTACCTTATGTCGTCG-3',

c) sir-2.1 del rev - 5'-CAGATAGTTCATACTGAAAATCT and

d) sir-2.1 del fwd - 5'-AATCCCAATTGAACTCGCTG-3'.

The annealing temperature was calculated using a Tm Calculator (New England

Biolabs;https://www.neb.com/tools-and-resources/interactive-tools/tm-calculator).

4.3 RESULTS

4.3.1 EFFECTS OF RESVERATROL ON LIFESPAN

A drug screen had been performed in the lab on the *dnj-14(ok237)* mutants before the initiation of this study. Six drugs with either known neuroprotective or lifespan extending properties (Mithramycin, Trichostatin-A, Mianserin, Ethosuximide, C2-8 and Resveratrol) were analysed for their effect on the lifespan of *dnj-14(ok237)* mutants. Mithramycin and Trichostatin-A had previously been shown to reduce polyQ neurotoxicity in worms (Voisine et al., 2007). Mianserin, a human antidepressant, and ethosuximide, a human anticonvulsant, were respectively shown to increase lifespan in worms (Collins et al., 2008, Petrascheck et al., 2009). C2-8 , a small compound, was shown to be highly brain penetrable, non-toxic and was highly efficient in reducing neuronal atrophy in Huntington's disease model in mice (Chopra et al., 2007). The sixth drug used in the drug screen was resveratrol. In the study, resveratrol along with ethosuximide significantly rescued the lifespan of the *dnj*-14*(ok237)* worms. These experiments were repeated (Figure 4.1A,B) and the results were as found earlier with resveratrol and ethosuximide increasing the lifespan of the *dnj-14(ok237)* mutants significantly (mean lifespan in days of adulthood with SEM: N2 Et OH=17.52 ± 0.71; *dnj-14(ok237)* Et OH=14.57 ± 0.56; *dnj-14(ok237)* Resv= 18.57 ± 0.80; N2 PBS=17.95 ± 0.88; *dnj-14(ok237)* PBS=14.77 ± 0.93; *dnj-14(ok237)* Eth=16.25 ± 0.95). However, the work on ethosuximide was carried over by another PhD student and hence, in this study resveratrol has been

concentrated upon. A dose response experiment on both the wild-type and the *dnj-14(ok237)* worms was performed (Figure 4.2A and B) to determine the effect of varying doses of resveratrol on the lifespan of the worms. Concentrations varying from 0.1µM to 200µM were used in this experiment and it was observed that resveratrol had no effect on the lifespan of the wild-type worms. In the mutants, however, resveratrol did affect the lifespan of the worms and 100µM was found to be the optimal dose (mean lifespan in days of adulthood with SEM: N2: Et OH=19.04 ± 0.7; 1µM=18.83 ± 0.7; 100µM=19.25 ± 0.77. *dnj-14(ok237)*: Et OH=16.40 ± 0.87; 0.1µM=16.52 ± 0.82; 1µM=17 ± 0.85; 10µM=17.04 ± 0.8; 50µM=17.4 ± 0.67; 100µM=19.13 ± 0.87; 200µM=18.64 ± 0.83). The optimal dose increase in survival was found to be 16.65% compared to the lifespan under the vehicle ethanol (Figure 4.2C). The finding that no increase or only a marginal increase in lifespan was observed in the wild-type worms corroborated with the earlier study which reported inconsistencies in resveratrol mediated increase in lifespan (Bass et al., 2007). The effect of resveratrol on lifespan was specific to the *dnj-14* mutants suggesting that resveratrol acts on a pathway specific to *dnj-14* mutants.

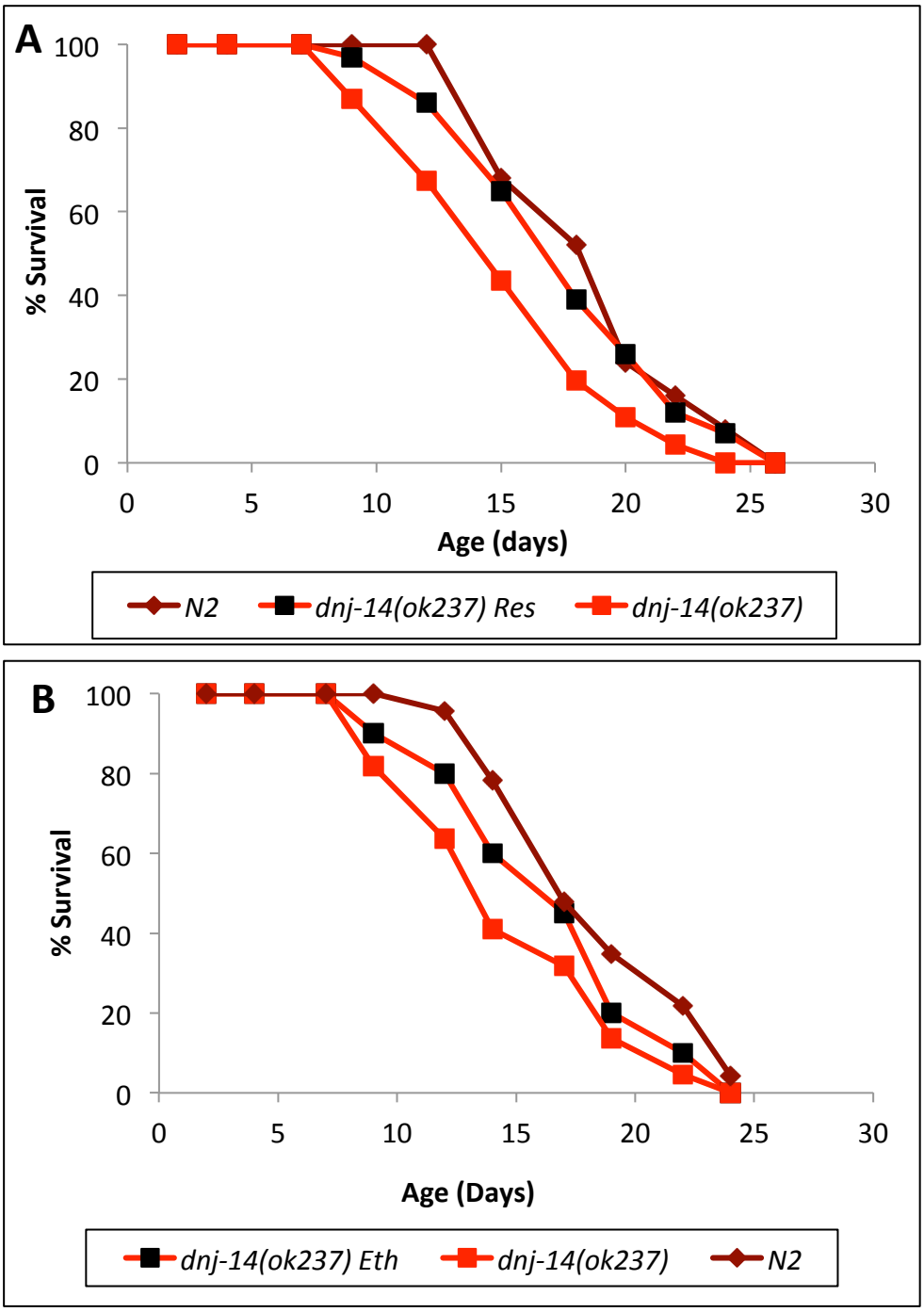

Figure 4.1: Resveratrol and ethosuximide rescues lifespan in *dnj*-14: A) and B) Shows effect of resveratrol and ethosuximide treatment on N2 and *dnj-14(ok237).* Worms were age synchronized by letting ten worms lay eggs overnight and 25 of the progeny was transferred on to seeded drug/control plates. Worms were monitored every alternate day and transferred to fresh plates to prevent progeny formation. Concentrations used: Resveratrol – 100µM in Et OH, Ethosuximide: 2.8mM in PBS. Mean lifespan in days of adulthood with SEM – N2 Et OH=17.52 ± 0.71; *dnj-14(ok237)* Et OH=14.57 ± 0.56; *dnj-14(ok237)* Resv= 18.57 ± 0.80; N2 PBS=17.95 ± 0.88; *dnj-14(ok237)* PBS=14.77 ± 0.93; *dnj-14(ok237)* Eth=16.25 ± 0.95. n=25 for all conditions. Log Rank test was used to calculate significance and both resveratrol and ethosuximide increased the lifespan significantly compared to the control. P<0.05 was considered to be significant.

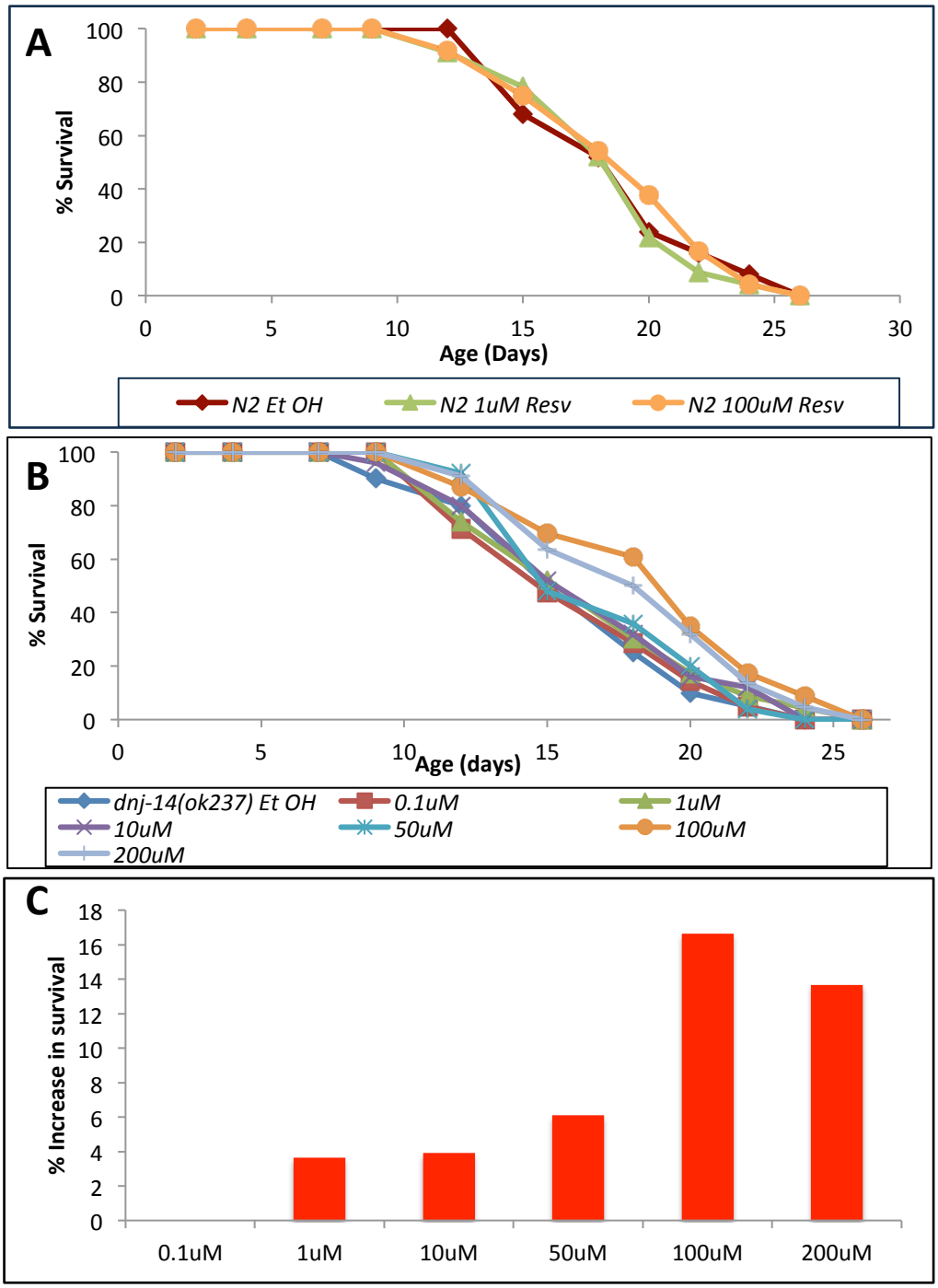

Figure 4.2: Dose Response with Resveratrol: A) and B) Shows dose response for Resveratrol treatment on N2 and *dnj-14(ok237)*. Worms were age synchronized as explained before and were monitored every alternate day and transferred to fresh plates to prevent progeny formation. Mean lifespan in days of adulthood with SEM – N2: Et OH=19.04 ± 0.7; 1µM=18.83 ± 0.7; 100µM=19.25 ± 0.77. *dnj-14(ok237)*: Et OH=16.40 ± 0.87; 0.1µM=16.52 ± 0.82; 1µM=17 ± 0.85; 10µM=17.04 ± 0.8; 50µM=17.4 ± 0.67; 100µM=19.13 ± 0.87; 200µM=18.64 ± 0.83. n=25 for all conditions. Log Rank test was used to calculate significance and *dnj-14(ok237)* 100µM and 200µM were found to be significant compared to *dnj-14(ok237)* EtOH. P<0.05 was considered to be significant. C) Shows percentage increase in survival of *dnj-14(ok237)* mutants compared to the control. *dnj-14(ok237)* 0.1µM – 0%; 1µM – 3.66%; 10µM – 3.90%; 50µM – 6.1%; 100µM – 16.64%; 200µM – 13.66%. n=25 for all conditions 100µM resveratrol had the highest effect on the lifespan of *dnj-14(ok237)* mutants.

4.3.2 CHEMOSENSATION AND NEURODEGENERATION

Resveratrol has previously been described in studies to be neuroprotective (Sharma and Gupta, 2002, Sinha et al., 2002, Yang and Piao, 2003). More recently, resveratrol has been shown to rescue neurodegeneration in a chronic mouse model for multiple sclerosis (Fonseca-Kelly et al., 2012). As it has been previously observed that resveratrol has a positive effect the lifespan of *dnj-14* mutants, we wanted to further investigate the neuroprotective effect of resveratrol in the *dnj-14* mutants. The *dnj-14* mutants have a chemosensory defect as illustrated in food race and chemotaxis assays. This phenotype manifested itself later as neurodegeneration in the sensory cilia of the *dnj-14* mutants. Worms were grown on resveratrol containing NGM plates and a food race assay was performed on day 6 of adulthood. Interestingly, we found a complete rescue of the phenotype in both the *dnj-14* mutants (Figure 4.3A). This was surprising as the food race phenotype seen in the *dnj*-14 mutants was severe and a complete rescue with resveratrol treatment was not expected. Chemotaxis assays were also performed on the *dnj-14* mutants treated with resveratrol, and like in the food race assay, resveratrol rescued the chemotaxis defect seen in the *dnj-14* mutants (Figure 4.3B).

Next these worms were analysed for neurodegeneration assays. Earlier it was shown that the *dnj-14* mutants show an abnormal expression of GFP in the head with the loss of cell bodies. If resveratrol is indeed neuroprotective, as suggested by the chemosensory assays, the expression pattern of GFP in the

head of the resveratrol treated worms would be similar to the wild type. Worms were grown on NGM plates containing 100µM resveratrol and analysed for neuroprotection in the head. Out of the twenty worms analysed, 45% of the worms treated with resveratrol showed abnormal expression of GFP in the head (Figure 4.4A,B). The rest of the worms displayed expression of GFP similar to the wild-type and hence showed signs of rescue. Among the untreated mutants the percentage of the worms that showed this phenotype was 70.45% (Figure 4.4B). This shows that although resveratrol completely rescues the chemosensory phenotypes in *dnj-14* early on in the worm's lifespan, it cannot completely rescue the neurons from dying.

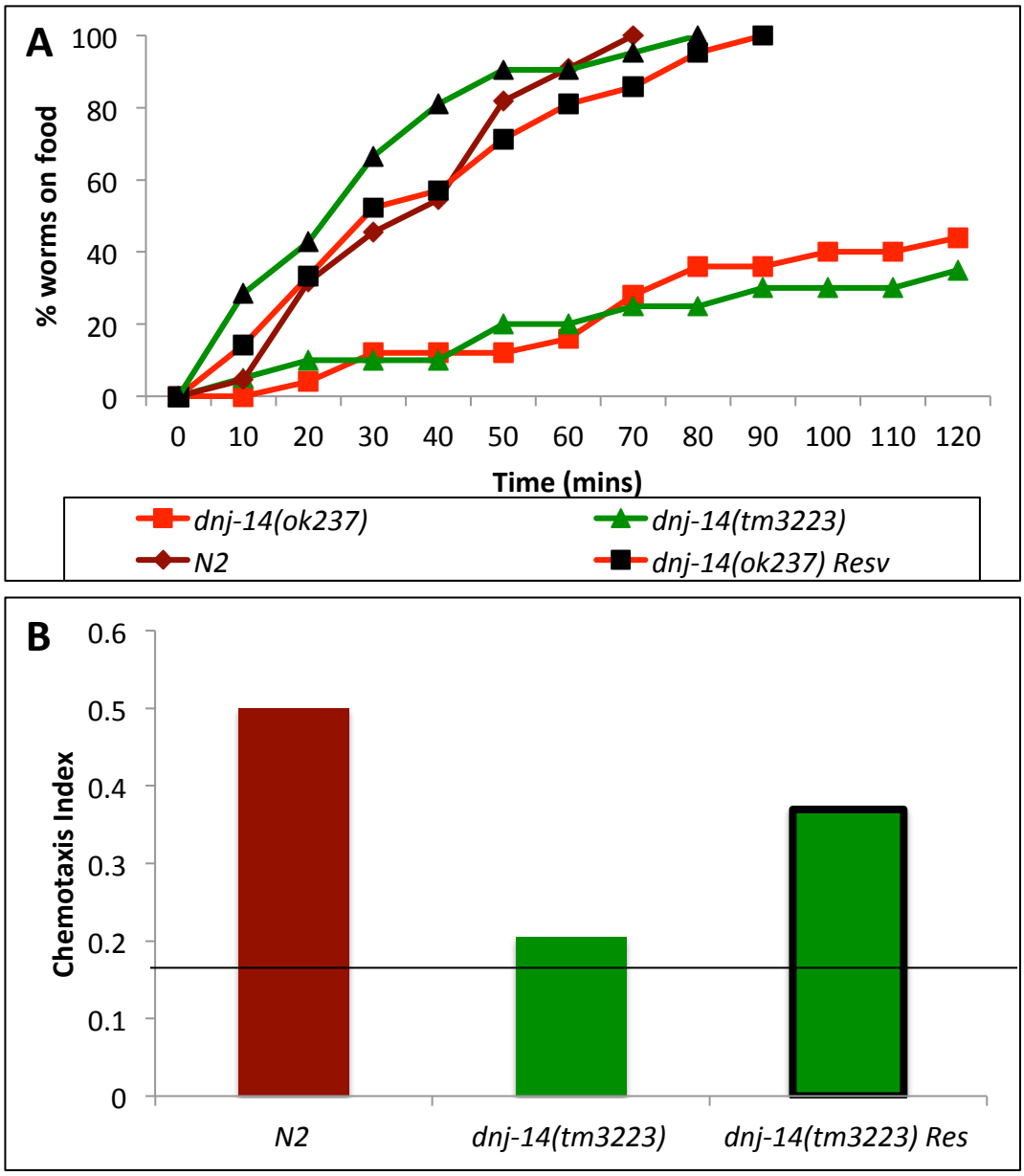

Figure 4.3: Resveratrol rescues chemosensory defects in *dnj-14.* A) Shows food race assay performed on six-day old worms on NGM plates containing resveratrol (100µM). Ethanol was used as vehicle control. Worms were washed in M9 buffer and placed on the corner of an NGM plate with 30µL of OP50 on the opposite corner. Worms reaching the food every 10 minutes were noted down till 120 minutes. Resveratrol rescues food race defects in *dnj-14* mutants significantly. Resveratrol has minimal effect on the wild-type N2 which was insignificant. Data pooled from two independent biological replicate studies. and n_{N2}=45, $n_{N2\ Resv}$=46, $n_{dnj\text{-}14(tm3223)}$=45, $n_{dnj\text{-}14\ Resv}$=47. Log-Rank test was used to calculate significance and P<0.05 was considered as significant. B) Shows chemotaxis assays performed with isomayl alcohol on six day old worms. Worms were washed in M9 buffer and placed on the centre of a chemotaxis plate with 1µL of isoamyl alcohol and ethanol on either side of the plate. After 90 minutes, chemotaxis index was calculated as (number of worms on drug-number of worms on control)/total number of worms. Chemotaxis index of 0.11 was considered baseline for false positives. Data pooled from from two independent biological replicate studies and n_{N2}=75, $n_{dnj\text{-}14(tm3223)}$=77, $n_{dnj\text{-}14\ Resv}$=96.

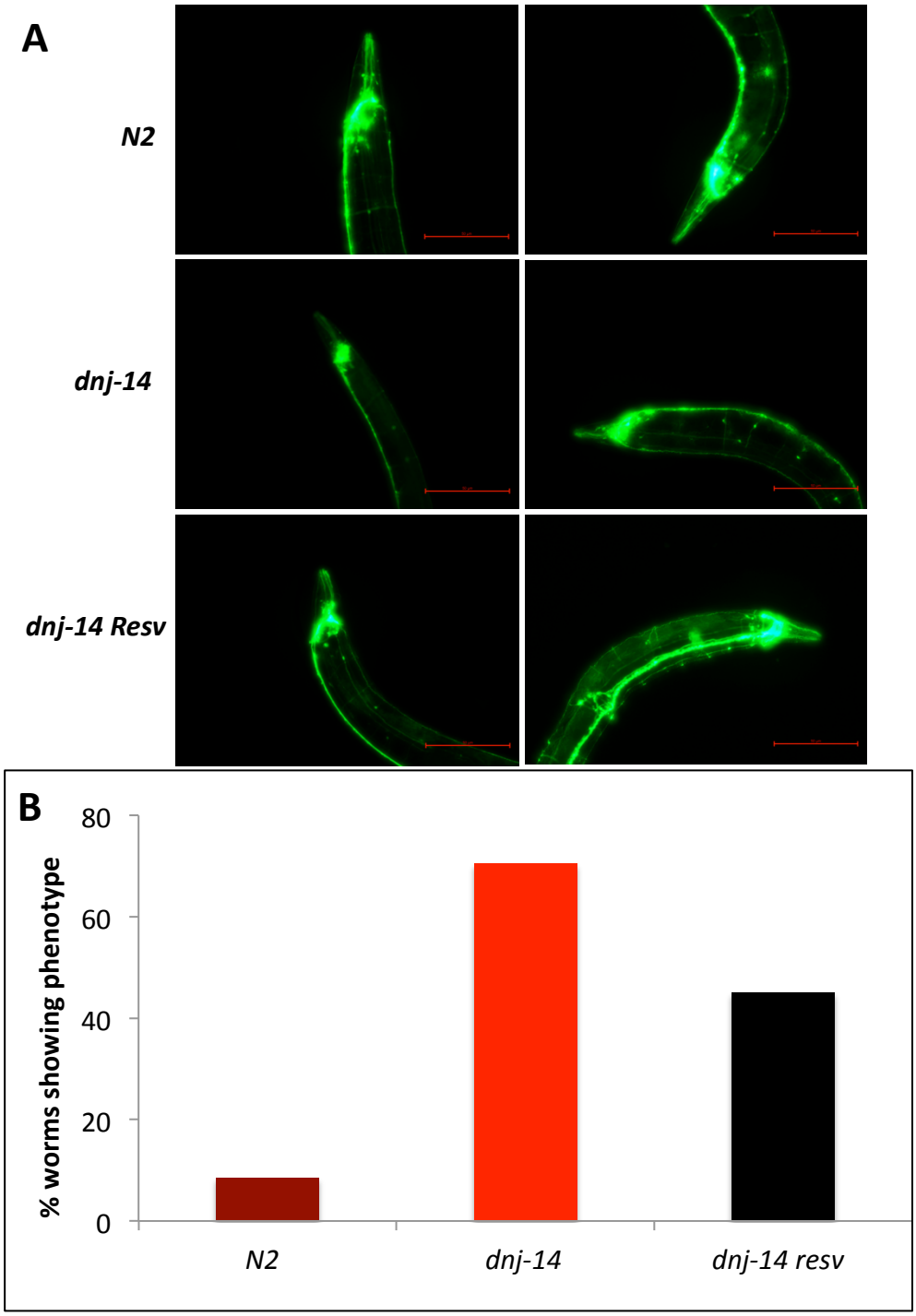

Figure 4.4: Neurodegeneration partially rescued by resveratrol treatment. A) Shows typical images of the abnormal snout phenotype of N2 (top row), *dnj-14(ok237)* (middle row) and *dnj-14(ok237)* treated with resveratrol (bottom row). In the wild-type N2, the neurons in the head look normal with all the cell bodies and processes intact as seen by the GFP expression. In the mutant, we see loss of GFP expression and loss of neuronal cell bodies. This is indicative of neurodegeneration. In mutants treated with resveratrol, a partial rescue of this phenotype was seen. The snout of the animal was short like the mutant, but the cell bodies and the processes were intact in rescued worms. B) Shows percentage of worms showing the abnormal snout phenotype in wild-type N2 and *dnj-14(ok237)* ± resveratrol. N2 = 8.57%, n=35; *dnj-14(ok237)*=70.45%, n=44; *dnj-14(ok237)* Resv=45%, n=20. All worms imaged were aged at day 15 of adulthood. Scale bars=50µM.

4.3.3 MECHANISM OF RESVERATROL ACTION

4.3.3.1 PHOSPHODIESTERASE INHIBITION

Previous studies have revealed several pathways through which resveratrol could possibly act. It is known to activate protein kinase C (PKC) which could render protection against cell death (Pany et al., 2012). Treatment of resveratrol has shown to increase levels of glutathione and reduce the generation of reactive oxygen species (Albani et al., 2010). A study in mice suggested that resveratrol improves health and survival by activating AMP kinase activity (Baur et al., 2006). A more recent, comprehensive study in Cell showed that resveratrol, in cells and mice, acts by inhibiting PDE4 increasing cAMP levels leading to the activation of AMPK pathway. This increases the NAD levels and the activity of Sirt1 in the cells (Park et al., 2012). The above study also showed that rolipram, a PDE4 inhibitor, mimicked the effect of resveratrol in mice. Hence if the effect of resveratrol could be mimicked by rolipram in the *dnj-14* mutants, it could be reasoned that resveratrol acts by inhibiting PDE4 in the mutants as well.

NGM plates containing rolipram were poured and *dnj-14(tm3223)* worms were grown on these plates and their lifespan was analysed (Figure 4.5 B). Just like resveratrol, rolipram rescued the lifespan of *dnj-14(tm3223)* mutants completely. The effect of the drug was absent on the wild type N2 worms (Figure 4.5 A) (Mean lifespan in days of adulthood with SEM: N2: Et OH=19.13 ± 0.72; Res=18.39 ± 0.75; Rol=19.29 ± 0.76. *dnj-14(tm3223)*: Et OH=14.64 ± 0.96;

Res=18.08 ± 0.85; Rol: 18.79 ± 0.97). Chemosensory assays like food race assay and chemotaxis to isoamyl alcohol, were performed on worms grown on rolipram on day 6 of the worms' adulthood. Food race assay was performed and rolipram completely rescued the phenotype of the *dnj-14(tm3223)* worms (Figure 4.6 A). The rescue was also seen with chemotaxis assay on isoamyl alcohol (Figure 4.6 B). Hence, it could be inferred that rolipram mimics resveratrol in the *dnj-14* mutants as seen by the rescue of lifespan and chemosensory defects and hence it could be suggested that resveratrol might act through the inhibition of PDE4.

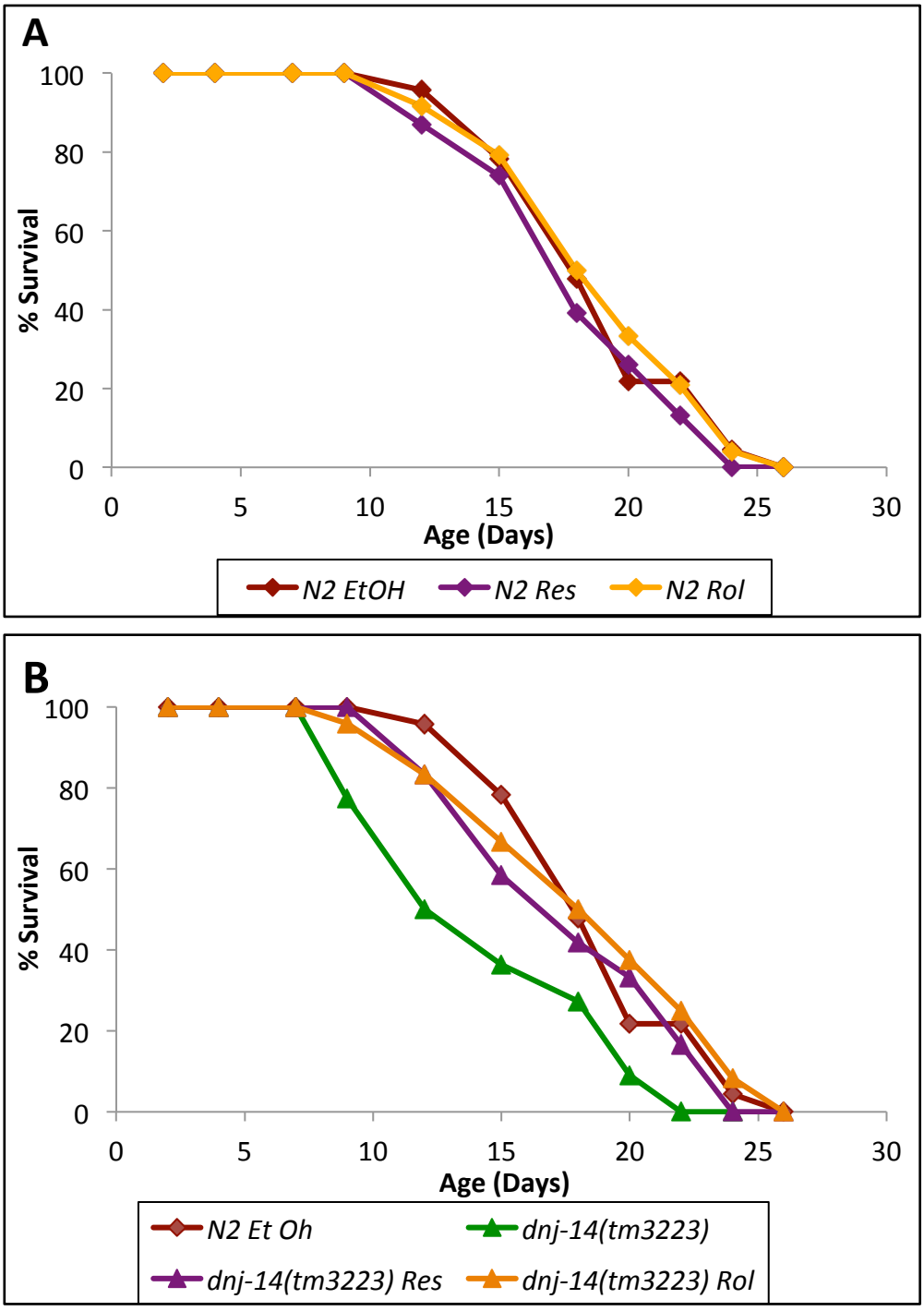

Figure 4.5: Rolipram rescues lifespan of *dnj-14* similar to resveratrol. A) and B) Shows effects of Resveratrol and a Phoshphodiesterase-4 inhibitor – Rolipram (Rol) (100µM each) on N2 and *dnj-14(tm3223)* mutants. Experiment was performed as described earlier. Mean lifespan in days of adulthood with SEM – N2: Et OH=19.13 ± 0.72 (n=48); Res=18.39 ± 0.75 (n=50); Rol=19.29 ± 0.76 (n=48). *dnj-14(tm3223)*: Et OH=14.64 ± 0.96 (n=45); Res=18.08 ± 0.85 (n=50); Rol: 18.79 ± 0.97 (n=46). Data pooled from two independent biological replicate studies. Log Rank test was used to calculate significance and *dnj-14(tm3223)* treated with both drugs were found to be significant compared to *dnj-14(tm3223)* EtOH. The effect of drugs on the wild-type N2 was insignificant. $P<0.05$ was considered to be significant.

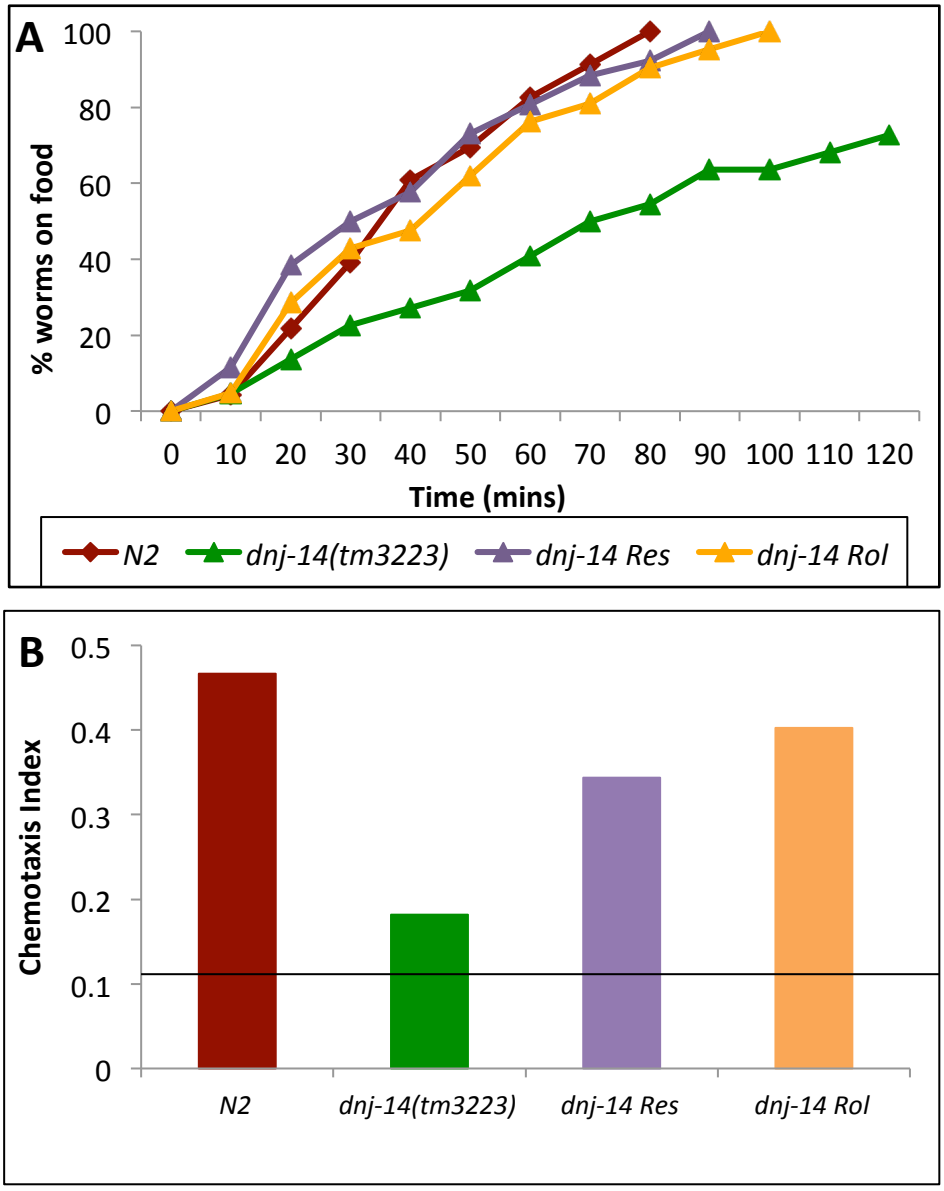

Figure 4.6: Rolipram rescues food race and chemotaxis assays in *dnj*-14. A) Shows food race assay performed on six day old worms as described earlier. Resveratrol and rolipram (100µM) significantly rescues food race defects in both *dnj-14* mutants significantly. Resveratrol has minimal effect on the wild-type N2 which was insignificant. Data pooled from two independent biological replicate studies. n_{N2}=45, $n_{dnj\text{-}14(tm3223)}$=45, $n_{dnj\text{-}14\ Resv}$=47, $n_{dnj\text{-}14\ Rol}$=47. Log-Rank test was used to calculate significance and P<0.05 was considered as significant. B) Shows chemotaxis to isoamyl alcohol performed on six day old worms as described earlier. Similar to food race, resveratrol and rolipram have a significant effect. Chemotaxis index of 0.11 was considered baseline for false positives. Data pooled from two independent biological replicate studies. n_{N2}=75, $n_{dnj\text{-}14(tm3223)}$=77, $n_{dnj\text{-}14\ Resv}$=96; $n_{dnj\text{-}14\ Rolipram}$= 77. for all strains.

4.3.3.2 RESVERATROL AND SIRTUIN INDEPENDENCY

According to Park *et al.*, downstream to inhibition of phosphodiesterase is activation of Sirt1 (Park et al., 2012) which is speculated to extend survival via a dietary restriction like mechanism (Wood et al., 2004, Viswanathan et al., 2005). It is possible that resveratrol might act by activation of *sir-2.1* (*C. elegans* homologue of Sirt1) in the *dnj-14* mutants. *sir-2.1(ok434)* mutants were obtained from CGC and crossed with *dnj-14(tm3223)* mutants to obtain *sir-2.1;dnj-14* double mutants (Figure 4.7). These worms were then grown on resveratrol plates and assayed for lifespan. If resveratrol acts in a pathway that is dependent on sirtuins, the extension of lifespan in the double mutant should be abrogated.

Surprisingly, it was found that the *sir-2.1;dnj-14* double mutants showed a complete rescue of lifespan by treatment with resveratrol (Figure 4.8). The *sir-2.1;dnj-14* double mutant without resveratrol treatment was slightly short lived, albeit marginally insignificant (P=0.0608), compared to *dnj-14(tm3223)* mutants. The lifespan of the *sir-2.1(ok434)* mutant was not significantly different from the wild type N2 and treatment with resveratrol did not have any effect on the extension of lifespan (mean lifespan in days of adulthood with SEM: N2 Et OH=20 ± 0.83; *dnj-14(tm3223)*=16.43 ± 0.81; *sir-2.1(ok434)*=18.46 ± 0.92; *sir-2.1(ok434)* Res=19.23 ± 0.91; *dnj-14;sir-2.1*=14.48 ± 0.66; *dnj-14;sir-2.1* Res: 20.54 ± 0.77). These findings were very interesting as it suggests that resveratrol acts on the *dnj-14* mutants in a *sir-2.1* independent pathway.

However, chemosensory assays on the *sir-2.1;dnj-14* double mutants revealed interesting results. Surprisingly, both food race and chemotaxis assays were completely rescued in the *sir-2.1;dnj-14* double mutants (Figure 4.9 A, B). This suggests that loss of *sir-2.1* in *dnj-14* mutants has a neuroprotective effect in rescuing the chemosensory defects of *dnj-14* mutants. However, from the above results clearly resveratrol acts on the *dnj-14* mutants in a PDE inhibition dependent and *sir-2.1* independent manner in at least rescuing the lifespan phenotype of the *dnj-14* mutants.

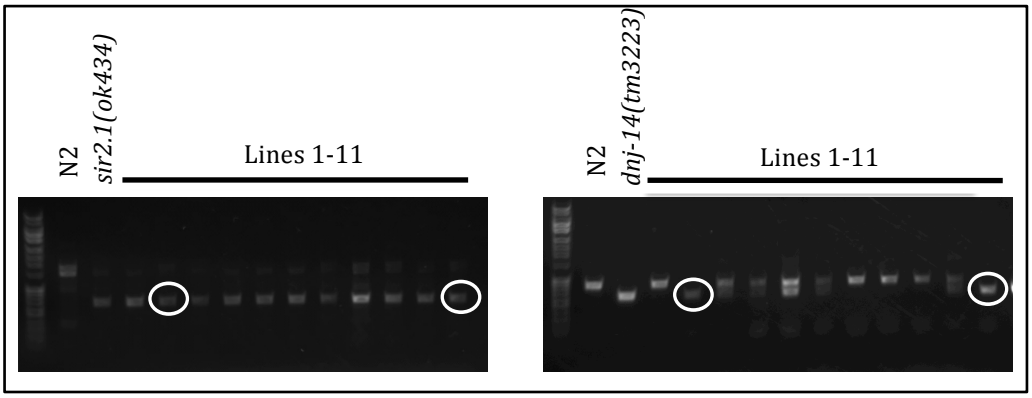

Figure 4.7: PCR confirmation of *sir-2.1;dnj-14* double mutant lines: Shows agarose gel electrophoresis of the PCR amplified DNA from the two lines of the *sir-2.1(ok434);dnj-14(tm3223)* double mutant. *sir-2.1(ok434)* mutant hermaphrodites were crossed on to *dnj-14(tm3223)* male worms and the F2 progeny was segregated. DNA from the segregated lines was extracted and amplified through PCR and analyzed using agarose gel electrophoresis.

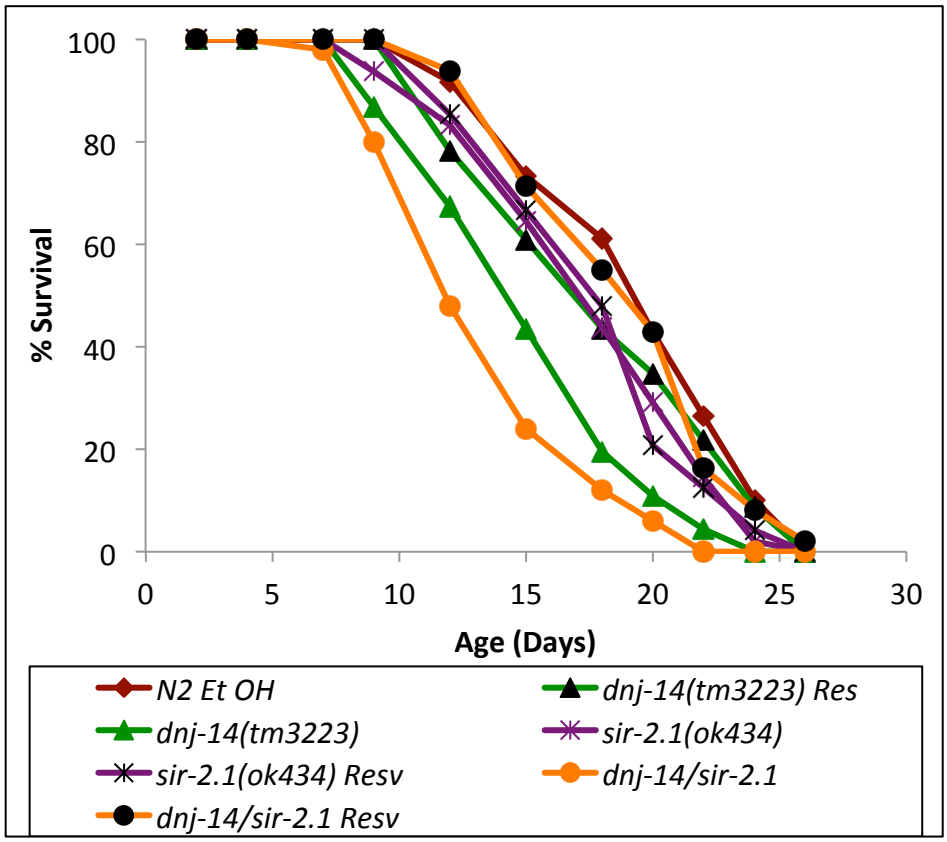

Figure 4.8: Analysis of lifespan of the *sir-2.1;dnj-14* double mutant. Shows lifespan of the *sir-2.1;dnj-14* double mutant ± Resveratrol. As illustrated, the mechanism of action of resveratrol is independent of *sir-2.1.* The lifespan of *sir-2.1* single mutant is not affected by resveratrol and under control conditions, the lifespan of the single mutant is similar to wild-type N2. The lifespan of *sir-2.1;dnj-14* double mutant under the control is lower than *dnj-14* single mutant (P=0.0608) but is significantly rescued upon treatment with resveratrol (P<0.05) Mean lifespan in days of adulthood with SEM – N2 Et OH=20 ± 0.83 (n=49); *dnj-14(tm3223)*=16.43 ± 0.81 (n=50); *sir-2.1(ok434)*=18.46 ± 0.92 (n=48); *sir-2.1(ok434)* Resv=19.23 ± 0.91 (n=48); *dnj-14;sir-2.1*=14.48 ± 0.66 (n=50); *dnj-14;sir-2.1* Resv: 20.54 ± 0.77 (n=49). Data pooled from two independent biological replicate studies. Log-Rank test was used to calculate significance and P<0.05 was considered as significant. Ethanol was used as a vehicle control for all experiments.

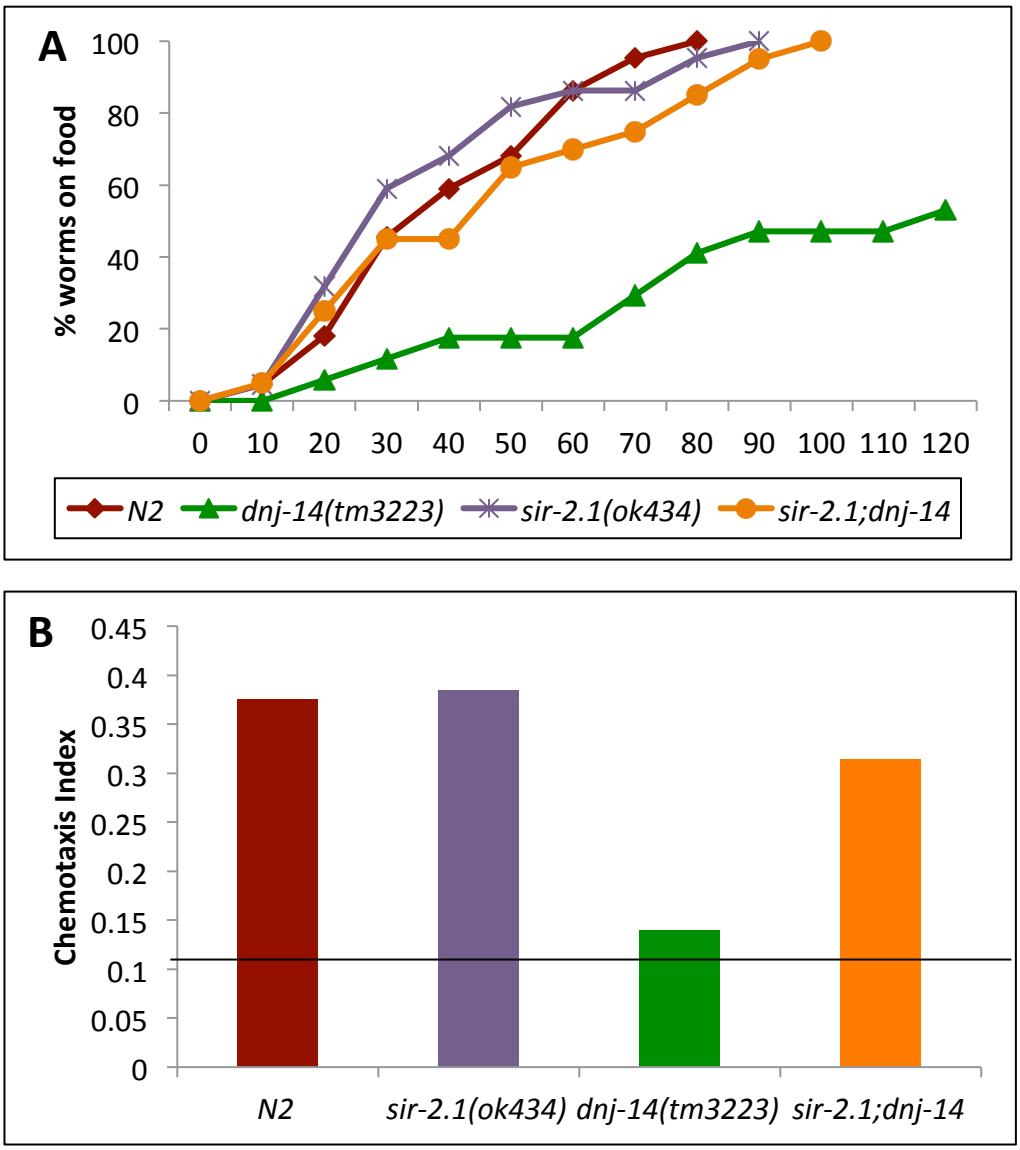

Figure 4.9: *sir-2.1* deletion in *dnj-14* rescues chemosensory defect as seen by food race assay and chemotaxis. A) Shows food race assay performed on six day old worms as described earlier. Food race assay rescued significantly in *sir-2.1;dnj-14* double mutant compared to *dnj-14(tm3223)*. *sir-2.1(ok434)* single mutant insignificant to the wild-type N2. Data pooled from two independent biological replicate studies and n=50 for all strains. Log rank test performed to calculate significance and $P<0.05$ was considered significant. B) Shows chemotaxis to isoamyl alcohol performed on six day old worms. Similar to food race, *sir-2.1;dnj-14* have a significant increase in chemotaxis index compared to *dnj-14(tm3223)*. Chemotaxis index of 0.11 was considered baseline for false positives. Data pooled from two independent biological replicate studies. . $n_{N2}=60$, $n_{dnj\text{-}14(tm3223)}=51$, $n_{sir\text{-}2.1(ok434)}= 69$; $n_{sir\text{-}2.1;dnj\text{-}14}=77$.

4.3.4 RESVERATROL RELATED COMPOUNDS

It has been shown earlier in this study that resveratrol significantly rescued the lifespan of *dnj-14* mutants in a *sir-2.1* independent manner and this was found to be specific to the mutants as resveratrol had no effect on the wild type worms. Resveratrol also affected the neurodegeneration phenotype of the *dnj-14* mutants in a positive manner. However, the dosage of resveratrol was relatively high which meant the potency of resveratrol as a drug was quite low. Hence, compounds similar to resveratrol in structure were tested on the *dnj-14* mutants to see if they were more potent. These could potentially form scaffolding compounds in the future to a more efficient drug which could be then used to treat neurodegenerative diseases.

We obtained three compounds namely, p-propenylanisole (Resv1), 2-propenylphenol (Resv4) and 3,4-dimethoxyresveratrol (Resv5) (Figure 4.10) tested the *dnj-14(ok237)* worms for survival on treatment with the analogues. The concentrations used for these experiments were the same as the optimal concentration of resveratrol (100µM in ethanol). It was observed that Resv1 and Resv4 compounds had an effect similar to resveratrol on the survival of the *dnj-14(ok237)* worms (Figure 4.11 B). Resv5 however failed to increase the lifespan of *dnj-14(ok237)* worms. The rescue effect albeit not as complete as resveratrol, was found to be significant ($P<0.05$; Log-Rank test) and the effect of these drugs were insignificant on the wild-type N2 (Figure 4.11 A) (mean lifespan in days of adulthood with SEM: N2: Et OH=14.28 ± 0.52; Res=14.95 ±

0.44; Resv1=15.42 ± 0.55; Revs4=15.77 ± 0.55; Resv5=14.56 ± 0.35. *dnj-14(ok237):* Et OH=13.02 ± 0.65; Resv=15.32 ± 0.68; Resv1=15.10 ± 0.73; Resv4=13.99 ± 0.61; Resv5=11.69 ± 0.51). These experiments were performed by M. Ayala under my supervision.

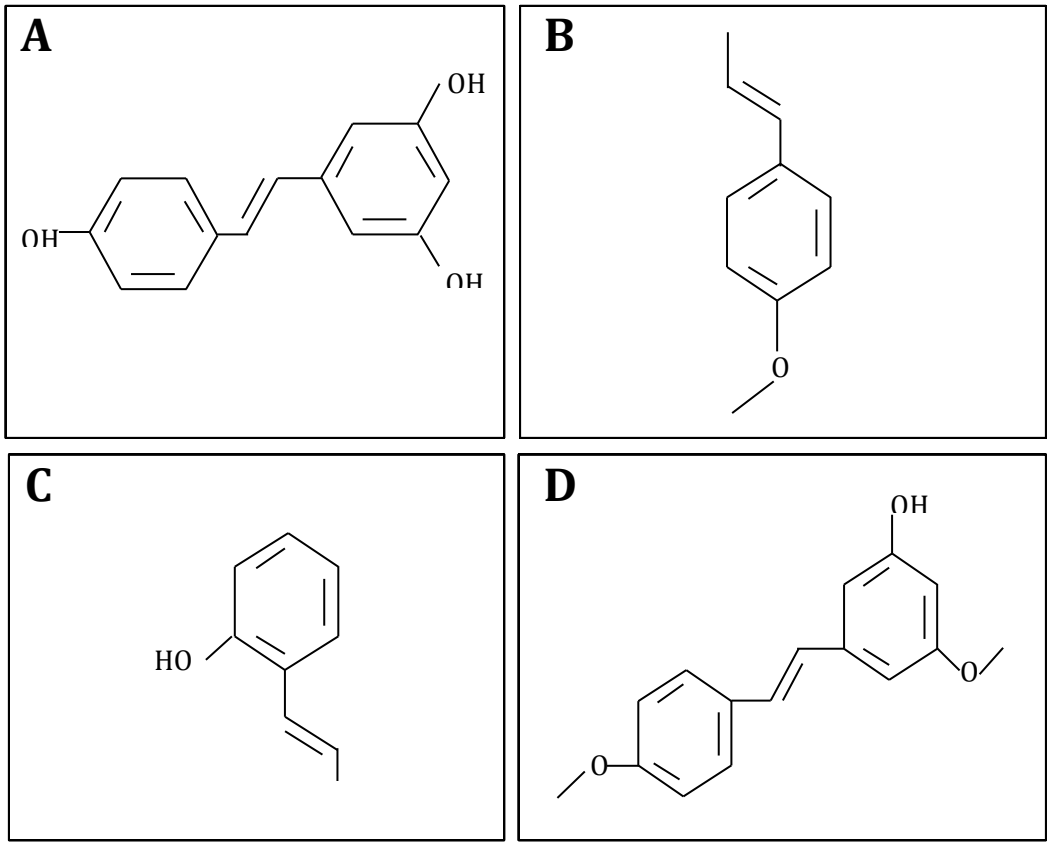

Figure 4.10: Structures of Resveratrol and similar compounds: Shows structures of Resveratrol, Resv1, Resv4 and Resv5 (A, B, C and D) respectively.

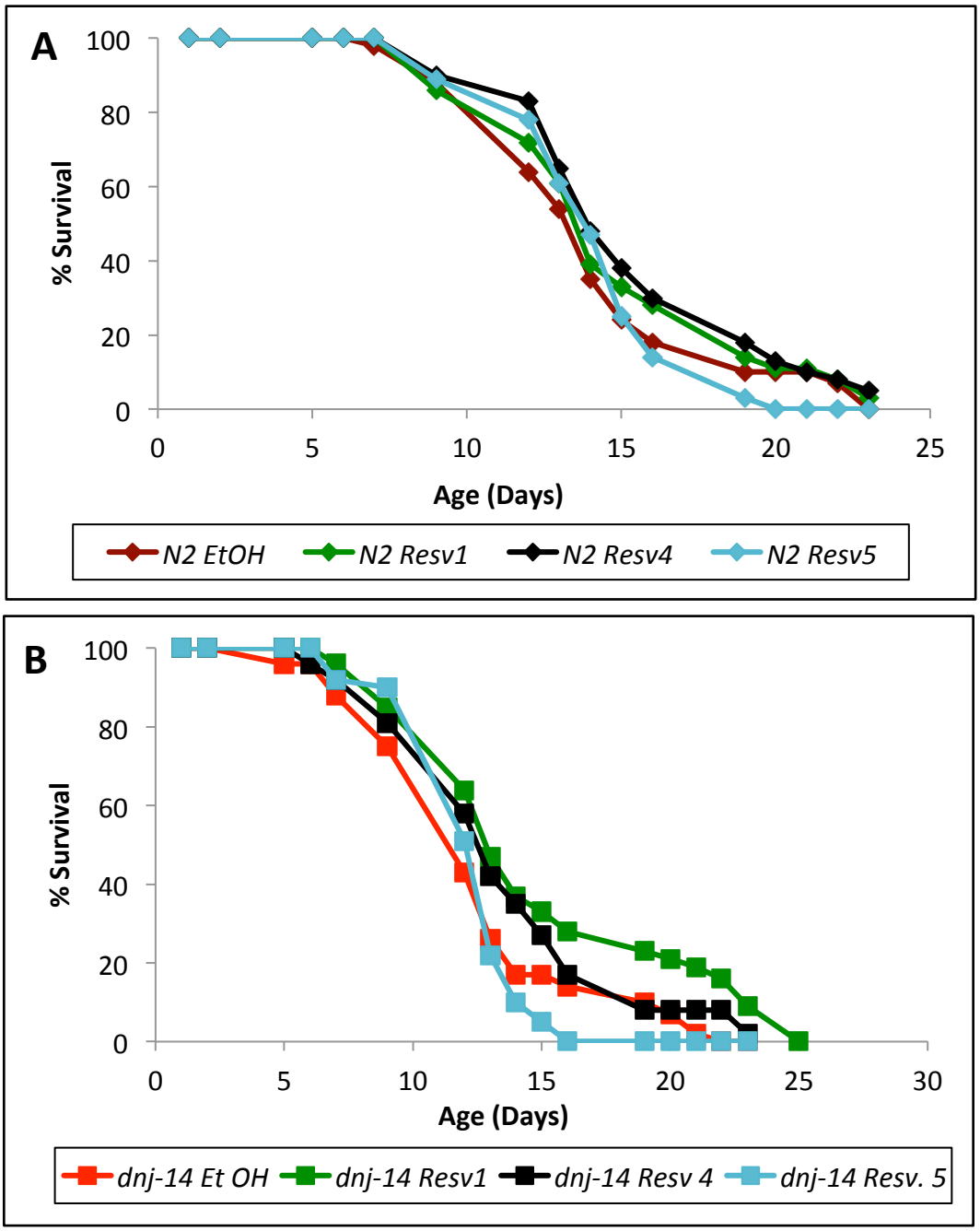

Figure 4.11: Resveratrol analogues rescue the lifespan of *dnj-14(ok237)* mutants. A) and B) Shows effect of Resveratrol analogues Resv1, Resv4 and Resv5 100µM each, on the lifespan of *dnj-14(ok237)* mutants. Above represented are pooled data from two independent biological replicate studies. Mean lifespan in days of adulthood with SEM – N2: Et OH=14.28 ± 0.52; Res=14.95 ± 0.44; Resv1=15.42 ± 0.55; Revs4=15.77 ± 0.55; Resv5=14.56 ± 0.35. *dnj-14(ok237):* Et OH=13.02 ± 0.65; Resv=15.32 ± 0.68; Resv1=15.10 ± 0.73; Resv4=13.99 ± 0.61; Resv5=11.69 ± 0.51. Ethanol (Et OH) was used as vehicle control. Lifespan of *dnj-14(ok237)* treated with Resv1 and Resv4 were significant to *dnj-14(ok237)* and the effect of drugs on wild-type were not significant. Resv5 did not have an effect on the lifespan of *dnj-14(ok237).* N=50 for all strains and conditions. Log-Rank test was used to calculate significance and $P<0.05$ was considered as significant.

4.4 DISCUSSION

In this chapter, both the *dnj-14* mutant alleles were used to illustrate the positive effects of resveratrol on the phenotype of these worms. For most experiments, apart from Figure 4.1 and Figure 4.11, outcrossed strains were used. The phenotypes of both outcrossed and non-outcrossed *dnj-14* worms should be same and hence it would be possible to compare the effect of resveratrol on these two directly. Some experiments were performed on only one of the *dnj-14* mutant strains as it has previously been established in chapter 3 that both the mutant strains were phenocopies of each other.

It was found that resveratrol completely rescued most of the phenotypes seen in the *dnj-14* mutants. It also rescued lifespan significantly and the optimal dose of resveratrol used on the mutants was found to be 100µM. This rescue of lifespan was found to be specific to both mutants of *dnj-14* as resveratrol had very minimal (statistically insignificant) or no effect on the lifespan of the wild-type N2. This was inconsistent with most results reported in earlier studies wherein an increase in the lifespan of the wild-type was seen (Wood et al., 2004, Gruber et al., 2007). Our results of the wild-type were consistent with the findings of another group which showed that the effect of resveratrol on the lifespan extension was debatable (Bass et al., 2007). However, the effect on the *dnj-14* mutants in our study revealed a clear rescue of lifespan.

Several studies in the past have revealed that a mutation in *daf-2*, which

encodes for the insulin-like growth factor 1 (IGF1), almost doubles the lifespan of the worms (Kenyon et al., 1993). This extension of lifespan in the *daf-2* mutants was shown to be mediated by DAF-16, the *C. elegans'* FOXO transcription factor (Lin et al., 1997). Functional DAF-16 is required for the activation of the *daf-2/daf-16* pathway, and hence if resveratrol were to act through this pathway, a *dnj-14;daf-16* double mutant should block the lifespan extending effects of seen in *daf-2* mutants. However, if resveratrol treatment on these double mutants does increase the lifespan, it would mean that resveratrol acts independent of the *daf-2/daf-16* pathway. A recent report has shown that in an amylotrophic lateral sclerosis model in worms, resveratrol protected against neurodegeneration and increased the lifespan in a *daf-16* and *sir-2.1* dependent manner (Tauffenberger et al., 2013). As it has been shown in this study that resveratrol acts independent of *sir-2.1* on the *dnj14* mutants, it would be interesting to investigate its dependency on *daf-16.*

Another mechanism through which resveratrol can mediate lifespan extension is through dietary restriction. In mice, there is evidence that resveratrol mimics the transcriptionary aspects of dietary restriction by delaying age-related deterioration without extending the lifespan (Pearson et al., 2008). An earlier report also suggested that resveratrol treated mice fed on a high calorie diet showed improved health and survival (Baur et al., 2006). SKN-1, the worm homologue of mammalian Nrf2, involved in cellular stress response to toxins (Osburn and Kensler, 2008), has been shown to be required for dietary

restriction mediated lifespan extension (Bishop and Guarente, 2007). However, *skn-1* has been shown to be directly inhibited by the *daf-2/daf-16* pathway (Tullet et al., 2008), suggesting an intersection between these two pathways.

Another regulator of dietary restriction could be the TOR (Target Of Rapamycin) pathway. RNAi of TOR in worms produces a longevity phenotype that is independent of the *daf-2/daf-16* pathway (Vellai et al., 2003). Most studies showed that reduction of TOR in worms already subjected to dietary restriction yielded no further increase in lifespan (Lee et al., 2006, Hansen et al., 2007), suggesting that TOR could be a key regulator of dietary restriction. Perhaps a more interesting aspect of the TOR pathway is its regulation of autophagy (Hars et al., 2007, Hansen et al., 2008).

In *C. elegans,* studies have shown that resveratrol promotes longevity through the regulation of the autophagic gene *bec-1* (Morselli et al., 2010). This cross talk between autophagy and resveratrol seems very interesting as there is enough evidence to suggest that the induction of autophagy confers neuroprotection in mice (Sarkar et al., 2009, Schaeffer et al., 2012), flies (Ravikumar et al., 2006) and cell culture studies (Berger et al., 2006, Williams et al., 2006). Several studies have identified resveratrol to be neuroprotective (Sharma and Gupta, 2002, Sinha et al., 2002, Yang and Piao, 2003, Fonseca-Kelly et al., 2012). As it has been shown by our experiments that resveratrol rescues neurodegenerative phenotype in the *dnj-14* mutants, one possibility could be

that resveratrol promotes autophagy in *dnj-14* mutants. However, this resveratrol dependent induction of autophagy was shown to be dependent on *sir-2.1* (Morselli et al., 2010). Several other studies on longevity and neuroprotection have shown that resveratrol acts through *sir-2.1* (Parker et al., 2005, Tauffenberger et al., 2013). On the contrary, in the *dnj-14* mutants resveratrol action was shown to be independent of *sir-2.1* activity. Some reports suggest that resveratrol acts in a sirtuin independent manner shown in rats (Zhang, 2006) and lower invertebrates (Bass et al., 2007). Rolipram indeed mimicked the effects of resveratrol in the *dnj-14* mutants suggesting that resveratrol could act through inhibition of PDEs as seen before in mice (Park et al., 2012). Downstream of PDE inhibition is the activation of AMP kinase (Park et al., 2012) and AMP kinase is also a known regulator of autophagy (Lee et al., 2010, Kim et al., 2011, Mao and Klionsky, 2011). Hence, this further strengthens the idea that in the *dnj-14* mutants, resveratrol could act through induction of autophagy. Resveratrol treatment on mutants of autophagic genes, *bec-1* and *aak-2* (*C. elegans'* homologue of AMP kinase), in a *dnj-14* mutant background would enable us to identify the exact mechanism of resveratrol action.

Another interesting result observed in the *dnj-14* mutants was the effects of drugs similar in structure to resveratrol on the worms' lifespan. Two drugs, Resv1 and Resv4 were shown to rescue the lifespan of *dnj-14(ok237)* worms significantly. These drugs had minimal or no effect on the lifespan of the wild-type N2. Resv1 is widely used as a flavouring agent in several alcoholic drinks,

seasonings, confectionary applications and oral hygiene products. It has also been shown to have antimicrobial properties against bacteria, yeast and fungi (De et al., 2002). Resv4 has been shown to prevent 6-hydroxydopamine (6OHDA) induced dopamine depression in mouse striatum (Kabuto et al., 2007). Therefore, functionally, these drugs have been known to have different properties compared to resveratrol. The fact that they induce an effect similar to resveratrol on the lifespan of *dnj-14* mutants, suggests that there could be similarities in certain domains of their chemical structure. An earlier study screened a large library of resveratrol related compounds to identify allosteric activators of Sirt1 (Milne et al., 2007). As the effect of resveratrol in *dnj-14* mutants is independent of *sir-2.1*, these compounds would be unlikely to induce a response similar to resveratrol in the *dnj-14* mutants. However these drugs could be key in identifying more potent synthetic compounds which mimic the sirtuin independent effects of resveratrol in *dnj-14* mutants and also for structure function studies on resveratrol. Hence with the help of resveratrol, Resv1 and Resv4, a whole variety of synthetic compounds could be tested and the *dnj-14* model offers a great platform for high throughput screens with these compounds.

The other remarkable result of the deletion of *sir-2.1* in *dnj-14* mutants was the rescue of the chemosensory defects seen in *dnj-14* mutants. Interestingly, the lifespan of the *dnj-14;sir-2.1* double mutants was lower than the *dnj-14* mutant. However, this reduction was marginally insignificant with a P value of 0.06. This

could be explained as follows. We hypothesise that the lifespan of the *dnj-14* mutants is much lower but as a result of the chemosensory degeneration, a slight increase in lifespan is seen. This could be explained by the findings of a previous study which indicated that mutations in proteins involved in chemosensation leading to chemosensory inability results in an extension in lifespan (Alcedo and Kenyon, 2004). However, in the *dnj-14* mutants, as more neurons degenerate with advancing age, the worms die prematurely and hence have a reduced lifespan compared to the wild-type N2.

The loss of deacetylase activity of Sirt1 in mice has been shown to render neuroprotection in the cerebellar granule neurons (Pfister et al., 2008). It has also been shown that genetic or pharmacological reduction of Sirt2 provides neuroprotection in a fly model of Huntington's disease (Pallos et al., 2008). Interestingly, *sir-2.1* in *C. elegans* is involved in repressing a protein called ABU-11 (Viswanathan et al., 2005) which is involved in ER stress response and expressed in the ciliated sensory neurons (Blacque et al., 2005). Hence, in *dnj-14* mutants, loss of *sir-2.1* would result in the overexpression of *abu-11* which could help prevent neurodegeneration of sensory neurons resulting in a rescue of chemosensory assays. It was also shown that resveratrol also increases ABU-11 in worms (Viswanathan et al., 2005) and hence this could explain why both resveratrol and *sir-2.1* deletion has the same effect on the chemosensory assays seen in *dnj-14* mutants.

CHAPTER 5: INTERACTION BETWEEN CSP AND SNAP-25 IN *C. ELEGANS*

5.1 INTRODUCTION

5.1.1 EXOCYTOSIS AND NEURONAL SNARE PROTEINS

Exocytosis in the neuronal synapse is essential for the release of neurotransmitters and hence in the maintenance of neuronal homeostasis. A key group of proteins that regulate this process is the neuronal SNARE (soluble N-ethylmaleimide-sensitive factor-attachment protein receptor) complex. Functionally, SNARE proteins can be divided into: v-SNAREs composed of synaptobrevin bound to the vesicle and t-SNAREs composed of plasmalemmal proteins, syntaxin1 and SNAP-25 (Chapman et al., 1994).

The core SNARE complex is composed of both v-SNARE and t-SNARE proteins. Structurally, the SNARE proteins are also classified as R and Q-SNAREs. R-SNAREs contribute an arginine (R) residue in the formation of the zero ionic layer in the assembled core of the SNARE complex whereas Q-SNAREs donate a glutamine (Q) (Bruns, 1997). The R-SNAREs in neurons is made of synaptobrevin and the Q-SNAREs are made of syntaxin and SNAP-25. The SNARE complex is a four α-helix bundle with one α-helix contributed by synaptobrevin, one by syntaxin and two by SNAP-25 (synaptosome associated protein of 25kDa) (Sollner et al., 1993). These SNARE proteins are specific substrates to eight clostiridial neurotoxins (one tetanus toxin, TeNT, and seven botulinum toxins, BoNT/A-G) (Schiavo et al., 2000a). These neurotoxins were shown to specifically bind and cleave a fragment of SNARE proteins at their cytosolic regions

(Simpson, 2004). This discovery epitomized the physiological importance of these proteins in the neuronal synapse.

5.1.2 SNAP-25 AND ITS ROLE IN EXOCYTOSIS

SNAP-25 is expressed in neurons on the cytoplasmic face of the plasma membrane in the synaptic terminal, all through the axons and also in small amounts in the secretory vesicles (Hanson et al., 1997). It has two isoforms, SNAP-25a and SNAP-25b, which are expressed differentially. SNAP-25a is expressed early in development and SNAP-25b is expressed during and after synaptogenesis (Wilson et al., 1996).

SNAP-25 is a hydrophilic protein that is palmitoylated at the centre flanked by two highly conserved α-helices at the N and C terminus (Hodel, 1998). It contains a small membrane targeting sequence that spans from amino acid 85-120 consisting of four cysteine residues that are palmitoylated and a QPARV motif that is important for DHHC interaction (Greaves et al., 2010). In the plasma membrane, SNAP-25 can form complexes with syntaxin which then bind to synaptobrevin to form the highly stable four helix bundle, the SNARE complex (Sutton et al., 1998). Moreover, there is evidence that SNAP-25 stoichiometrically binds to the putative calcium sensor, synaptotagmin and this interaction is thought to be very important in the calcium dependent release of neurotransmitters (Montecucco et al., 2005). SNAP-25 is cleaved by BoNT A, E and C1 at the C terminus thereby truncating the protein; BoNT A and E cleaves SNAP-25 exclusively whereas BoNT C1 also cleaves syntaxin (Schiavo et al., 2000b) leading to paralysis in clinically developed botulinism and thereby illustrating its importance in neurotransmission.

Although loss of SNAP-25 in mice results in developmental lethality heterozygous mice expressing a 50% reduction in SNAP-25 are still viable while exhibiting spontaneous hyperactivity (Wilson et al., 1996, Oliver and Davies, 2009). This hyperactivity was shown to be rescued by the treatment of D-amphetamine (Hess et al., 1996), a drug that promotes the release of dopamine through a non-vesicular mode (Floor and Meng, 1996). This indicates a lowered synaptic dopamine release in these SNAP-25 mutants. Polymorphisms in SNAP-25 have recently been shown to be a risk factor in the development of attention-deficit hyperactivity disorder, ADHD (Thapar et al., 2005). Also another study indicated that a heterozygous deletion in SNAP-25 affected the size of the vesicle pools and the kinetics of priming/depriming of vesicles (Bark, 2009) making it one of the most important players in the exocytotic machinery.

5.1.3 SNAP-25, CSP AND NEURODEGENERATION

The possibility that a deficiency in SNARE complex assembly might lead to neurodegenerative disorders can be substantiated by the reduction of synaptic proteins and the assembly of the SNARE complex in brain homogenates of patients suffering from Alzheimer's and Parkinson's diseases (Sharma et al., 2012b). This is consistent with previous studies in dementia patients wherein a reduction in synaptic proteins was seen in their brain samples (Head et al., 2009, Beeri et al., 2012). This suggests a link between neurodegenerative diseases, neurodegeneration and the SNARE complex. There is also a reduction in the levels of SNARE complex and SNARE proteins in CSP knockout mice (Sharma et al., 2011). More importantly, the same study also showed that the facilitation of SNAP-25 into the SNARE complex was chaperoned by CSP (Sharma et al., 2011). CSP knockout mice, as explained before, exhibit progressive pre-synaptic neurodegeneration (Fernandez-Chacon et al., 2004). It was also shown that heterozygous loss of SNAP-25 in CSP knockout mice worsened the neurodegeneration phenotype, which was rescued by the overexpression of SNAP-25 (Sharma et al., 2012a). These studies suggest that the proper functioning of the SNARE complex is important and its regulation of exocytosis plays a key neuroprotective role. Having earlier shown that the conservation in the neurodegenerative phenotypes exist between higher mammals such as mice and lower vertebrates like C. elegans, it remains to be seen whether the mechanism of neurodegeneration is also the same in higher mammals and

lower vertebrates. Hence the basis of this study is to investigate the relationship between CSP and SNAP-25 in worms.

5.2 METHODS

The methodology remains similar to that mentioned in the earlier sections with the exception of the key points mentioned below.

5.2.1 *C. ELEGANS* STRAINS

Apart from the wild type N2, *dnj-14(ok237)* and *dnj-14(tm3223),* which were used in the previous chapter, the *ric-4(md1088)* strain obtained from the Caenorhabditis Genetics Center (University of Minnesota, Twin Cities, MN, USA) was used for experiments that are the focus of this chapter. Outcrossed *dnj-14* strains were used in most assays. *dnj-14(ok237)* was outcrossed six times whereas *dnj-14(tm3223)* was outcrossed five times.

5.2.2 PCR ANALYSIS OF *MD1088* MUTATION

Regions of the *ric-4* gene were amplified using PCR using many trial primers. These were then run on an agarose gel. The amplified DNA bands were excised and purified using GenElute™ Gel Extraction Kit (Sigma-Aldrich®). 20µL of the extracted DNA was added to a PCR tube containing 3.2pmoles of one of the primers used in the PCR reaction. The volume was made up to 32µL using Ambion® Nuclease-Free Water (Life technologies™) and was sent to the DNA Sequencing and Services™, University of Dundee, Dundee. The results were then analyzed using BLAST (http://blast.ncbi.nlm.nih.gov) and the quality of the

sequencing was determined by analysing the DNA chromatogram using DNA Baser Sequence Assembler (Heracle BioSoft®).

5.2.3 WORM CROSSING

The *dnj-14*;*ric-4* double mutant was made by first crossing the *dnj-14* mutant hermaphrodites with wild-type N2 male worms. The *dnj-14* male progeny obtained from the cross were then allowed to mate with *ric-4* hermaphrodites. The resulting F1 hermaphrodite progeny was heterozygous to both alleles. These worms were then picked onto replica NGM plates (40mm) such that each plate had a single worm on it. One-sixteenth of the resulting F2 progeny should be double mutants. The double mutants were genotyped using PCR analysis and agarose gel electrophoresis. Both *dnj-14(ok237)* and *dnj-14(tm3223)* mutants were used to obtain *dnj-14(ok237)*;*ric-4(md1088)* and *dnj-14(tm3223)*;*ric-4(md1088)* double mutants.

5.2.4 PCR ANALYSIS AND STRAIN VERIFICATION

DNA was extracted from the segregated F2 progeny obtained from the cross and amplified by a PCR as explained before. The primers used to amplify the DNA in this chapter includes:

a) *dnj-14* del rev - 5'-TGCTCTCAACAGACCCATAC-3',

b) tm3223 del full fwd: 5'-GCTTGTCTTACCTTATGTCGTCG-3',

c) *dnj-14* del full fwd: 5'-CAGATAGTTCATACTGAAAATCT-3',

d) *dnj-14* del mid fwd: 5'-ATTCGCACGATCCGAAAAAG-3',

e) *ric-4* ex5 rev: 5'-CGTGATTGAAAAATGGAGCTG-3'

f) *ric-4* ex5 fwd: 5'-.CCATGTTACGCAAATTGCCGA-3'.

The annealing temperature was calculated using a Tm Calculator (New England Biolabs;https://www.neb.com/tools-and-resources/interactive-tools/tm-calculator).

5.2.5 CONSTRUCTION OF P*dnj-14::ric4* PLASMID

The coding sequence of *ric-4*b, lacking exons, was synthesized by GeneArt (Invitrogen, UK) and sub-cloned immediately downstream of the putative *dnj-14* promoter (bases -1 to -560 relative to the ATG start codon) into the pPD117.01 plasmid with the GFP-coding region excised.

5.2 RESULTS

5.2.1 PHENOTYPIC ANALYSIS OF SNAP-25 IN *C. ELEGANS*

SNAP-25 has a single homologue in *C. elegans*, *ric-4* with a homology of 52%. The *ric-4* gene in *C. elegans* has two isoforms, *ric-4*a and *ric-4*b with differences only in the N-terminal domain with the *ric-4*b isoform having a longer N-terminus (Figure 5.1 A). RIC-4 has two t-SNARE domains, α-helices, at the N and C-termini that are required for SNARE complex formation. These are flanked by a cysteine rich domain, which is palmitoylated (Lane and Liu, 1997) and involved in the facilitation of RIC-4 into membranes (Greaves et al., 2009). This region between the SNARE domains also consists of a conserved domain, which is the activation site for the DHHC palmitoyl transferases, which palmitolyate the cysteine residues (Greaves et al., 2010) (Figure 5.1 B).

Two mutant alleles were obtained for analysis of *ric-4*. The gk322 contained an 822bp deletion at the N-terminus of the *ric-4*a gene. The second allele, *md1088*, had no available information regarding the mutation. Mutants containing the *md1088* allele however were shown in previous studies to have a short lifespan and were resistant to aldicarb (Miller et al., 1996, Shen et al., 2005). Aldicarb assay, which is an indirect read out of the neurotransmission at the synapse, was performed on both mutant types and the results suggested that both the *ric-4* alleles, *md1088* and *gk322*, showed an increased resistance to aldicarb (Figure 5.2 A). The *md1088* allele had significantly increased resistance compared to the gk322 ($P<0.01$) and the wild-type N2 ($P<0.001$). The resistance

to aldicarb of *md1088* mutants were shown in previous reports as well (Miller et al., 1996).

Locomotion assays were performed on these two mutant alleles of *ric-4* and it was found that the *md1088* allele had a slight but significant reduction in locomotion ($P<0.05$) (Figure 5.2 B). The gk322 mutants however showed locomotion levels similar to wild-type N2 (Figure 5.2 B). Moreover, the locomotion of *md1088* mutant was similar to that of the *dnj-14* mutants. Therefore all further work was carried out on the *md1088* mutants. Lifespan assays were then performed on these mutants and it was again found that similar to *dnj-14* mutants, *ric-4(md1088)* mutants had a significant reduction in lifespan (Figure 5.3). This was rescued significantly by the treatment of resveratrol (Figure 5.3). These results suggested that there could be an interaction between *ric-4* and *dnj-14*. However, the mutation in the *md1088* mutants needed to be established before this interaction could be investigated further.

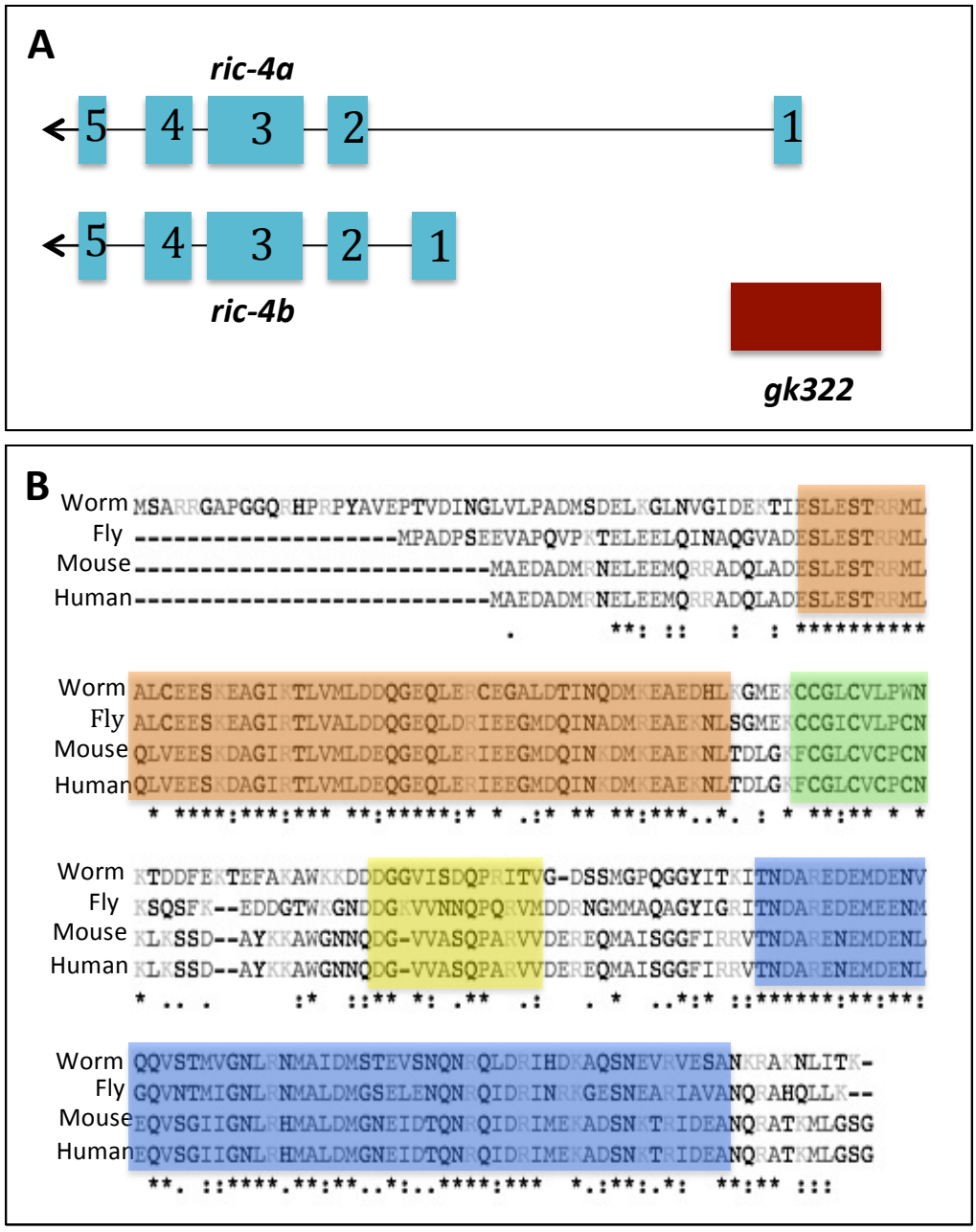

Figure 5.1: Genetic analysis and homology of *ric-4* gene: A) Shows the two isoforms of *ric-4* – *ric-4a* and *ric-4b* which differs in the position and sequence of the first exon. The first exon of *ric-4a* smaller than that of *ric-4b* and is further upstream separated by huge intron. The *gk322* allele has a 822 bp deletion near the first exon of *ric-4a.* B) Shows multiple sequence alignment of RIC-4 and its SNAP-25 homologues in flies, mice and humans respectively. Also highlighted are the conserved regions – the N-terminal tSNARE domain (brown), the cysteine rich domain (green), binding site for the DHHC palmitoly transferase (yellow) and the C-terminal tSNARE domain (blue).

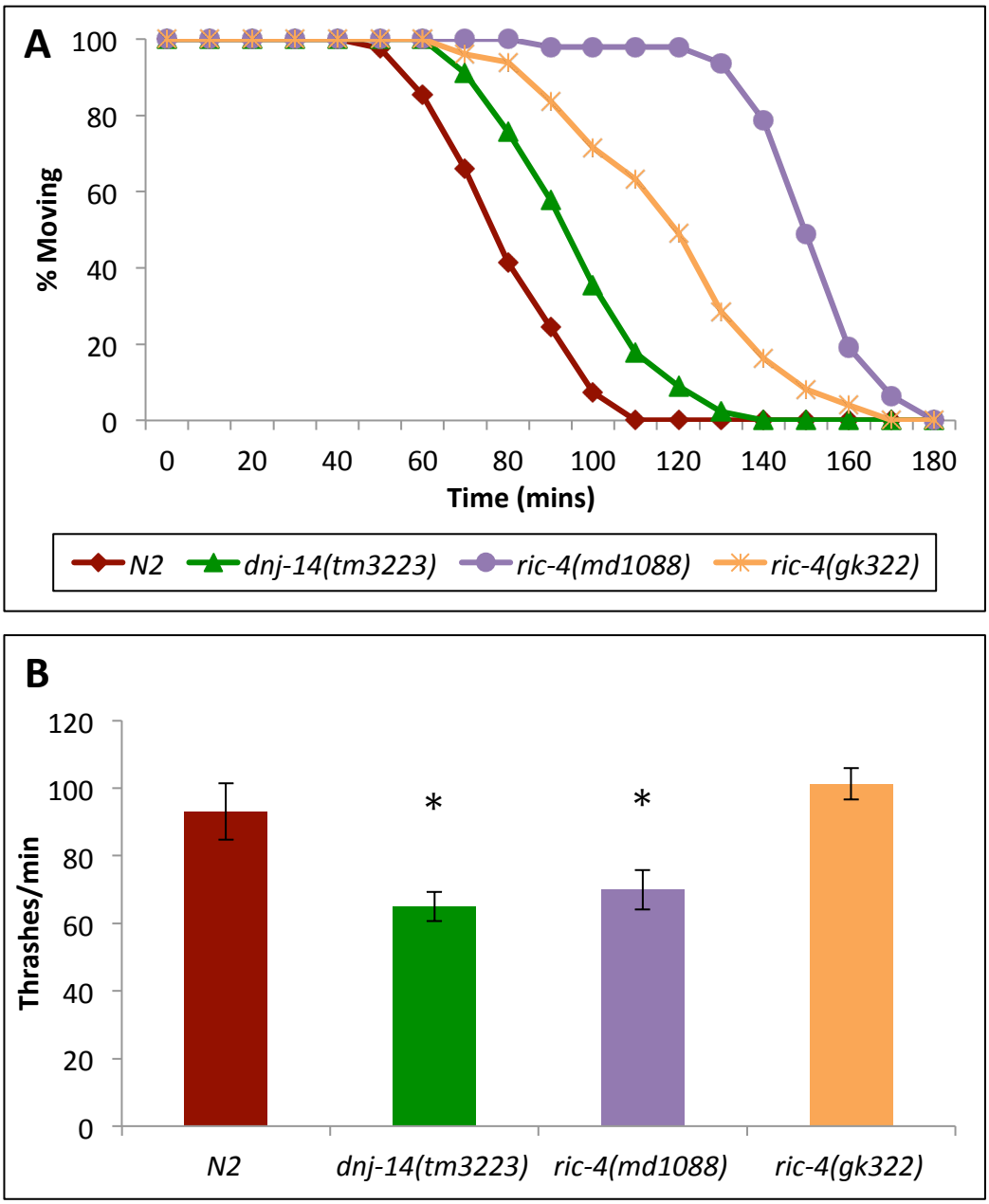

Figure 5.2: Aldicarb resistance and locomotion variance of *ric-4* mutants: A) Shows aldicarb resistance of both the *ric-4* mutant alleles, *md1088* and *gk322*. About 20-25 worms were age synchronized to day 6 of adulthood and picked on to plates containing 1mM alidcarb. Number of worms paralyzed were counted every ten minutes till every worm paralyzed. All three mutant strains are significantly 'ric' compared to the wild-type N2 ($P<0.05$) with the *ric-4(md1088)* worms being highly resistant. Above represented are pooled data from two independent biological replicate studies. Mean paralysis time (mins): N2=82.2 ± 2.4 (n=41); *dnj-14(tm3223)*=98.89 ± 2.61 (n=45); *ric-4(md1088)*=153.83 ± 2.22 (n=47); *ric-4(gk322)*=121.43 ± 3.48 (n=49). Log-Rank test was used to calculate significance and $P<0.05$ was considered as significant. B) Shows locomotion of mutant strains in Dent's Ringer solution. Worms were age synchronized to day 6 of adulthood and placed on a drop of Dent's Ringer solution and the number of thrashes were counted per minute. The *ric-4(md1088)* mutants thrash at a similar level compared to the *dnj-14(tm3223)* mutant and both were significantly lower than the wild-type. Mean thrashing rates per minute: N2=93.13 ± 8.36; *dnj-14(tm3223)*=64.93 ± 3.57; *ric-4(md1088)*=69.93 ± 4.31; *ric-4(gk322)*=101.26 ± 5.81. N=20 for all strains. Student's t-test was used to calculate significance (*) and $P<0.05$ was considered significant.

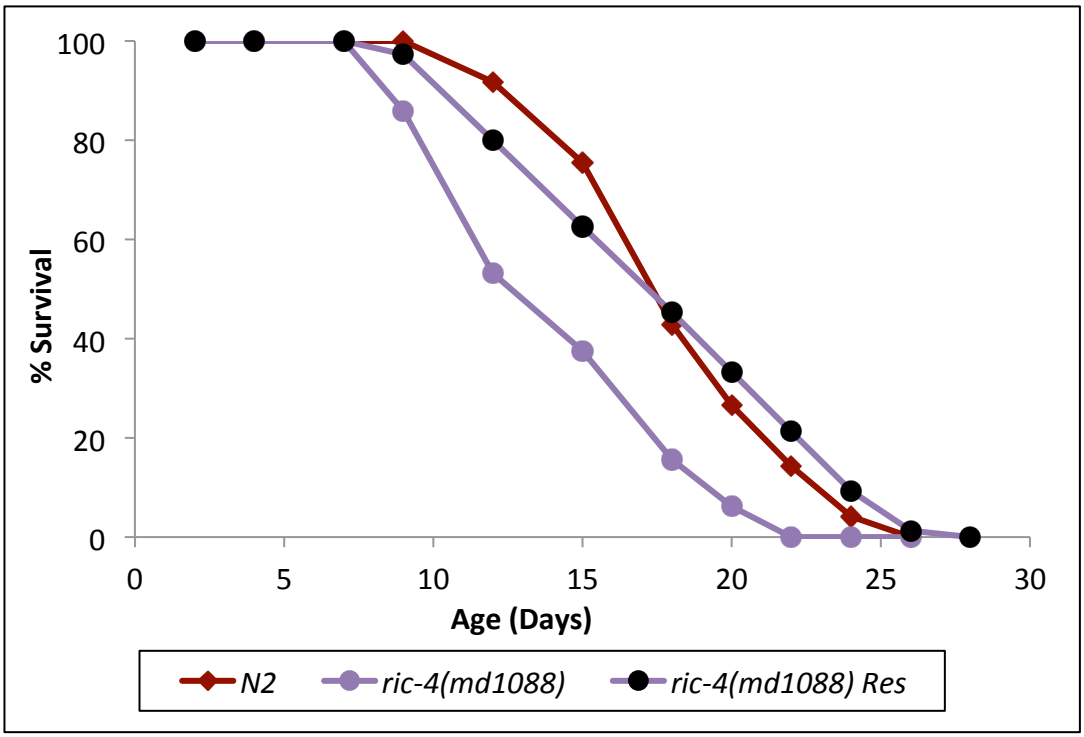

Figure 5.3: Short lifespan of *ric-4(md1088)* rescued by treatment of resveratrol: Shows lifespan assay performed on *ric-4(md1088)* worms upon treatment with 100µM resveratrol. Figure shows that resveratrol significantly (P<0.05) rescues the lifespan of *ric-4(md1088)* worms similar to the effect seen in *dnj-14* mutants. Ethanol was used as the vehicle control. Above represented are pooled data from three independent biological replicate studies. Mean lifespan in days: N2=18.78 ± 0.51 (n=71); *ric-4(md1088)*=14.73 ± 0.49 (n=64); *ric-4(md1088)* Resv=18.41 ± 0.51 (n=75). Log-Rank test was used to calculate significance and P<0.05 was considered as significant.

5.3.2 GENETIC ANALYSIS OF *MD1088* ALLELE

The *md1088* mutant was identified in a screen for aldicarb resistant mutants performed by Prof. James Rand in which two strains with elevated levels of transposon Tc1 activity; RM25 and TR638 were used (Miller et al., 1996). Tc1 transposon is a 1610 base pair element with inverted terminal repeats which would jump along genes and attach itself to sites containing the activation sequence CAAAT adding an extra AT during insertion (Rosenzweig et al., 1983). This results in a Tc1 transposon insertion being flanked by an imperfect palindrome (CAAATA:Tc1:TATATG) thereby making the insertion stable (Rosenzweig et al., 1983). This suggested that the *md1088* allele could have an insertion rather than a deletion.

Hence primers were made along the coding regions of *ric-4* (Figure 5.4 A) and were PCR amplified. The amplified DNA was then purified and subsequently sequenced. It was found that the *md1088* allele contained a mutation at the end of exon 3 of *ric-4*, which corresponded to a 1.6kb insertion of the Tc1 transposon (Figure 5.4 A and B). The mutation leads to the addition of 14 amino acids after Tyr162 leading to an early truncation. This would mean that if translated, the mutant RIC-4 would contain just the first t-SNARE domain (Figure 5.4 C). The truncated protein would also contain the cysteines required for membrane association and the palmitolylation site for these cysteines.

Western blots were performed on worm lysates of wild type and mutants to establish whether the truncated protein is expressed or not. However, in the mutants, in spite of observing a lower band at the predicted molecular weight of the truncated protein, a band for the wild-type RIC-4 could not be observed in the wild-type N2 despite repeated attempts (Data not shown).

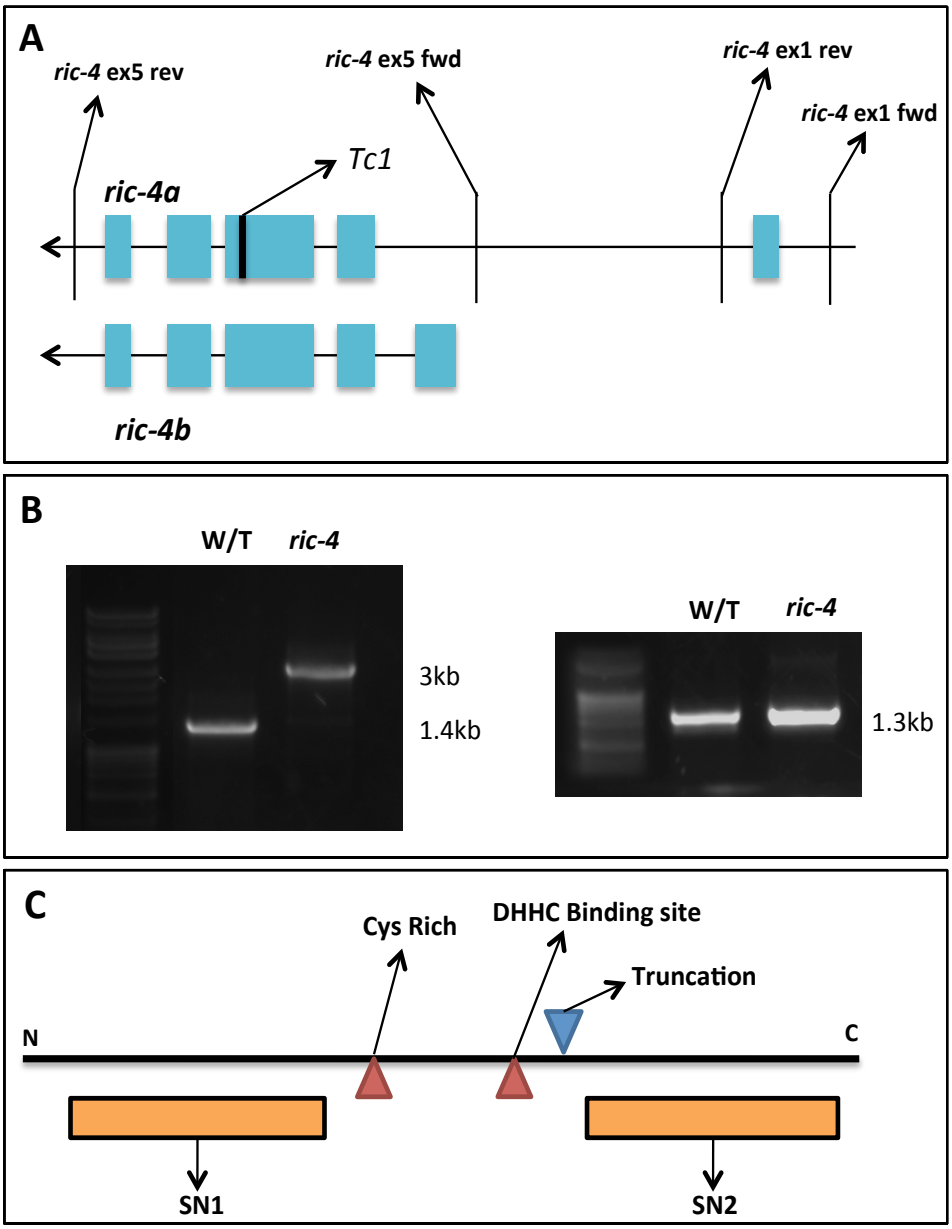

Figure 5.4: Molecular analysis of the *md1088* allele reveals a Tc1 transposon insertion: A) Shows the binding site of the primers prepared to analyse the mutation in the *md1088* allele and also shows the Tc1 transposon insertion site. B) Agarose gel showing PCR amplified DNA samples of two exon domains in the *ric-4* gene niche. In the right panel, it can be seen that both the wild-type and the mutant have bands of similar size suggesting there is no insertion or deletion in that region. In the left panel, it can be seen that the *ric-4* mutants have a 1.6kb insertion corresponding to Tc1 transposon. C) Shows the secondary structure of RIC-4 protein with the individual SNARE domains, the cysteine rich region, binding site for the DHHC palmitoyl transferase and the truncation site in the *ric-4* mutant.

5.3.3 ANALYSIS OF RIC-4;*DNJ-14* DOUBLE MUTANT

To investigate the interaction of RIC-4 and DNJ-14 in vivo, both mutant strains were crossed with each other to form a double mutant. With the mutation in the *ric-4* mutants now established these worms could be genotyped using PCR analysis. Male *dnj-14* worms were crossed with the *ric-4* hermaphrodites and the resulting F1 progeny were grown on replica plates. The F2 generation was screened for both the mutant alleles by genotyping. On isolation, the double mutants were observed to be viable with normal movement on the plate.

Similar to the characterization of the *ric-4(md1088)* mutant, thrashing assays were performed on the double mutant at days 3 and 6 of adulthood so the phenotypes could be compared with the individual mutants. It was observed that locomotion was reduced in these double mutants as compared to the wild-type N2, but not significantly different from the individual mutants (Figure 5.5 A). Lifespan assays were then performed on the double mutant worms to ascertain whether the double mutants exhibit a further reduction in survival compared with the individual mutants. As shown in Figure 5.5 B the *ric-4*;*dnj-14* double mutants had a lifespan that was comparable to the individual mutants (mean Lifespan in days of adulthood: N2 - 18.33±0.65; *dnj-14(ok237)* - 14.19±0.68; *ric-4(md1088)* - 14.82±0.61; *dnj-14;ric-4* - 14.80±0.62).

In the case of the *dnj-14* and *ric-4* individual mutants, the lifespan of these double mutants was also shown to be rescued by the treatment of resveratrol

(Figure 5.6) (mean Lifespan in days of adulthood: N2 - 19.54±0.85; *dnj-14(tm3223)* - 14.83±0.88; *ric-4(md1088)* - 15.30±0.56; *dnj-14;ric-4* - 14.88±0.63; *dnj-14*;*ric-4* Resv - 17.80±0.58) suggesting a genetic epistasis between DNJ-14 and RIC-4 in worms. Thus it could be inferred that the interaction between CSP and SNAP-25 is conserved in *C. elegans*.

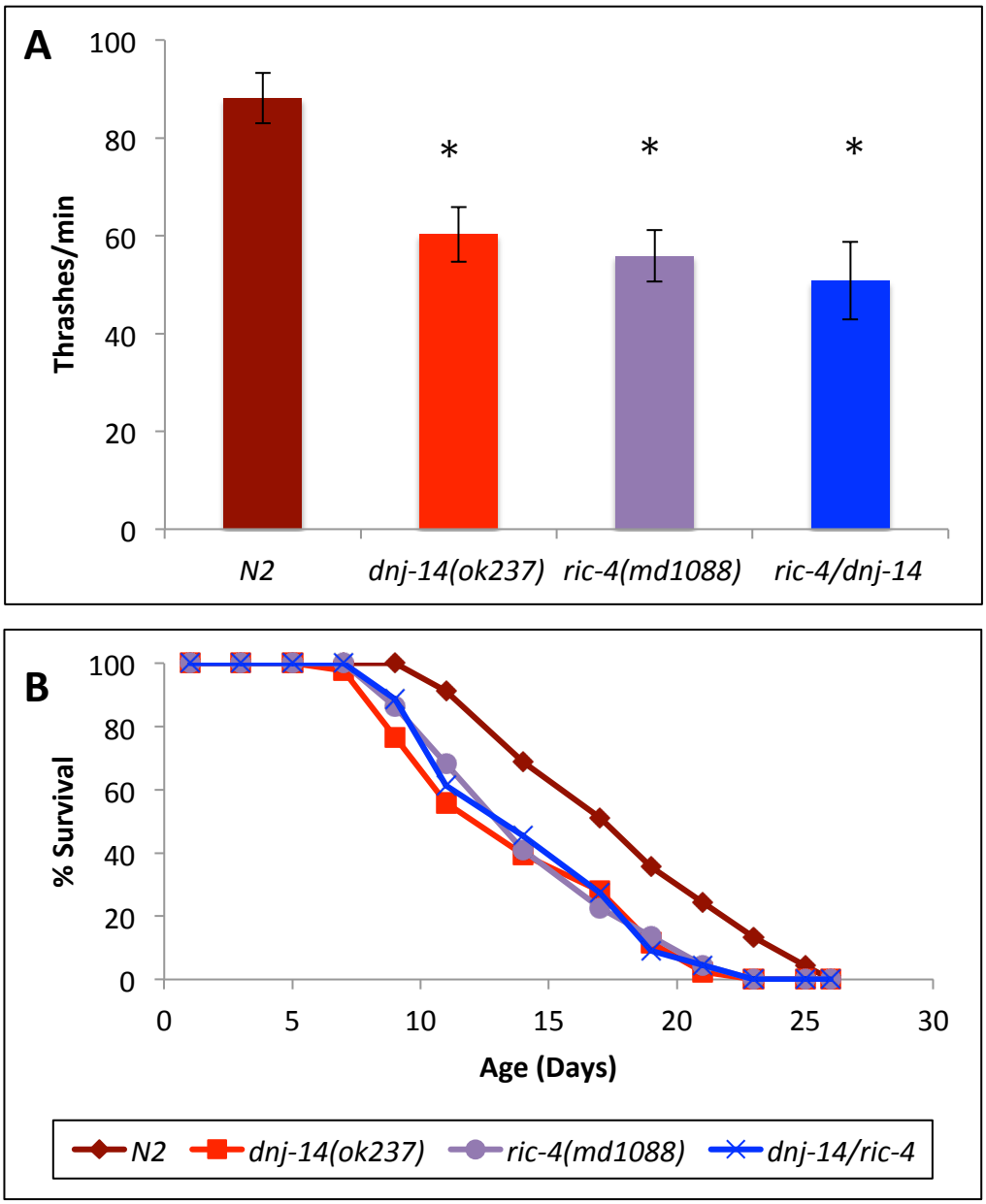

Figure 5.5: *dnj-14;ric-4* double mutant phenotypically similar to the individual mutants: A) Shows thrashing assays performed on worms aged at day 6 of adulthood. The figure shows the double mutants thrash similar to the individual mutants and are significantly lower than the wild-type N2. Mean thrashing rates/minute: N2=88.1 ± 5.13; *dnj-14(ok237)*=60.3 ± 5.61; *ric-4(md1088)*=55.9 ± 5.25; *dnj-14(ok237);ric-4(md1088)*=50.8 ± 7.9. N=20 for all strains. Student's t-test was used to calculate significance (*) and P<0.05 was considered significant. B) Shows lifespan assay performed on the *dnj-14;ric-4* double mutant with the wild-type N2 and the individual mutants as control. It is seen that the lifespan of the double mutant is similar to that of the individual mutants and significantly lower than the wild-type N2. Above represented are pooled data from three independent biological replicate studies. Mean lifespan in days of adulthood: N2=18,33 ± 0.65 (n=45); *dnj-14(ok237)*=14.19 ± 0.68 (n=43); *ric-4(md1088)*=14.82 ± 0.61 (n=44); *dnj-14;ric-4*=14.80 ± 0.62 (n=44). Log-Rank test was used to calculate significance and P<0.05 was considered as significant.

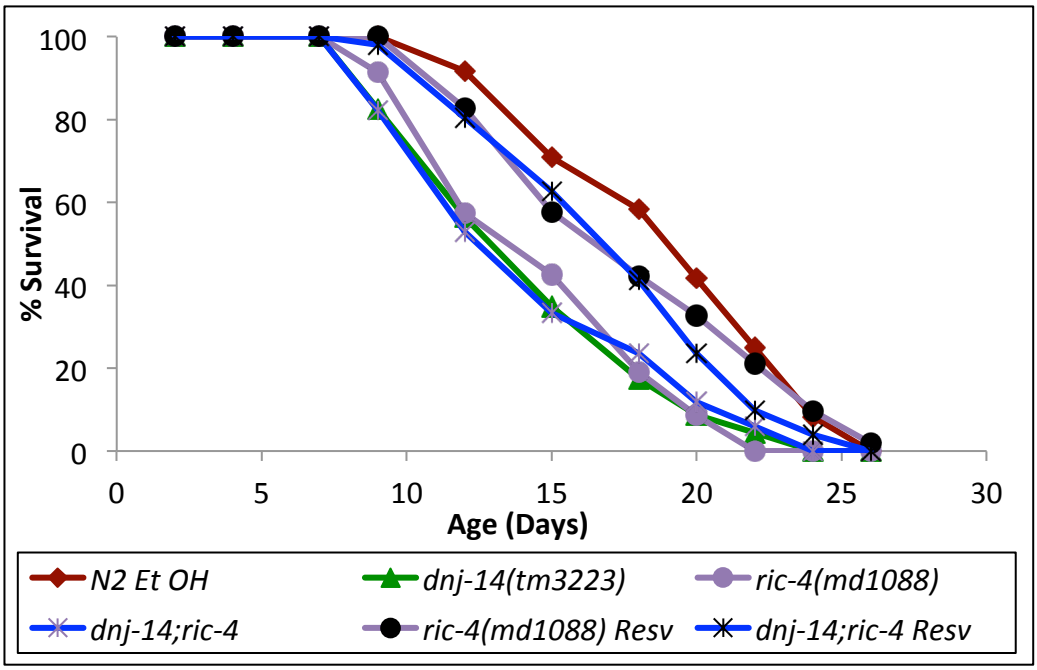

Figure 5.6: Resveratrol rescues the lifespan of the *dnj-14;ric-4* double mutant: Figure shows lifespan analysis performed on the *dnj-14(tm3223);ric-4(md1088)* double mutant in the presence of 100µM resveratrol. Wild-type N2 and the individual mutants were used as control. It can be clearly seen that the lifespan of the double mutant was significantly rescued with the treatment of resveratrol similar to the individual mutants. Above represented (except N2 and *dnj-14(tm3223)*) are pooled data from two independent biological replicate studies. Mean lifespan in days of adulthood: N2=19.54 ± 0.85 (n=24); *dnj-14(tm3223)*=14.83 ± 0.88 (n=23); *ric-4(md1088)*=15.30 ± 0.56 (n=47); *ric-4(md1088)* Resv=18.37 ± 0.64 (n=52); *dnj-14(tm3223);ric-4(md1088)*=14.88 ± 0.63 (n=51); *dnj-14(tm3223);ric-4(md1088)* Resv=17.80 ± 0.58 (n=51). Log-Rank test was used to calculate significance and P<0.05 was considered as significant.

5.3.4 OVEREXPRESSION OF RIC-4 IN DNJ-14 MUTANTS

As mentioned before, overexpression of SNAP-25 rescues the phenotype of the CSP knockout mice (Sharma et al., 2011). Hence it was postulated that regulation of exocytosis by the SNARE complex could play a key role in neuroprotection. In worms, as explained above, it has been established that there is genetic epistasis between DNJ-14 and RIC-4, however what remains to be seen is whether the over expression of RIC-4 rescued the phenotype of the *dnj-14* mutants.

Hence, a transgenic strain had to be created which over expresses RIC-4 in a *dnj-14* mutant background. The promoter sequence of *ric-4* has not been characterized and due to the presence of a huge intron in the middle of *ric-4a*, the second isoform *ric-4b* was cloned into a construct driven by the *dnj-14* promoter. This construct was injected into wild-type N2 worms and the injected transgenic lines were crossed into the *dnj-14(tm3223)* strains to maintain same levels of expression of RIC-4. Dr. Hannah McCue constructed these transgenic lines. Lifespan assays were then performed on these lines and it was found that the *dnj-14* mutants with RIC-4 overexpression (*dnj-14(tm3223)* OE), showed a significant rescue in lifespan as compared to the *dnj-14(tm3223)* mutants (Figure 5.7 A). The transgenic N2 OE control worms however did show a slight decrease in lifespan (Mean lifespan in days of adulthood: N2 - 19.58±1.06; N2 OE - 18.56±0.76; *dnj-14(tm3223)* - 14.52±0.82; *dnj-14(tm3223)* OE - 17.75±0.68)

but this was insignificant (P>0.05) compared to the lifespan of the wild-type N2 (Figure 5.7 A).

Next, food race assays were performed on these transgenic strains and it was seen that the overexpression of RIC-4 had a significant positive impact on the food race phenotype of the *dnj-14* mutants (Figure 5.7 B). These results indicate that the overexpression of RIC-4 does have a positive effect on the phenotypes of the *dnj-14* mutants. However, to analyse the rescue effect of overexpression on the neurodegeneration phenotype, integrated and stable transgenic lines would have to be created.

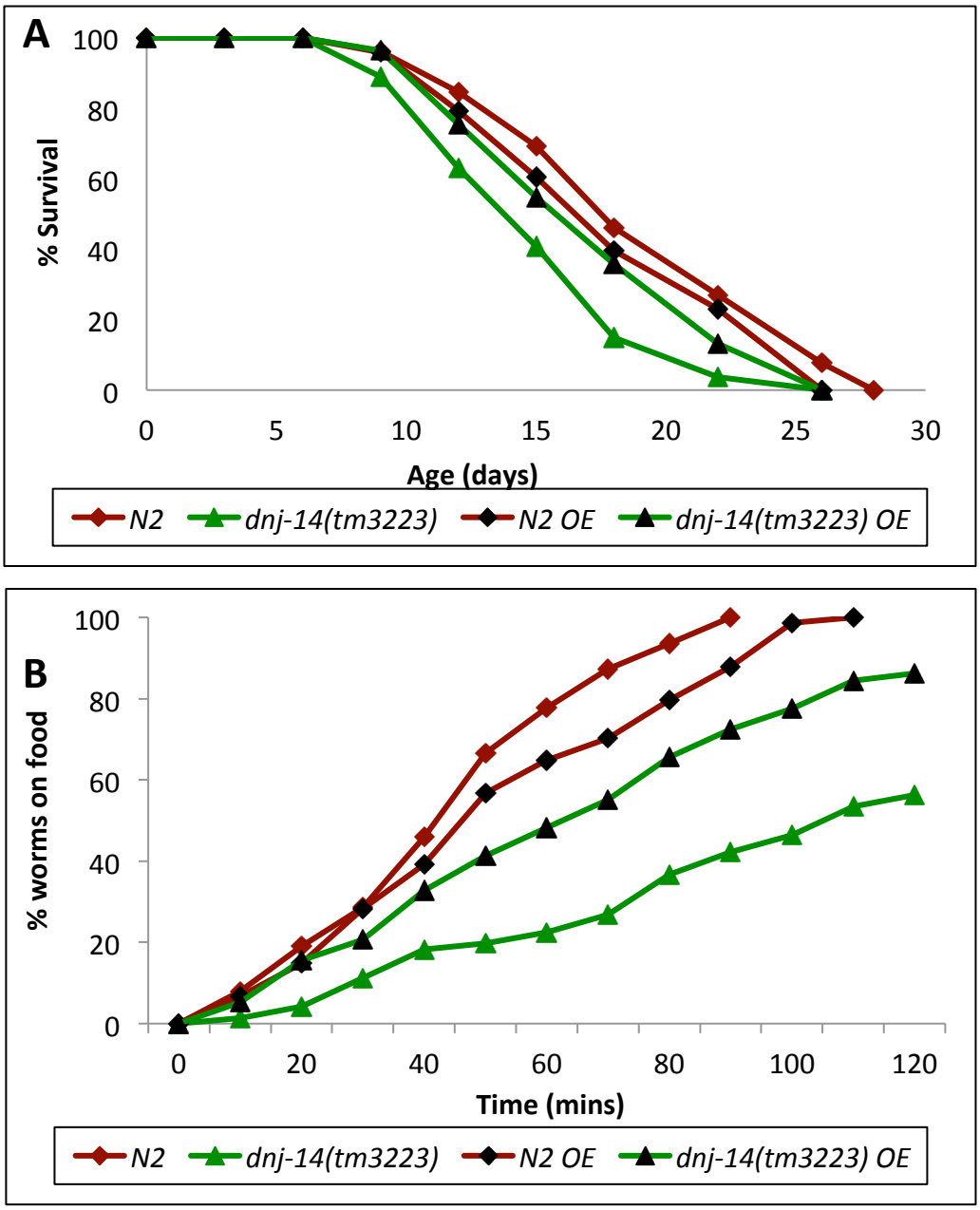

Figure 5.7: Overexpression of *ric-4* in *dnj-14* rescues lifespan and food race defects: A) Figure shows lifespan analysis performed on the transgenic wild-type N2 and *dnj*-14 mutants (N2 OE and *dnj-14(tm3223) OE)*. Wild-type N2 and *dnj-14(tm3223)* mutants were used as control. It can be clearly seen that the lifespan of the transgenic mutant was significantly increased. Above represented (except N2 and *dnj-14(tm3223)*) are pooled data from two independent biological replicate studies. Mean lifespan in days of adulthood: N2=19.58 ± 1.06 (n=26); *dnj-14(tm3223)*=14.52 ± 0.82 (n=27); N2 OE=18.56 ± 0.76 (n=48); *dnj-14(tm3223)* OE=17.75 ± 0.68 (n=53). Log-Rank test was used to calculate significance and P<0.05 was considered as significant. B) Shows food race assay performed on six-day old worms on NGM. Worms were washed in M9 buffer and placed on the corner of an NGM plate with 30µL of OP50 on the opposite corner. Worms reaching the food every 10 minutes were noted down till 120 minutes. Overexpression of *ric-4* in *dnj-14(tm3223)* rescues food race defects in *dnj-14* mutants significantly. Above data was pooled from from two independent biological replicate studies. and n_{N2}=63, $n_{N2\ OE}$=74, $n_{dnj\text{-}14(tm3223)}$=71, $n_{dnj\text{-}14(tm3223)\ OE}$=58. Log-Rank test was used to calculate significance and P<0.05 was considered as significant.

5.4 DISCUSSION

In this study, it has been shown that mutation in *ric-4* (homologue of SNAP-25 in *C. elegans*) in worms leads to phenotypes similar to the loss of *dnj*-14. The *ric-4(md1088)* mutants have a severe neurotransmission defect, which is read out as a large resistance to aldicarb. Similar to the *dnj*-14 mutants, the *ric-4* worms show a reduction in locomotion and lifespan. The type of mutation in the *ric-4(md1088)* worms, which could potentially lead to the expression of a truncated protein, makes these results interesting as loss of SNAP-25 in mice results in lethality (Washbourne et al., 2002).

In Drosophila, it has been shown that only in the absence of SNAP-25, another similar protein, SNAP-24 compensates for its loss and this compensation was absent in the presence of mutant forms of SNAP-25 (Vilinsky et al., 2002). This could be explained by the fact that SNAP-24 was shown to be able to form SNARE complexes with syntaxin and synaptobrevin in a different study (Niemeyer and Schwarz, 2000). It has also been shown that SNAP-23, another protein belonging to the SNAP-25 family, was shown to form ternary complexes with other SNARE proteins with albeit half the stability compared with the ternary complex formed by SNAP-25 (Montana et al., 2009). This suggests that SNAP-25 could be substituted for in some systems but not mice.

Interestingly the *ric-4(md1088)* mutants in *C. elegans* are viable and superficially wild-type. Hence, this suggests the possibility of other proteins with t-SNARE

domains, which could either lend a α-helix to form the SNARE complex or could completely substitute RIC-4 and form a faulty SNARE complex, which could possibly explain the abnormality in neurotransmission seen in the mutant. There are two possible candidate proteins for this in *C. elegans*, AEX-4 and SNAP-29. These two proteins respectively have 46% and 42% homology to RIC-4 and have t-SNARE domains. AEX-4 is an intestinal protein, which controls the defecation motor program in worms and contains a single t-SNARE domain (Mahoney et al., 2008). It has homology to both isoforms of RIC-4 and could donate the second α-helix required to make the SNARE complex. SNAP-29 in worms is expressed in many cell types and also some neurons (Kang et al., 2011). It has two t-SNARE motifs and is involved in endosome recycling (Kang et al., 2011). SNAP-29 is different from the other members of the SNAP family of worm proteins in that it does not have cysteine residues. Hence, SNAP-29 at least in itself might not compensate for the loss of RIC-4 in *C. elegans* as SNAP-25 in higher organisms require cysteine mediated membrane association for its activity (Gonzalo and Linder, 1998, Gonzalo et al., 1999). It is also interesting to note that targeting of SNAP-25 to the membranes is mediated by its association with the N-terminal SNARE domain of syntaxin (Vogel et al., 2000). Hence it would be interesting to see if either one of AEX-4 and SNAP-29 interacts with syntaxin.

RNAi of *ric-4* was shown to have a resistance to aldicarb similar to the *ric-4(md1088)* mutants (Sieburth et al., 2005). This cannot be compared to a null

mutant of *ric-4* (which could potentially be lethal) as in RNAi experiments the entire gene activity is not eliminated. Therefore, in the *ric-4(md1088)* mutant (which is likely to express a partly functional protein), it is not known if the phenotypes seen are due to a reduction in the SNARE complex or just due to faulty SNARE complex assembly. If it were due to the former, then certainly analysis of transgenic mutants overexpressing aex-4 and snap-29 would give more insights to the mechanism of action of the *ric-4(md1088)* mutant and perhaps would give an answer as to how this worm is viable.

Another possibility would be that the truncated RIC-4 is overexpressed and the N-terminal t-SNARE domain forms a dimer compensating for the loss of the second t-SNARE domain. As mentioned before, the SNARE complex is formed by the donation of two t-SNARE domains by SNAP-25 and one each by syntaxin and synaptobrevin (Sutton et al., 1998). It was shown in in vitro studies that a high level of promiscuity exists in the interaction of individual SNARE proteins (Fasshauer et al., 1999). It was shown that during the assembly of the SNARE complex, the interaction between the N-terminal SNARE domain of SNAP-25 and syntaxin serves as the on-pathway (Fasshauer and Margittai, 2004). This suggests that if the truncated RIC-4 gene is expressed in the mutant, the binary complex with syntaxin could potentially be formed thereby nucleating the SNARE complex.

Also, it was shown that in in vitro studies, antiparallel configurations of SNARE domains could form and this could be the reason behind the relatively slow rates of vesicle fusion observed in reconstituted fusion experiments in vitro (Weninger et al., 2003). Therefore, if the truncated *ric-4* is overexpressed it could mean that the N-terminal SNARE domain compensates for the loss of the C-terminal SNARE domain either in a parallel or an antiparallel configuration. It would be interesting to see if overexpression of just the C-terminal domain of *ric-4* rescues the phenotype of the *ric-4(md1088)* mutants. FRET analysis of transgenic strains expressing fluorescent-tagged SNARE domains would also help in explaining the SNARE complex assembly in the *ric-4(md1088)* mutant.

Studies in CSP KO mice showed progressive sensorimotor dysfunction, presynaptic neurodegeneration and premature death (Fernandez-Chacon et al., 2004). Moreover, when CSP KO mice had reduced levels of SNAP-25, the phenotype worsened (Sharma et al., 2012a) as mentioned before. In Drosophila lacking CSP, a much more severe phenotype was seen that is not really progressive as seen in mice (Umbach et al., 1994). Hence, it would prove to be much more difficult to analyse the knock down of SNAP-25 in flies. Hence, *C. elegans* gives an ideal platform to investigate the conservation of this interaction in lower organisms. A functional double mutant in *C. elegans* between *dnj*-14 and *ric-4*, which are homologues of CSP and SNAP-25 respectively, could exhibit a similar phenotype as seen in mice. However, our results suggest that the phenotype of the double mutant of *dnj*-14 and *ric-4* is

no worse than the individual mutants. The data suggests that there is genetic epistasis in the DNJ-14-RIC-4 pathway.

There is a difference in the genotypes of the double mutants used in the mouse study (Sharma et al., 2012a) and the one used in this study. In mice, a knock down in SNAP-25 levels is obtained by using a heterozygous SNAP-25 mutant. Effectively, there is a 50% reduction in the levels of SNAP-25 in the mouse mutant. In contrast, in the *ric-4*;*dnj*-14 double mutant, there is no loss of RIC-4 but all of the expressed RIC-4 is mutated and presumably lacks the C-terminal SNARE domain. Although it has been shown that CSP chaperones SNAP-25 (Sharma et al., 2011), its interaction has not been well characterized.

The data shown in this study seem to suggest that in *C. elegans*, DNJ-14 could have a specific role in chaperoning the C-terminal SNARE domain of RIC-4 into the SNARE complex. The overexpression of *ric-4* in *dnj*-14*(tm3223)* mutants also rescued the lifespan and the food race phenotypes in this study. This finding is consistent with the CSP mouse model where overexpression of SNAP-25 rescues the CSP KO phenotype. Moreover, this finding also hints at a possible role for *DNJ-14* in facilitating the C-terminal SNARE domain of RIC-4 into the SNARE complex. Clearly, overexpression of individual SNARE domains of RIC-4 in *dnj-14* mutants would reveal more insights into the interaction between *ric-4* and *dnj-14*.

Another interesting aspect of CSP KO is its transgenic rescue by the overexpression of α-synuclein (Chandra et al., 2005) in a pathway, presumably, different from the one involving CSP and SNAP-25 (Sharma et al., 2012). There are reports that α-synuclein promotes SNARE complex assembly in vivo and in vitro presumably by acting as a synaptobrevin chaperone (Burre et al., 2010), however, α-synuclein or a homologue is not endogenously expressed in *C. elegans* so the hypothesis that a similar protein acting as a chaperone in the absence of DNJ-14 seems implausible. However, it would be interesting to see if expression of transgenic α-synuclein does rescue this phenotype. A lot of questions need to be answered before the role of RIC-4/DNJ-14 interaction could be understood. The nature of the double mutant makes it very important in unravelling the mechanisms involved in ageing and neurodegeneration in neurodegenerative diseases.

CHAPTER 6: CONCLUSIONS

6.1 OVERVIEW OF RESULTS

CSP knock outs in mice and *Drosophila* have been the subjects of extensive study in the past. Although both these mutants exhibit similar phenotypes like neurodegeneration and short lifespan, there is a huge difference in the onset and severity of phenotypes. The onset of phenotypes in mice is age-dependent whereas in *Drosophila* the onset is very early. Also, the phenotype seen in *Drosophila* mutants is more severe compared to knock outs in mice with more than 95% of the flies dying before they reach adulthood. These differences in CSP knock outs in mice and *Drosophila* led to the idea of conceiving a model in *Caenorhabditis elegans*.

Initial studies of the *dnj-14* (CSP homologue in *C. elegans*) mutant revealed a reduced lifespan and also a slight but significant reduction in locomotion on performing thrashing assay. The severity of the phenotype was more similar to mice than *Drosophila*. The worms also exhibited a neurotransmission defect by day 5 of adulthood.

The *dnj-14* mutants also exhibited age-dependent neurodegeneration which was classified as puncta along the nerve cords and abnormal *gfp* expression in the head. Although the neurodegeneration in the nerve cords could not be characterised the loss of *gfp* in the head region corresponded to chemosensory defects. Also, the lifespan and chemosensory phenotypes were rescued by the

injection of a transgene containing the *dnj-14* gene driven by its endogenous promoter. All these findings indicate that the *dnj-14* mutants are similar to the CSP knock out mice and hence can be used as a model for neurodegeneration.

Furthermore, the lifespan and chemosensory phenotypes of the *dnj-14* mutants were shown to be rescued by treatment with resveratrol. A partial rescue of neurodegeneration phenotype was also seen. This suggested that *dnj-14* could be used as a model to screen compounds neuroprotective in nature. The mechanism of resveratrol action was deduced to be PDE4 inhibition-dependent as rolipram could mimic resveratrol in rescuing *dnj-14*. It was also observed that resveratrol acted independent of *sir-2.1,* which was interesting as several studies have shown that resveratrol acts in a *sir-2.1*-dependent manner.

Interaction between CSP and SNAP-25 in *C. elegans* was the next aspect investigated. The mutation in *ric-4*, the worm homologue for SNAP-25, was analysed and it was observed that the *ric-4* mutants were phenotypically similar to *dnj-14*. The *ric-4* mutants showed a slower thrashing rate and a reduction in lifespan which was rescued by treatment with resveratrol. This similarity prompted us to analyse the *ric-4;dnj-14* double mutant, which indicated a phenotypic similarity to the individual mutants. The double mutant like the individual mutants had a reduced lifespan and thrashing rate. This suggested the existence of genetic epistasis between *dnj-14* and *ric-4* in *C. elegans* similar to the genetic interaction previously reported in mice. Moreover,

overexpression of *ric-4* in the *dnj-14* mutants rescued the lifespan and chemosensory phenotypes of the *dnj-14* mutants, as seen in mice. These findings suggest a similarity between the worm *dnj-14* model and the CSP model in mice which could be used further be used to investigate drug targets and other high throughput screens to identify novel therapies for neurodegenerative diseases.

6.2 FUTURE WORK

It has been established that loss of *dnj-14* in *C. elegans* leads to neurodegeneration. However, the exact type of neurons that degenerate in the worm head and along the nerve cords is still unclear. To further investigate this, the *gfp* expression patterns in specific subtypes of neurons in the *dnj-14* mutants could be observed. For example, IL-2 neurons could be analysed by studying the expression pattern of *gfp* in *klp-6* expressing neurons.

As the *dnj-14* mutants are similar to CSP mutants in mice, it would be interesting to analyse single copy inserted transgenic rescue lines containing specific mutations to better understand the structure-function relationship of DNJ-14. Transgenic lines which have multiple copies of the gene leads to many-fold overexpression which could be deleterious to the mutant as seen in the reduction of thrashing rate in the rescue lines explained in chapter 3. Transgenic lines expressing the ANCL mutation could be used to establish a working model for the disease. More importantly, it would be interesting to see if the insertion of human CSP could rescue the phenotype of *dnj-14* mutants to investigate the evolutionary conservation of CSP function.

Although, resveratrol rescued lifespan and chemosensory phenotypes completely, it only rescued the neurodegeneration phenotype partially. Thus further investigation is essential to see if resveratrol is indeed neuroprotective in *dnj-14* mutants. Resv1 and Resv4, resveratrol related compounds, and

rolipram all of which increased lifespan could be tested for neurodegeneration in *dnj-14* mutants. Also another important aspect to analyse is the mechanism of resveratrol action. Our data has indicated that resveratrol acts in a *sir-2.1* independent manner but its dependency on PDE4 inhibition is attributed to the fact that rolipram mimics resveratrol. Thus first with the help of we would need to identify if rolipram inhibits PDE4 in *C. elegans*. If so, a functional mutant of PDE4 in *C. elegans* could be crossed to detect any effect on the phenotype of *dnj-14* mutants. Also, there exists a possibility that resveratrol could be neuroprotective in nature by enhancing AMP kinase activity (Park et al., 2012). It is widely accepted that AMP kinase is a known regulator of several processes including autophagy in *C. elegans*. Hence treatment of resveratrol to an *aak-2* (*C. elegans'* homologue of AMP kinase) mutation in *dnj-14* background could provide a more mechanistic insight into resveratrol action.

Overexpression of *ric-4* in *dnj-14* mutants rescued the lifespan and food race phenotypes in *dnj-14* mutants. Rescue of the food race phenotype could be an indication that the overexpression of *ric-4* leads to neuroprotection in *dnj-14* mutants similar to CSP knock out mice (Sharma et al., 2012a). Hence, neurodegeneration assays could be performed on these transgenic lines to check if they are protected against neurodegeneration.

Another important aspect that needs to be investigated is whether the lifespan phenotype and the neurodegeneration phenotype act in the same pathway.

The fact that resveratrol seems to rescue both neurodegeneration and lifespan suggests they might act in the same pathway but more work in this direction is needed to be certain of this fact. AMP kinase (*aak-2* in *C. elegans*) which is a known regulator of autophagy enhances neurodegeneration when mutated in a neurodegenerative disease model (Lee et al., 2010, Kim et al., 2011, Mao and Klionsky, 2011, Vingtduex et al., 2011). Hence, if a *dnj-14;aak-2* double mutant shows lifespan and neurodegeneration phenotypes similar to the *dnj-14* mutants, it would be fair to say that neurodegeneration and reduction in lifespan occurs in the same pathway which could possibly depend on the regulation of autophagy. With all this information, the *dnj-14* model could well prove to be important in finding pathways and drug targets which are generally neuroprotective against several neurodegenerative diseases.

REFERENCES

1. Albani D, Polito L, Signorini A, Forloni G (2010) Neuroprotective Properties of Resveratrol in Different Neurodegenerative Disorders. Biofactors 36:370-376.

2. Alcedo J, Kenyon C (2004) Regulation of *C. elegans* Longevity by Specific Gustatory and Olfactory Neurons. Neuron 41:45-55.

3. Arsov T, Smith KR, Damiano J, Franceschetti S, Canafoglia L, Bromhead CJ, Andermann E, Vears DF, Cossette P, Rajagopalan S, McDougall A, Sofia V, Farrell M, Aguglia U, Zini A, Meletti S, Morbin M, Mullen S, Andermann F, Mole SE, Bahlo M, Berkovic SF (2011) Kuf's Disease, the Major Adult Form of Neuronal Ceroid Lipofuscinosis, Caused by Mutations in CLN6. Am J Hum Genet 88:566-573.

4. Athar M, Back JH, Tang X, Kim KH, Kopelovich L, Bickers DR, Kim AL (2007) Resveratrol: A Review of Preclinical Studies for Human Cancer Prevention. Toxicol Appl Pharmacol 224:274-283.

5. Auld VJ, Fetter RD, Broadie K, Goodman CS (1995) Gliotactin, a Novel Transmembrane Protein on Peripheral Glia, Is Required to Form the Blood-Nerve Barrier in *Drosophila*. Cell 81:757-767.

6. Bales KR, Verina T, Dodel RC, Du Y, Altstiel L, Bender M, Hyslop P, Johnstone EM, Little SP, Cummins DJ, Piccardo P, Ghetti B, Paul SM (1997) Lack of Apolipoprotein E Dramatically Reduces Amyloid Beta-Peptide Deposition. Nat Genet 17:263-264.

7. Bargmann CI, Hartwieg E, Horvitz HR (1993) Odorant-Selective Genes and

Neurons Mediate Olfaction in *C. elegans*. Cell 74:515-527.

8. Bark C (2009) SNAP-25 and Gene-Targeted Mouse Mutants. Mechanisms of Exocytosis, vol. 1152 (Zorec, R. et al., eds), pp 145-153.

9. Bass TM, Weinkove D, Houthoofd K, Gems D, Partridge L (2007) Effects of Resveratrol on Lifespan in *Drosophila melanogaster* and *Caenorhabditis elegans*. Mech Ageing Dev 128:546-552.

10. Bates EA, Victor M, Jones AK, Shi Y, Hart AC (2006) Differential Contributions of *Caenorhabditis elegans* Histone Deacetylases to Huntingtin Polyglutamine Toxicity. J Neurosci 26:2830-2838.

11. Baur JA, Pearson KJ, Price NL, Jamieson HA, Lerin C, Kalra A, Prabhu VV, Allard JS, Lopez-Lluch G, Lewis K, Pistell PJ, Poosala S, Becker KG, Boss O, Gwinn D, Wang M, Ramaswamy S, Fishbein KW, Spencer RG, Lakatta EG, Le Couteur D, Shaw RJ, Navas P, Puigserver P, Ingram DK, de Cabo R, Sinclair DA (2006) Resveratrol Improves Health and Survival of Mice on a High-Calorie Diet. Nature 444:337-342.

12. Beeri MS, Haroutunian V, Schmeidler J, Sano M, Fam P, Kavanaugh A, Barr AM, Honer WG, Katsel P (2012) Synaptic Protein Deficits Are Associated with Dementia Irrespective of Extreme Old Age. Neurobiol Aging 33:1125 e1121-1128.

13. Benitez BA, Alvarado D, Cai Y, Mayo K, Chakraverty S, Norton J, Morris JC, Sands MS, Goate A, Cruchaga C (2011) Exome-Sequencing Confirms *DNAJC5* Mutations as Cause of Adult Neuronal Ceroid-Lipofuscinosis. PLoS ONE 6:e26741.

14. Berger Z, Ravikumar B, Menzies FM, Oroz LG, Underwood BR, Pangalos MN, Schmitt I, Wullner U, Evert BO, O'Kane CJ, Rubinsztein DC (2006) Rapamycin Alleviates Toxicity of Different Aggregate-Prone Proteins. Hum Mol Genet 15:433-442.

15. Bishop NA, Guarente L (2007) Two Neurons Mediate Diet-Restriction-Induced Longevity in *C. elegans*. Nature 447:545-549.

16. Blacque OE, Perens EA, Boroevich KA, Inglis PN, Li C, Warner A, Khattra J, Holt RA, Ou G, Mah AK, McKay SJ, Huang P, Swoboda P, Jones SJ, Marra MA, Baillie DL, Moerman DG, Shaham S, Leroux MR (2005) Functional Genomics of the Cilium, a Sensory Organelle. Curr Biol 15:935-941.

17. Boal F, Le Pevelen S, Ziepluch C, Scotti P, Lang J (2007) Cysteine-String Protein Isoform Beta (CSP-beta) Is Targeted to the Trans-Golgi Network as a Non-Palmitoylated CSP in Clonal Beta-Cells. Biochim Biophys Acta 1773:109-119.

18. Boal F, Zhang H, Tessier C, Scotti P, Lang J (2004) The Variable C-Terminus of Cysteine String Proteins Modulates Exocytosis and Protein-Protein Interactions. Biochemistry 43:16212-16223.

19. Braun JE, Wilbanks SM, Scheller RH (1996) The Cysteine String Secretory Vesicle Protein Activates Hsc70 Atpase. J Biol Chem 271:25989-25993.

20. Brenner S (1974) The Genetics of *Caenorhabditis elegans*. Genetics 77:71-94.

21. Brignull HR, Moore FE, Tang SJ, Morimoto RI (2006) Polyglutamine Proteins at the Pathogenic Threshold Display Neuron-Specific Aggregation

in a Pan-Neuronal *Caenorhabditis elegans* Model. J Neurosci 26:7597-7606.

22. Bronk P, Nie ZP, Klose MK, Dawson-Scully K, Zhang JH, Robertson RM, Atwood HL, Zinsmaier KE (2005) The Multiple Functions of Cysteine-String Protein Analyzed at *Drosophila* Nerve Terminals. J Neurosci 25:2204-2214.
23. Bronk P, Wenniger JJ, Dawson-Scully K, Guo X, Hong S, Atwood HL, Zinsmaier KE (2001) *Drosophila* Hsc70-4 Is Critical for Neurotransmitter Exocytosis in Vivo. Neuron 30:475-488.
24. Brookmeyer R, Johnson E, Ziegler-Graham K, Arrighi HM (2007) Forecasting the Global Burden of Alzheimer's Disease. Alzheimers Dement 3:186-191.
25. Brooks J, Ding J, Simon-Sanchez J, Paisan-Ruiz C, Singleton AB, Scholz SW (2009) Parkin and PINK1 Mutations in Early-Onset Parkinson's Disease: Comprehensive Screening in Publicly Available Cases and Control. J Med Genet 46:375-381.
26. Brown H, Larsson O, Branstrom R, Yang SN, Leibiger B, Leibiger I, Fried G, Moede T, Deeney JT, Brown GR, Jacobsson G, Rhodes CJ, Braun JE, Scheller RH, Corkey BE, Berggren PO, Meister B (1998) Cysteine String Protein (CSP) Is an Insulin Secretory Granule-Associated Protein Regulating Beta-Cell Exocytosis. EMBO J 17:5048-5058.
27. Bruns D (1997) A Structural Change Occurs Upon Binding of Syntaxin to SNAP-25. J Biol Chem 272:4582-4590.

28. Burre J, Sharma M, Tsetsenis T, Buchman V, Etherton MR, Sudhof TC (2010) Alpha-Synuclein Promotes SNARE-Complex Assembly in vivo and in vitro. Science 329:1663-1667.

29. Cao S, Gelwix CC, Caldwell KA, Caldwell GA (2005) Torsin-Mediated Protection from Cellular Stress in the Dopaminergic Neurons of *Caenorhabditis elegans*. J Neurosci 25:3801-3812.

30. Carnemolla A, Fossale E, Agostoni E, Michelazzi S, Calligaris R, De Maso L, Del Sal G, MacDonald ME, Persichetti F (2009) Rrs1 Is Involved in Endoplasmic Reticulum Stress Response in Huntington Disease. J Biol Chem 284:18167-18173.

31. Chalfie M, Sulston J (1981) Developmental Genetics of the Mechanosensory Neurons of *Caenorhabditis elegans*. Dev Biol 82:358-370.

32. Chamberlain LH, Burgoyne RD (1997a) Activation of the ATPase Activity of Heat-Shock Proteins Hsc70/Hsp70 by Cysteine-String Protein. Biochem J 322:853-858.

33. Chamberlain LH, Burgoyne RD (1997b) The Molecular Chaperone Function of the Secretory Vesicle Cysteine String Proteins. J Biol Chem 272:31420-31426.

34. Chamberlain LH, Burgoyne RD (1998a) Cysteine String Protein Functions Directly in Regulated Exocytosis. Mol Biol Cell 9:2259-2267.

35. Chamberlain LH, Burgoyne RD (1998b) The Cysteine-String Domain of the Secretory Vesicle Cysteine-String Protein Is Required for Membrane Targeting. Biochemical Journal 335:205-209.

36. Chamberlain LH, Burgoyne RD (2000) Cysteine-String Protein: The Chaperone at the Synapse. J Neurochem 74:1781-1789.

37. Chamberlain LH, Graham ME, Kane S, Jackson JL, Maier VH, Burgoyne RD, Gould GW (2001) The Synaptic Vesicle Protein, Cysteine-String Protein, Is Associated with the Plasma Membrane in 3T3-L1 Adipocytes and Interacts with Syntaxin 4. J Cell Sci 114:445-455.

38. Chandra S, Gallardo G, Fernandez-Chacon R, Schluter OM, Sudhof TC (2005) Alpha-Synuclein Cooperates with CSP-alpha in Preventing Neurodegeneration. Cell 123:383-396.

39. Chapman ER, An S, Barton N, Jahn R (1994) SNAP-25, a t-SNARE which Binds to Both Syntaxin and Synaptobrevin Via Domains That May Form Coiled Coils. J Biol Chem 269:27427-27432.

40. Chen X, Burgoyne RD (2012) Identification of Common Genetic Modifiers of Neurodegenerative Diseases from an Integrative Analysis of Diverse Genetic Screens in Model Organisms. BMC Genomics 13:71.

41. Chen X, Yan SD (2006) Mitochondrial a Beta: A Potential Cause of Metabolic Dysfunction in Alzheimer's Disease. IUBMB Life 58:686-694.

42. Chiang H-C, Iijima K, Hakker I, Zhong Y (2009) Distinctive Roles of Different Beta-Amyloid 42 Aggregates in Modulation of Synaptic Functions. Faseb Journal 23:1969-1977.

43. Chopra V, Fox JH, Lieberman G, Dorsey K, Matson W, Waldmeier P, Housman DE, Kazantsev A, Young AB, Hersch S (2007) A Small-Molecule Therapeutic Lead for Huntington's Disease: Preclinical Pharmacology and Efficacy of C2-8 in the R6/2 Transgenic Mouse. Proc Natl Acad Sci U S A 104:16685-16689.

44. Ciechanover A, Brundin P (2003) The Ubiquitin Proteasome System in Neurodegenerative Diseases: Sometimes the Chicken, Sometimes the Egg. Neuron 40:427-446.

45. Citron M, Oltersdorf T, Haass C, McConlogue L, Hung AY, Seubert P, Vigo-Pelfrey C, Lieberburg I, Selkoe DJ (1992) Mutation of the Beta-Amyloid Precursor Protein in Familial Alzheimer's Disease Increases Beta-Protein Production. Nature 360:672-674.

46. Clark LN, Wang Y, Karlins E, Saito L, Mejia-Santana H, Harris J, Louis ED, Cote LJ, Andrews H, Fahn S, Waters C, Ford B, Frucht S, Ottman R, Marder K (2006) Frequency of LRRK2 Mutations in Early- and Late-Onset Parkinson Disease. Neurology 67:1786-1791.

47. Cohen E, Bieschke J, Perciavalle RM, Kelly JW, Dillin A (2006) Opposing Activities Protect against Age-Onset Proteotoxicity. Science 313:1604-1610.

48. Collins JJ, Evason K, Pickett CL, Schneider DL, Kornfeld K (2008) The Anticonvulsant Ethosuximide Disrupts Sensory Function to Extend *C. elegans* Lifespan. PLoS Genet 4:e1000230.

49. Cooper AA, Gitler AD, Cashikar A, Haynes CM, Hill KJ, Bhullar B, Liu K, Xu K, Strathearn KE, Liu F, Cao S, Caldwell KA, Caldwell GA, Marsischky G, Kolodner RD, Labaer J, Rochet JC, Bonini NM, Lindquist S (2006) Alpha-Synuclein Blocks ER-Golgi Traffic and Rab1 Rescues Neuron Loss in Parkinson's Models. Science 313:324-328.

50. Crook R, Verkkoniemi A, Perez-Tur J, Mehta N, Baker M, Houlden H, Farrer M, Hutton M, Lincoln S, Hardy J, Gwinn K, Somer M, Paetau A, Kalimo H, Ylikoski R, Poyhonen M, Kucera S, Haltia M (1998) A Variant of Alzheimer's Disease with Spastic Paraparesis and Unusual Plaques Due to Deletion of Exon 9 of Presenilin 1. Nat Med 4:452-455.

51. Culetto E, Sattelle DB (2000) A Role for *Caenorhabditis elegans* in Understanding the Function and Interactions of Human Disease Genes. Hum Mol Genet 9:869-877.

52. Daigle I, Li C (1993) *apl-1*, a *Caenorhabditis elegans* Gene Encoding a Protein Related to the Human Beta-Amyloid Protein-Precursor. Proc Natl Acad Sci U S A 90:12045-12049.

53. Davies SW, Turmaine M, Cozens BA, DiFiglia M, Sharp AH, Ross CA, Scherzinger E, Wanker EE, Mangiarini L, Bates GP (1997) Formation of Neuronal Intranuclear Inclusions Underlies the Neurological Dysfunction in Mice Transgenic for the HD Mutation. Cell 90:537-548.

54. Dawson TM, Dawson VL (2003) Rare Genetic Mutations Shed Light on the Pathogenesis of Parkinson Disease. J Clin Invest 111:145-151.

55. Dawson TM, Ko HS, Dawson VL (2010) Genetic Animal Models of Parkinson's Disease. Neuron 66:646-661.

56. Dawson-Scully K, Bronk P, Atwood HL, Zinsmaier KE (2000) Cysteine-String Protein Increases the Calcium Sensitivity of Neurotransmitter Exocytosis in *Drosophila*. J Neurosci 20:6039-6047.

57. De M, De AK, Sen P, Banerjee AB (2002) Antimicrobial Properties of Star Anise (Illicium Verum Hook F). Phytother Res 16:94-95.

58. DePaolo J, Goker-Alpan O, Samaddar T, Lopez G, Sidransky E (2009) The Association between Mutations in the Lysosomal Protein Glucocerebrosidase and Parkinsonism. Mov Disord 24:1571-1578.

59. Dickson DW, Braak H, Duda JE, Duyckaerts C, Gasser T, Halliday GM, Hardy J, Leverenz JB, Del Tredici K, Wszolek ZK, Litvan I (2009) Neuropathological Assessment of Parkinson's Disease: Refining the Diagnostic Criteria. Lancet Neurol 8:1150-1157.

60. DiFiglia M, Sapp E, Chase K, Schwarz C, Meloni A, Young C, Martin E, Vonsattel JP, Carraway R, Reeves SA, et al. (1995) Huntingtin Is a Cytoplasmic Protein Associated with Vesicles in Human and Rat Brain Neurons. Neuron 14:1075-1081.

61. Eberle KK, Zinsmaier KE, Buchner S, Gruhn M, Jenni M, Arnold C, Leibold C, Reisch D, Walter N, Hafen E, Hofbauer A, Pflugfelder GO, Buchner E (1998) Wide Distribution of the Cysteine String Proteins in *Drosophila* Tissues Revealed by Targeted Mutagenesis. Cell Tissue Res 294:203-217.

62. Evans GJ, Wilkinson MC, Graham ME, Turner KM, Chamberlain LH, Burgoyne RD, Morgan A (2001) Phosphorylation of Cysteine String Protein by Protein Kinase A. Implications for the Modulation of Exocytosis. J Biol Chem 276:47877-47885.

63. Evans GJ, Morgan A (2002) Phosphorylation-Dependent Interaction of the Synaptic Vesicle Proteins Cysteine String Protein and Synaptotagmin I. Biochem J 364:343-347.

64. Evans GJ, Barclay JW, Prescott GR, Jo SR, Burgoyne RD, Birnbaum MJ, Morgan A (2006) Protein Kinase B/Akt Is a Novel Cysteine String Protein Kinase That Regulates Exocytosis Release Kinetics and Quantal Size. J Biol Chem 281:1564-1572.

65. Evans GJ, Morgan A (2002) Phosphorylation-Dependent Interaction of the Synaptic Vesicle Proteins Cysteine String Protein and Synaptotagmin I. Biochem J 364:343-347.

66. Faber PW, Voisine C, King DC, Bates EA, Hart AC (2002) Glutamine/Proline-Rich PQE-1 Proteins Protect *Caenorhabditis elegans* Neurons from Huntingtin Polyglutamine Neurotoxicity. Proc Natl Acad Sci U S A 99:17131-17136.

67. Fasshauer D, Antonin W, Margittai M, Pabst S, Jahn R (1999) Mixed and Non-Cognate SNARE Complexes. Characterization of Assembly and Biophysical Properties. J Biol Chem 274:15440-15446.

68. Fasshauer D, Margittai M (2004) A Transient N-Terminal Interaction of SNAP-25 and Syntaxin Nucleates SNARE Assembly. J Biol Chem 279:7613-7621.

69. Fernandez-Chacon R, Wolfel M, Nishimune H, Tabares L, Schmitz F, Castellano-Munoz M, Rosenmund C, Montesinos ML, Sanes JR, Schneggenburger R, Sudhof TC (2004) The Synaptic Vesicle Protein CSP Alpha Prevents Presynaptic Degeneration. Neuron 42:237-251.

70. Floor E, Meng L (1996) Amphetamine Releases Dopamine from Synaptic Vesicles by Dual Mechanisms. Neurosci Lett 215:53-56.

71. Fonseca-Kelly Z, Nassrallah M, Uribe J, Khan RS, Dine K, Dutt M, Shindler KS (2012) Resveratrol Neuroprotection in a Chronic Mouse Model of Multiple Sclerosis. Front Neurol 3.

72. Fonte V, Kapulkin WJ, Taft A, Fluet A, Friedman D, Link CD (2002) Interaction of Intracellular Beta Amyloid Peptide with Chaperone Proteins. Proc Natl Acad Sci U S A 99:9439-9444.

73. Fonte V, Kipp DR, Yerg J, 3rd, Merin D, Forrestal M, Wagner E, Roberts CM, Link CD (2008) Suppression of in Vivo Beta-Amyloid Peptide Toxicity by Overexpression of the Hsp-16.2 Small Chaperone Protein. J Biol Chem 283:784-791.

74. Fujiwara H, Hasegawa M, Dohmae N, Kawashima A, Masliah E, Goldberg MS, Shen J, Takio K, Iwatsubo T (2002) Alpha-Synuclein Is Phosphorylated in Synucleinopathy Lesions. Nat Cell Biol 4:160-164.

75. Gao X, Xu YX, Divine G, Janakiraman N, Chapman RA, Gautam SC (2002)

Disparate *in vitro* and *in vivo* Antileukemic Effects of Resveratrol, a Natural Polyphenolic Compound Found in Grapes. J Nut 132:2076-2081.

76. Garcia-Junco-Clemente P, Cantero G, Gomez-Sanchez L, Linares-Clemente P, Martinez-Lopez JA, Lujan R, Fernandez-Chacon R (2010) Cysteine String Protein-alpha Prevents Activity-Dependent Degeneration in GABAergic Synapses. J Neurosci 30:7377-7391.

77. Gonzalo S, Greentree WK, Linder ME (1999) SNAP-25 Is Targeted to the Plasma Membrane through a Novel Membrane-Binding Domain. J Biol Chem 274:21313-21318.

78. Gonzalo S, Linder ME (1998) SNAP-25 Palmitoylation and Plasma Membrane Targeting Require a Functional Secretory Pathway. Mol Biol Cell 9:585-597.

79. Goodman MB (2006) Mechanosensation. The *C. elegans* Research Community WormBook 10.1895/wormbook.1.62.1.

80. Gorleku OA, Chamberlain LH (2010) Palmitoylation and Testis-Enriched Expression of the Cysteine-String Protein Beta Isoform. Biochemistry 49:5308-5313.

81. Graham ME, Burgoyne RD (2000) Comparison of Cysteine String Protein (CSP) and Mutant Alpha-Snap Overexpression Reveals a Role for CSP in Late Steps of Membrane Fusion in Dense-Core Granule Exocytosis in Adrenal Chromaffin Cells. J Neurosci 20:1281-1289.

82. Graham ME, Prescott GR, Johnson JR, Jones M, Walmesley A, Haynes LP, Morgan A, Burgoyne RD, Barclay JW (2011) Structure-function Study of

Mammalian Munc18-1 and *C. elegans* UNC-18 Implicates Domain 3b in the Regulation of Exocytosis. PLoS ONE 6:e17999.

83. Greaves J, Gorleku OA, Salaun C, Chamberlain LH (2010) Palmitoylation of the SNAP-25 Protein Family: Specificity and Regulation by DHHC Palmitoyl Transferases. J Biol Chem 285:24629-24638.

84. Greaves J, Lemonidis K, Gorleku OA, Cruchaga C, Grefen C, Chamberlain LH (2012) Palmitoylation-Induced Aggregation of Cysteine-String Protein Mutants That Cause Neuronal Ceroid Lipofuscinosis. J Biol Chem 287:37330-37339.

85. Greaves J, Prescott GR, Fukata Y, Fukata M, Salaun C, Chamberlain LH (2009) The Hydrophobic Cysteine-Rich Domain of SNAP-25 Couples with Downstream Residues to Mediate Membrane Interactions and Recognition by DHHC Palmitoyl Transferases. Mol Biol Cell 20:1845-1854.

86. Greten-Harrison B, Polydoro M, Morimoto-Tomita M, Diao L, Williams AM, Nie EH, Makani S, Tian N, Castillo PE, Buchman VL, Chandra SS (2010) Alpha, Beta and Gamma Synuclein Triple Knockout Mice Reveal Age-Dependent Neuronal Dysfunction. Proc Natl Acad Sci U S A 107(45): 19573-19578

87. Gruber JAN, Tang SY, Halliwell B (2007) Evidence for a Trade-Off between Survival and Fitness Caused by Resveratrol Treatment of *Caenorhabditis elegans*. Ann N Y Acad Sci 1100:530-542.

88. Gundersen CB, Kohan SA, Souda P, Whitelegge JP, Umbach JA (2010) Cysteine String Protein beta Is Prominently Associated with Nerve

Terminals and Secretory Organelles in Mouse Brain. Brain Res 1332:1-11.

89. Gundersen CB, Mastrogiacomo A, Faull K, Umbach JA (1994) Extensive Lipidation of a Torpedo Cysteine String Protein. J Biol Chem 269:19197-19199.

90. Haass C, Hung AY, Schlossmacher MG, Teplow DB, Selkoe DJ (1993) Beta-Amyloid Peptide and a 3-kDa Fragment Are Derived by Distinct Cellular Mechanisms. J Biol Chem 268:3021-3024.

91. Hahn-Barma V, Deweer B, Durr A, Dode C, Feingold J, Pillon B, Agid Y, Brice A, Dubois B (1998) Are Cognitive Changes the First Symptoms of Huntington's Disease? A Study of Gene Carriers. J Neurol Neurosurg Psychiatry 64:172-177.

92. Hansen M, Chandra A, Mitic LL, Onken B, Driscoll M, Kenyon C (2008) A Role for Autophagy in the Extension of Lifespan by Dietary Restriction in *C. elegans*. PLoS Genet 4:e24.

93. Hansen M, Taubert S, Crawford D, Libina N, Lee SJ, Kenyon C (2007) Lifespan Extension by Conditions That Inhibit Translation in *Caenorhabditis elegans*. Aging Cell 6:95-110.

94. Hanson PI, Heuser JE, Jahn R (1997) Neurotransmitter Release - Four Years of SNARE Complexes. Curr Opin Neurobiol 7:310-315.

95. Harjes P, Wanker EE (2003) The Hunt for Huntingtin Function: Interaction Partners Tell Many Different Stories. Trends Biochem Sci 28:425-433.

96. Harrington AJ, Hamamichi S, Caldwell GA, Caldwell KA (2010) C.Elegans as a Model Organism to Investigate Molecular Pathways Involved with Parkinson's Disease. Dev Dyn 239:1282-1295.

97. Hars ES, Qi H, Ryazanov AG, Jin S, Cai L, Hu C, Liu LF (2007) Autophagy Regulates Ageing in *C. elegans*. Autophagy 3:93-95.

98. Hart AC, Sims S, Kaplan JM (1995) Synaptic Code for Sensory Modalities Revealed by *C. elegans* GLR-1 Glutamate Receptor. Nature 378:82-85.

99. Head E, Corrada MM, Kahle-Wrobleski K, Kim RC, Sarsoza F, Goodus M, Kawas CH (2009) Synaptic Proteins, Neuropathology and Cognitive Status in the Oldest-Old. Neurobiol Aging 30:1125-1134.

100. Hess EJ, Collins KA, Wilson MC (1996) Mouse Model of Hyperkinesis Implicates SNAP-25 in Behavioral Regulation. J Neurosci 16:3104-3111.

101. Hodel A (1998) Snap-25. Int J Biochem Cell Biol 30:1069-1073.

102. Hoffner G, Kahlem P, Djian P (2002) Perinuclear Localization of Huntingtin as a Consequence of Its Binding to Microtubules through an Interaction with Beta-Tubulin: Relevance to Huntington's Disease. J Cell Sci 115:941-948.

103. Houlden H, Singleton AB (2012) The Genetics and Neuropathology of Parkinson's Disease. Acta Neuropathol 124:325-338.

104. Housman D (1995) Gain of Glutamines, Gain of Function? Nat Genet 10:3-4.

105. Howitz KT, Bitterman KJ, Cohen HY, Lamming DW, Lavu S, Wood JG, Zipkin RE, Chung P, Kisielewski A, Zhang L-L, Scherer B, Sinclair DA (2003) Small

Molecule Activators of Sirtuins Extend *Saccharomyces cerevisiae* Lifespan. Nature 425:191-196.

106. Hung CW, Chen YC, Hsieh WL, Chiou SH, Kao CL (2010) Ageing and Neurodegenerative Diseases. Ageing Res Rev 9:S36-S46.
107. Huntington's Disease Collaborative Research Group A (1993) A Novel Gene Containing a Trinucleotide Repeat That Is Expanded and Unstable on Huntington's Disease Chromosomes. The Huntington's Disease Collaborative Research Group. Cell 72:971-983.
108. Ishikawa S, Taira T, Niki T, Takahashi-Niki K, Maita C, Maita H, Ariga H, Iguchi-Ariga SM (2009) Oxidative Status of DJ-1-Dependent Activation of Dopamine Synthesis through Interaction of Tyrosine Hydroxylase and 4-Dihydroxy-L-Phenylalanine (L-Dopa) Decarboxylase with DJ-1. J Biol Chem 284:28832-28844.
109. Jacobsen KT, Iverfeldt K (2009) Amyloid Precursor Protein and Its Homologues: A Family of Proteolysis-Dependent Receptors. Cell Mol Life Sci 66:2299-2318.
110. Jalanko A, Braulke T (2009) Neuronal Ceroid Lipofuscinoses. Biochim Biophys Acta 1793:697-709.
111. Jang M, Cai L, Udeani GO, Slowing KV, Thomas CF, Beecher CWW, Fong HHS, Farnsworth NR, Kinghorn AD, Mehta RG, Moon RC, Pezzuto JM (1997) Cancer Chemopreventive Activity of Resveratrol, a Natural Product Derived from Grapes. Science 275:218-220.

112. Jarrett JT, Berger EP, Lansbury PT, Jr. (1993) The Carboxy Terminus of the Beta Amyloid Protein Is Critical for the Seeding of Amyloid Formation: Implications for the Pathogenesis of Alzheimer's Disease. Biochemistry 32:4693-4697.

113. Jellinger KA (2011) Neurochemical Aspects of Neurotraumatic and Neurodegenerative Diseases. European Journal of Neurology 18:e104-e104.

114. Jensen PH, Nielsen MS, Jakes R, Dotti G, Goedert M (1998) Binding of Alpha-Synuclein to Brain Vesicles Is Abolished by Familial Parkinson's Disease Mutation. J Biol Chem 273:26292-26294.

115. Jin Y, Jorgensen E, Hartwieg E, Horvitz HR (1999) The *Caenorhabditis elegans* Gene UNC-25 Encodes Glutamic Acid Decarboxylase and Is Required for Synaptic Transmission but Not Synaptic Development. J Neurosci 19:539-548.

116. Johnson JR, Ferdek P, Lian LY, Barclay JW, Burgoyne RD, Morgan A (2009) Binding of UNC-18 to the N-terminus of Syntaxin is Essential for Neurotransmission in *Caenorhabditis elegans*. Biochem J 418:73-80.

117. Kabuto H, Tada M, Kohno M (2007) Eugenol [2-Methoxy-4-(2-Propenyl)Phenol] Prevents 6-Hydroxydopamine-Induced Dopamine Depression and Lipid Peroxidation Inductivity in Mouse Striatum. Biol Pharma Bull 30:423-427.

118. Kaeberlein M, McDonagh T, Heltweg B, Hixon J, Westman EA, Caldwell SD, Napper A, Curtis R, DiStefano PS, Fields S, Bedalov A, Kennedy BK (2005)

Substrate-Specific Activation of Sirtuins by Resveratrol. J Biol Chem 280:17038-17045.

119. Kang J, Bai Z, Zegarek MH, Grant BD, Lee J (2011) Essential Roles of SNAP-29 in *C. elegans*. Dev Biol 355:77-88.

120. Kang J, Lemaire HG, Unterbeck A, Salbaum JM, Masters CL, Grzeschik KH, Multhaup G, Beyreuther K, Muller-Hill B (1987) The Precursor of Alzheimer's Disease Amyloid A4 Protein Resembles a Cell-Surface Receptor. Nature 325:733-736.

121. Kaplan JM, Horvitz HR (1993) A Dual Mechanosensory and Chemosensory Neuron in *Caenorhabditis elegans*. Proc Natl Acad Sci U S A 90:2227-2231.

122. Karuppagounder SS, Pinto JT, Xu H, Chen H-L, Beal MF, Gibson GE (2009) Dietary Supplementation with Resveratrol Reduces Plaque Pathology in a Transgenic Model of Alzheimer's Disease. Neurochem Int 54:111-118.

123. Kautu BB, Carrasquilla A, Hicks ML, Caldwell KA, Caldwell GA (2013) Valproic Acid Ameliorates *C. elegans* Dopaminergic Neurodegeneration with Implications for ERK-MAPK Signaling. Neurosci Lett 541:116-119.

124. Kenyon C, Chang J, Gensch E, Rudner A, Tabtiang R (1993) A *C. elegans* Mutant That Lives Twice as Long as Wild Type. Nature 366:461-464.

125. Kim J, Kundu M, Viollet B, Guan K-L (2011) AMPK and mTOR Regulate Autophagy through Direct Phosphorylation of Ulk1. Nat Cell Biol 13:132-141.

126. Kimura Y, Okuda H (2001) Resveratrol Isolated from Polygonum Cuspidatum Root Prevents Tumor Growth and Metastasis to Lung and

Tumor-Induced Neovascularization in Lewis Lung Carcinoma-Bearing Mice. J Nut 131:1844-1849.

127. Kitada T, Asakawa S, Hattori N, Matsumine H, Yamamura Y, Minoshima S, Yokochi M, Mizuno Y, Shimizu N (1998) Mutations in the Parkin Gene Cause Autosomal Recessive Juvenile Parkinsonism. Nature 392:605-608.

128. Kitada T, Tong Y, Gautier CA, Shen J (2009) Absence of Nigral Degeneration in Aged Parkin/DJ-1/PINK1 Triple Knockout Mice. J Neurochem 111:696-702.

129. Kojro E, Fahrenholz F (2005) The Non-Amyloidogenic Pathway: Structure and Function of Alpha-Secretases. In: Subcellular Biochemistry, vol. 38 (Harris, J. R. F. F., ed), pp 105-127.

130. Kramer ML, Schulz-Schaeffer WJ (2007) Presynaptic Alpha-Synuclein Aggregates, Not Lewy Bodies, Cause Neurodegeneration in Dementia with Lewy Bodies. J Neurosci 27:1405-1410.

131. Lakso M, Vartiainen S, Moilanen AM, Sirvio J, Thomas JH, Nass R, Blakely RD, Wong G (2003) Dopaminergic Neuronal Loss and Motor Deficits in *Caenorhabditis elegans* Overexpressing Human Alpha-Synuclein. J Neurochem 86:165-172.

132. Landles C, Bates GP (2004) Huntingtin and the Molecular Pathogenesis of Huntington's Disease - Fourth in Molecular Medicine Review Series. EMBO Rep 5:958-963.

133. Lane SR, Liu Y (1997) Characterization of the Palmitoylation Domain of SNAP-25. J Neurochem 69:1864-1869.

134. Lee GD, Wilson MA, Zhu M, Wolkow CA, de Cabo R, Ingram DK, Zou S (2006) Dietary Deprivation Extends Lifespan in *Caenorhabditis elegans*. Aging Cell 5:515-524.

135. Lee HG, Perry G, Moreira PI, Garrett MR, Liu Q, Zhu X, Takeda A, Nunomura A, Smith MA (2005) Tau Phosphorylation in Alzheimer's Disease: Pathogen or Protector? Trends Mol Med 11:164-169.

136. Lee JW, Park S, Takahashi Y, Wang H-G (2010) The Association of AMPK with Ulk1 Regulates Autophagy. PLoS ONE 5:e15394.

137. Leveque C, Pupier S, Marqueze B, Geslin L, Kataoka M, Takahashi M, De Waard M, Seagar M (1998) Interaction of Cysteine String Proteins with the Alpha1a Subunit of the P/Q-Type Calcium Channel. J Biol Chem 273:13488-13492.

138. Lewis J, Dickson DW, Lin W-L, Chisholm L, Corral A, Jones G, Yen S-H, Sahara N, Skipper L, Yager D, Eckman C, Hardy J, Hutton M, McGowan E (2001) Enhanced Neurofibrillary Degeneration in Transgenic Mice Expressing Mutant Tau and App. Science 293:1487-1491.

139. Lewis J, Melrose H, Bumcrot D, Hope A, Zehr C, Lincoln S, Braithwaite A, He Z, Ogholikhan S, Hinkle K, Kent C, Toudjarska I, Charisse K, Braich R, Pandey RK, Heckman M, Maraganore DM, Crook J, Farrer MJ (2008) In Vivo Silencing of Alpha-Synuclein Using Naked Sirna. Mol Neurodegener 3:19.

140. Li ZG, Hong T, Shimada Y, Komoto I, Kawabe A, Ding Y, Kaganoi J, Hashimoto Y, Imamura M (2002) Suppression of N-

Nitrosomethylbenzylamine (NMBA)-Induced Esophageal Tumorigenesis in F344 Rats by Resveratrol. Carcinogenesis 23:1531-1536.

141. Liachko NF, Guthrie CR, Kraemer BC (2010) Phosphorylation Promotes Neurotoxicity in a *Caenorhabditis elegans* Model of TDP-43 Proteinopathy. J Neurosci 30:16208-16219.

142. Lin K, Dorman JB, Rodan A, Kenyon C (1997) DAF-16: An Hnf-3/Forkhead Family Member That Can Function to Double the Lifespan *of Caenorhabditis elegans*. Science 278:1319-1322.

143. Link CD (2006) *C. elegans* Models of Age-Associated Neurodegenerative Diseases: Lessons from Transgenic Worm Models of Alzheimer's Disease. Exp Gerontol 41:1007-1013.

144. Locke CJ, Fox SA, Caldwell GA, Caldwell KA (2008) Acetaminophen Attenuates Dopamine Neuron Degeneration in Animal Models of Parkinson's Disease. Neurosci Lett 439:129-133.

145. Luo Y (2006) Alzheimer's Disease, the Nematode *Caenorhabditis elegans*, and Ginkgo Biloba Leaf Extract. Life Sciences 78:2066-2072.

146. Lutz AK, Exner N, Fett ME, Schlehe JS, Kloos K, Lammermann K, Brunner B, Kurz-Drexler A, Vogel F, Reichert AS, Bouman L, Vogt-Weisenhorn D, Wurst W, Tatzelt J, Haass C, Winklhofer KF (2009) Loss of Parkin or PINK1 Function Increases DRP1-Dependent Mitochondrial Fragmentation. J Biol Chem 284:22938-22951.

147. Magga JM, Jarvis SE, Arnot MI, Zamponi GW, Braun JE (2000) Cysteine String Protein Regulates G Protein Modulation of N-Type Calcium Channels. Neuron 28:195-204.

148. Mahoney TR, Luo S, Nonet ML (2006) Analysis of Synaptic Transmission in *Caenorhabditis elegans* Using an Aldicarb-Sensitivity Assay. Nat Protoc 1:1772-1777.

149. Mao K, Klionsky DJ (2011) AMPK Activates Autophagy by Phosphorylating Ulk1. Circ Res 108:787-788.

150. Marambaud P, Zhao H, Davies P (2005) Resveratrol Promotes Clearance of Alzheimer's Disease Amyloid beta Peptides. J Biol Chem 280:37377-37382.

151. Mastrogiacomo A, Parsons SM, Zampighi GA, Jenden DJ, Umbach JA, Gundersen CB (1994) Cysteine String Proteins: A Potential Link between Synaptic Vesicles and Presynaptic Ca^{2+} Channels. Science 263:981-982.

152. Miller KG, Alfonso A, Nguyen M, Crowell JA, Johnson CD, Rand JB (1996) A Genetic Selection for *Caenorhabditis elegans* Synaptic Transmission Mutants. Proc Natl Acad Sci U S A 93:12593-12598.

153. Miller LC, Swayne LA, Chen L, Feng ZP, Wacker JL, Muchowski PJ, Zamponi GW, Braun JE (2003) Cysteine String Protein (CSP) Inhibition of N-Type Calcium Channels Is Blocked by Mutant Huntingtin. J Biol Chem 278:53072-53081.

154. Milne JC, Lambert PD, Schenk S, Carney DP, Smith JJ, Gagne DJ, Jin L, Boss O, Perni RB, Vu CB, Bemis JE, Xie R, Disch JS, Ng PY, Nunes JJ, Lynch AV, Yang H, Galonek H, Israelian K, Choy W, Iffland A, Lavu S, Medvedik O,

Sinclair DA, Olefsky JM, Jirousek MR, Elliott PJ, Westphal CH (2007) Small Molecule Activators of Sirt1 as Therapeutics for the Treatment of Type 2 Diabetes. Nature 450:712-716.

155. Mitchell P, Mould R, Dillon J, Glautier S, Andrianakis I, James C, Pugh A, Holden-Dye L, O'Connor V (2010) A Differential Role for Neuropeptides in Acute and Chronic Adaptive Responses to Alcohol: Behavioural and Genetic Analysis in *Caenorhabditis elegans*. PLoS ONE 5:e10422.

156. Mitsui J, Mizuta I, Toyoda A, Ashida R, Takahashi Y, Goto J, Fukuda Y, Date H, Iwata A, Yamamoto M, Hattori N, Murata M, Toda T, Tsuji S (2009) Mutations for Gaucher Disease Confer High Susceptibility to Parkinson Disease. Arch Neurol 66:571-576.

157. Mole SE, Mitchison HM, Munroe PB (1999) Molecular Basis of the Neuronal Ceroid Lipofuscinoses: Mutations in CLN1, CLN2, CLN3, and CLN5. Hum Mutat 14:199-215.

158. Montana V, Liu W, Mohideen U, Parpura V (2009) Single Molecule Measurements of Mechanical Interactions within Ternary Snare Complexes and Dynamics of Their Disassembly: SNAP-25 Vs. SNAP-23. J Physiol 587:1943-1960.

159. Montecucco C, Schiavo G, Pantano S (2005) Snare Complexes and Neuroexocytosis: How Many, How Close? Trends Biochem Sci 30:367-372.

160. Morselli E, Maiuri MC, Markaki M, Megalou E, Pasparaki A, Palikaras K, Criollo A, Galluzzi L, Malik SA, Vitale I, Michaud M, Madeo F, Tavernarakis N, Kroemer G (2010) Caloric Restriction and Resveratrol Promote

Longevity through the Sirtuin-1-Dependent Induction of Autophagy. Cell Death Dis 1:e10.

161. Narendra D, Tanaka A, Suen DF, Youle RJ (2009) Parkin-Induced Mitophagy in the Pathogenesis of Parkinson Disease. Autophagy 5:706-708.

162. Nariai M, Tanaka T, Okada T, Shirai C, Horigome C, Mizuta K (2005) Synergistic Defect in 60s Ribosomal Subunit Assembly Caused by a Mutation of Rrs1p, a Ribosomal Protein L11-Binding Protein, and 3'-Extension of 5S rRNA in Saccharomyces Cerevisiae. Nucleic Acids Res 33:4553-4562.

163. Nasir J, Floresco SB, O'Kusky JR, Diewert VM, Richman JM, Zeisler J, Borowski A, Marth JD, Phillips AG, Hayden MR (1995) Targeted Disruption of the Huntington's Disease Gene Results in Embryonic Lethality and Behavioral and Morphological Changes in Heterozygotes. Cell 81:811-823.

164. Nass R, Hall DH, Miller DM, 3rd, Blakely RD (2002) Neurotoxin-Induced Degeneration of Dopamine Neurons in *Caenorhabditis elegans*. Proc Natl Acad Sci U S A 99:3264-3269.

165. Neumann J, Bras J, Deas E, O'Sullivan SS, Parkkinen L, Lachmann RH, Li A, Holton J, Guerreiro R, Paudel R, Segarane B, Singleton A, Lees A, Hardy J, Houlden H, Revesz T, Wood NW (2009) Glucocerebrosidase Mutations in Clinical and Pathologically Proven Parkinson's Disease. Brain 132:1783-1794.

166. Nie Z, Ranjan R, Wenniger JJ, Hong SN, Bronk P, Zinsmaier KE (1999)

Overexpression of Cysteine-String Proteins in *Drosophila* Reveals Interactions with Syntaxin. J Neurosci 19:10270-10279.

167. Niemeyer BA, Schwarz TL (2000) Snap-24, a Drosophila Snap-25 Homologue on Granule Membranes, Is a Putative Mediator of Secretion and Granule-Granule Fusion in Salivary Glands. J Cell Sci 113:4055-4064.
168. Ninkina N, Peters OM, Connor-Robson N, Lytkina O, Sharfeddin E, Buchman VL (2012) Contrasting Effects of alpha-Synuclein and gamma-Synuclein on the Phenotype of Cysteine String Protein-alpha Null Mutant Mice Suggest Distinct Function of These Proteins in Neuronal Synapses. J Biol Chem 287:44471-44477.
169. Nishikori S, Yamanaka K, Sakurai T, Esaki M, Ogura T (2008) P97 Homologs from *Caenorhabditis elegans*, CDC-48.1 and CDC-48.2, Suppress the Aggregate Formation of Huntingtin Exon1 Containing Expanded PolyQ Repeat. Genes Cells 13:827-838.
170. Nollen EAA, Garcia SM, van Haaften G, Kim S, Chavez A, Morimoto RI, Plasterk RHA (2004) Genome-Wide RNA Interference Screen Identifies Previously Undescribed Regulators of Polyglutamine Aggregation. Proc Natl Acad Sci U S A 101:6403-6408.
171. Noskova L, Stranecky V, Hartmannova H, Pristoupilova A, Baresova V, Ivanek R, Hulkova H, Jahnova H, van der Zee J, Staropoli JF, Sims KB, Tyynela J, Van Broeckhoven C, Nijssen PC, Mole SE, Elleder M, Kmoch S (2011) Mutations in DNAJC5, Encoding Cysteine-String Protein Alpha,

Cause Autosomal-Dominant Adult-Onset Neuronal Ceroid Lipofuscinosis. Am J Hum Genet 89:241-252.

172. Oliver PL, Davies KE (2009) Interaction between Environmental and Genetic Factors Modulates Schizophrenic Endophenotypes in the SNAP-25 Mouse Mutant Blind-Drunk. Hum Mol Genet 18:4576-4589.

173. Osburn WO, Kensler TW (2008) Nrf2 Signaling: An Adaptive Response Pathway for Protection against Environmental Toxic Insults. Mutat Res 659:31-39.

174. Paisan-Ruiz C, Jain S, Evans EW, Gilks WP, Simon J, van der Brug M, Lopez de Munain A, Aparicio S, Gil AM, Khan N, Johnson J, Martinez JR, Nicholl D, Carrera IM, Pena AS, de Silva R, Lees A, Marti-Masso JF, Perez-Tur J, Wood NW, Singleton AB (2004) Cloning of the Gene Containing Mutations That Cause PARK8-Linked Parkinson's Disease. Neuron 44:595-600.

175. Pallos J, Bodai L, Lukacsovich T, Purcell JM, Steffan JS, Thompson LM, Marsh JL (2008) Inhibition of Specific HDACs and Sirtuins Suppresses Pathogenesis in a *Drosophila* Model of Huntington's Disease. Hum Mol Genet 17:3767-3775.

176. Pany S, Majhi A, Das J (2012) PKC Activation by Resveratrol Derivatives with Unsaturated Aliphatic Chain. PLoS ONE 7:e52888.

177. Park SJ, Ahmad F, Philp A, Baar K, Williams T, Luo H, Ke H, Rehmann H, Taussig R, Brown AL, Kim MK, Beaven MA, Burgin AB, Manganiello V, Chung JH (2012) Resveratrol Ameliorates Aging-Related Metabolic Phenotypes by Inhibiting cAMP Phosphodiesterases. Cell 148:421-433.

178. Parker JA, Arango M, Abderrahmane S, Lambert E, Tourette C, Catoire H, Neri C (2005) Resveratrol Rescues Mutant Polyglutamine Cytotoxicity in Nematode and Mammalian Neurons (Vol 37, Pg 349, 2005). Nature Genetics 37:555.

179. Parker JA, Connolly JB, Wellington C, Hayden M, Dausset J, Neri C (2001) Expanded Polyglutamines in *Caenorhabditis elegans* Cause Axonal Abnormalities and Severe Dysfunction of PLM Mechanosensory Neurons without Cell Death. Proc Natl Acad Sci U S A 98:13318-13323.

180. Parker JA, Metzler M, Georgiou J, Mage M, Roder JC, Rose AM, Hayden MR, Neri C (2007) Huntingtin-Interacting Protein 1 Influences Worm and Mouse Presynaptic Function and Protects *Caenorhabditis elegans* Neurons against Mutant Polyglutamine Toxicity. J Neurosci 27:11056-11064.

181. Pearson KJ, Baur JA, Lewis KN, Peshkin L, Price NL, Labinskyy N, Swindell WR, Kamara D, Minor RK, Perez E, Jamieson HA, Zhang Y, Dunn SR, Sharma K, Pleshko N, Woollett LA, Csiszar A, Ikeno Y, Le Couteur D, Elliott PJ, Becker KG, Navas P, Ingram DK, Wolf NS, Ungvari Z, Sinclair DA, de Cabo R (2008) Resveratrol Delays Age-Related Deterioration and Mimics Transcriptional Aspects of Dietary Restriction without Extending Life Span. Cell Metab 8:157-168.

182. Petrascheck M, Ye X, Buck LB (2009) A High-Throughput Screen for Chemicals That Increase the Lifespan of *Caenorhabditis elegans*. Ann N Y Acad Sci 1170:698-701.

183. Pfister JA, Ma C, Morrison BE, D'Mello SR (2008) Opposing Effects of

Sirtuins on Neuronal Survival: Sirt1-Mediated Neuroprotection Is Independent of Its Deacetylase Activity. PLoS ONE 3:e4090.

184. Ramadan H, Al-Din AS, Ismail A, Balen F, Varma A, Twomey A, Watts R, Jackson M, Anderson G, Green E, Mole SE (2007) Adult Neuronal Ceroid Lipofuscinosis Caused by Deficiency in Palmitoyl Protein Thioesterase 1. Neurology 68:387-388.

185. Ranjan R, Bronk P, Zinsmaier KE (1998) Cysteine String Protein Is Required for Calcium Secretion Coupling of Evoked Neurotransmission in *Drosophila* but Not for Vesicle Recycling. J Neurosci 18:956-964.

186. Rapoport M, Dawson HN, Binder LI, Vitek MP, Ferreira A (2002) Tau Is Essential to Beta-Amyloid-Induced Neurotoxicity. Proc Natl Acad Sci U S A 99:6364-6369.

187. Ravikumar B, Berger Z, Vacher C, O'Kane CJ, Rubinsztein DC (2006) Rapamycin Pre-Treatment Protects against Apoptosis. Hum Mol Genet 15:1209-1216.

188. Ravikumar B, Vacher C, Berger Z, Davies JE, Luo SQ, Oroz LG, Scaravilli F, Easton DF, Duden R, O'Kane CJ, Rubinsztein DC (2004) Inhibition of mTOR Induces Autophagy and Reduces Toxicity of Polyglutamine Expansions in Fly and Mouse Models of Huntington Disease. Nature Genetics 36:585-595.

189. Ridley RM, Frith CD, Crow TJ, Conneally PM (1988) Anticipation in Huntington's Disease Is Inherited through the Male Line but May Originate in the Female. J Med Genet 25:589-595.

190. Rosenzweig B, Liao LW, Hirsh D (1983) Sequence of the *C. elegans* Transposable Element Tc1. Nucleic Acids Res 11:4201-4209.

191. Rubinsztein DC, Carmichael J (2003) Huntington's Disease: Molecular Basis of Neurodegeneration. Expert Rev Mol Med 5:1-21.

192. Ruiz R, Casanas JJ, Sudhof TC, Tabares L (2008) Cysteine String Protein-Alpha Is Essential for the High Calcium Sensitivity of Exocytosis in a Vertebrate Synapse. Eur J Neurosci 27:3118-3131.

193. Sakahira H, Breuer P, Hayer-Hartl MK, Hartl FU (2002) Molecular Chaperones as Modulators of Polyglutamine Protein Aggregation and Toxicity. Proc Natl Acad Sci U S A 99:16412-16418.

194. Sarkar S, Ravikumar B, Floto RA, Rubinsztein DC (2009) Rapamycin and Mtor-Independent Autophagy Inducers Ameliorate Toxicity of Polyglutamine-Expanded Huntingtin and Related Proteinopathies. Cell Death Differ 16:46-56.

195. Schaeffer V, Lavenir I, Ozcelik S, Tolnay M, Winkler DT, Goedert M (2012) Stimulation of Autophagy Reduces Neurodegeneration in a Mouse Model of Human Tauopathy. Brain 135(Pt7): 2169-2177.

196. Scheff SW, Price DA, Schmitt FA, DeKosky ST, Mufson EJ (2007) Synaptic Alterations in Ca1 in Mild Alzheimer Disease and Mild Cognitive Impairment. Neurology 68:1501-1508.

197. Scherzinger E, Sittler A, Schweiger K, Heiser V, Lurz R, Hasenbank R, Bates GP, Lehrach H, Wanker EE (1999) Self-Assembly of Polyglutamine-

Containing Huntingtin Fragments into Amyloid-Like Fibrils: Implications for Huntington's Disease Pathology. Proc Natl Acad Sci U S A 96:4604-4609.

198. Schiavo G, Matteoli M, Montecucco C (2000) Neurotoxins Affecting Neuroexocytosis. Physiol Rev 80:717-766.
199. Schilling G, Sharp AH, Loev SJ, Wagster MV, Li SH, Stine OC, Ross CA (1995) Expression of the Huntington's Disease (LT15) Protein Product in HD Patients. Hum Mol Genet 4:1365-1371.
200. Selkoe DJ (2002) Alzheimer's Disease Is a Synaptic Failure. Science 298:789-791.
201. Shaham S (2010) Chemosensory Organs as Models of Neuronal Synapses. Nat Rev Neurosci 11:212-217.
202. Sharma M, Burre J, Bronk P, Zhang Y, Xu W, Sudhof TC (2012a) CSP alpha Knockout Causes Neurodegeneration by Impairing SNAP-25 Function. EMBO Journal 31:829-841.
203. Sharma M, Burre J, Sudhof TC (2011) CSP alpha Promotes SNARE-Complex Assembly by Chaperoning SNAP-25 During Synaptic Activity. Nat Cell Biol 13:30-U74.
204. Sharma M, Burre J, Sudhof TC (2012b) Proteasome Inhibition Alleviates Snare-Dependent Neurodegeneration. Sci Transl Med 4:147ra113.
205. Sharma M, Gupta YK (2002) Chronic Treatment with Trans Resveratrol Prevents Intracerebroventricular Streptozotocin Induced Cognitive Impairment and Oxidative Stress in Rats. Life Sciences 71:2489-2498.

206. Sharp AH, Loev SJ, Schilling G, Li SH, Li XJ, Bao J, Wagster MV, Kotzuk JA, Steiner JP, Lo A, et al. (1995) Widespread Expression of Huntington's Disease Gene (LT15) Protein Product. Neuron 14:1065-1074.

207. Shen N, Datta D, Schaffer C, LeDuc P, Ingber D, Mazur E (2005) Ablation of Cytoskeletal Filaments and Mitochondria in Cells Using a Femtosecond Laser Nanoscissor. Mech Chem Biosys 2:17 - 26.

208. Sidransky E, Nalls MA, Aasly JO, Aharon-Peretz J, Annesi G, Barbosa ER, Bar-Shira A, Berg D, Bras J, Brice A, Chen CM, Clark LN, Condroyer C, De Marco EV, Durr A, Eblan MJ, Fahn S, Farrer MJ, Fung HC, Gan-Or Z, Gasser T, Gershoni-Baruch R, Giladi N, Griffith A, Gurevich T, Januario C, Kropp P, Lang AE, Lee-Chen GJ, Lesage S, Marder K, Mata IF, Mirelman A, Mitsui J, Mizuta I, Nicoletti G, Oliveira C, Ottman R, Orr-Urtreger A, Pereira LV, Quattrone A, Rogaeva E, Rolfs A, Rosenbaum H, Rozenberg R, Samii A, Samaddar T, Schulte C, Sharma M, Singleton A, Spitz M, Tan EK, Tayebi N, Toda T, Troiano AR, Tsuji S, Wittstock M, Wolfsberg TG, Wu YR, Zabetian CP, Zhao Y, Ziegler SG (2009) Multicenter Analysis of Glucocerebrosidase Mutations in Parkinson's Disease. N Engl J Med 361:1651-1661.

209. Sieburth D, Ch'ng Q, Dybbs M, Tavazoie M, Kennedy S, Wang D, Dupuy D, Rual JF, Hill DE, Vidal M, Ruvkun G, Kaplan JM (2005) Systematic Analysis of Genes Required for Synapse Structure and Function. Nature 436:510-517.

210. Simpson LL (2004) Identification of the Major Steps in Botulinum Toxin Action. Annu Rev Pharmacol Toxicol 44:167-193.

211. Sinha K, Chaudhary G, Kumar Gupta Y (2002) Protective Effect of Resveratrol against Oxidative Stress in Middle Cerebral Artery Occlusion Model of Stroke in Rats. Life Sciences 71:655-665.

212. Skovronsky DM, Lee VMY, Trojanowskiz JQ (2006) Neurodegenerative Diseases: New Concepts of Pathogenesis and Their Therapeutic Implications. Annu Rev Pathol 1:151-170.

213. Sleigh JN, Buckingham SD, Esmaeili B, Viswanathan M, Cuppen E, Westlund BM, Sattelle DB (2011) A Novel Caenorhabditis Elegans Allele, Smn-1(Cb131), Mimicking a Mild Form of Spinal Muscular Atrophy, Provides a Convenient Drug Screening Platform Highlighting New and Pre-Approved Compounds. Hum Mol Genet 20:245-260.

214. Sollner T, Whiteheart SW, Brunner M, Erdjument-Bromage H, Geromanos S, Tempst P, Rothman JE (1993) SNAP Receptors Implicated in Vesicle Targeting and Fusion. Nature 362:318-324.

215. Spillantini MG, Crowther RA, Jakes R, Hasegawa M, Goedert M (1998) Alpha-Synuclein in Filamentous Inclusions of Lewy Bodies from Parkinson's Disease and Dementia with Lewy Bodies. Proc Natl Acad Sci U S A 95:6469-6473.

216. Strittmatter WJ, Saunders AM, Schmechel D, Pericak-Vance M, Enghild J, Salvesen GS, Roses AD (1993) Apolipoprotein E: High-Avidity Binding to Beta-Amyloid and Increased Frequency of Type 4 Allele in Late-Onset Familial Alzheimer Disease. Proc Natl Acad Sci U S A 90:1977-1981.

217. Sutton RB, Fasshauer D, Jahn R, Brunger AT (1998) Crystal Structure of a Snare Complex Involved in Synaptic Exocytosis at 2.4Å Resolution. Nature 395:347-353.

218. Tan EK, Skipper L, Chua E, Wong MC, Pavanni R, Bonnard C, Kolatkar P, Liu JJ (2006) Analysis of 14 LRRK2 Mutations in Parkinson's Plus Syndromes and Late-Onset Parkinson's Disease. Mov Disord 21:997-1001.

219. Tanaka K, Sugiura Y, Ichishita R, Mihara K, Oka T (2011) KLP-6: A Newly Identified Kinesin That Regulates the Morphology and Transport of Mitochondria in Neuronal Cells. J Cell Sci 124:2457-2465.

220. Tauffenberger A, Julien C, Parker JA (2013) Evaluation of Longevity Enhancing Compounds against Transactive Response DNA-Binding Protein-43 Neuronal Toxicity. Neurobiol Aging 34:2175-2182.

221. Thapar A, O'Donovan M, Owen MJ (2005) The Genetics of Attention Deficit Hyperactivity Disorder. Hum Mol Genet 14:R275-R282.

222. Tiraboschi P, Hansen LA, Thal LJ, Corey-Bloom J (2004) The Importance of Neuritic Plaques and Tangles to the Development and Evolution of AD. Neurology 62:1984-1989.

223. Tobaben S, Thakur P, Fernández-Chacón R, Südhof TC, Rettig J, Stahl B (2001) A Trimeric Protein Complex Functions as a Synaptic Chaperone Machine. Neuron 31:987-999.

224. Tobaben S, Varoqueaux F, Brose N, Stahl B, Meyer G (2003) A Brain-Specific Isoform of Small Glutamine-Rich Tetratricopeptide Repeat-

Containing Protein Binds to Hsc70 and the Cysteine String Protein. J Biol Chem 278:38376-38383.

225. Tullet JM, Hertweck M, An JH, Baker J, Hwang JY, Liu S, Oliveira RP, Baumeister R, Blackwell TK (2008) Direct Inhibition of the Longevity-Promoting Factor SKN-1 by Insulin-Like Signaling in *C. elegans*. Cell 132:1025-1038.

226. Umbach JA, Zinsmaier KE, Eberle KK, Buchner E, Benzer S, Gundersen CB (1994) Presynaptic Dysfunction in Drosophila CSP Mutants. Neuron 13:899-907.

227. Valente EM, Bentivoglio AR, Dixon PH, Ferraris A, Ialongo T, Frontali M, Albanese A, Wood NW (2001) Localization of a Novel Locus for Autosomal Recessive Early-Onset Parkinsonism, PARK6, on Human Chromosome 1p35-p36. Am J Hum Genet 68:895-900.

228. van Ham TJ, Breitling R, Swertz MA, Nollen EA (2009) Neurodegenerative Diseases: Lessons from Genome-Wide Screens in Small Model Organisms. EMBO Mol Med 1:360-370.

229. Velier J, Kim M, Schwarz C, Kim TW, Sapp E, Chase K, Aronin N, DiFiglia M (1998) Wild-Type and Mutant Huntingtins Function in Vesicle Trafficking in the Secretory and Endocytic Pathways. Exp Neurol 152:34-40.

230. Velinov M, Dolzhanskaya N, Gonzalez M, Powell E, Konidari I, Hulme W, Staropoli JF, Xin W, Wen GY, Barone R, Coppel SH, Sims K, Brown WT, Züchner S (2012) Mutations in the Gene *DNAJC5* Cause Autosomal Dominant Kufs Disease in a Proportion of Cases: Study of the Parry Family

and 8 Other Families. PLoS ONE 7:e29729.

231. Vellai T, Takacs-Vellai K, Zhang Y, Kovacs AL, Orosz L, Muller F (2003) Genetics: Influence of TOR Kinase on Lifespan in *C. elegans*. Nature 426:620.

232. Vesa J, Hellsten E, Verkruyse LA, Camp LA, Rapola J, Santavuori P, Hofmann SL, Peltonen L (1995) Mutations in the Palmitoyl Protein Thioesterase Gene Causing Infantile Neuronal Ceroid Lipofuscinosis. Nature 376:584-587.

233. Vilinsky I, Stewart BA, Drummond J, Robinson I, Deitcher DL (2002) A *Drosophila* SNAP-25 Null Mutant Reveals Context-Dependent Redundancy with SNAP-24 in Neurotransmission. Genetics 162:259-271.

234. Vingtdeux, V., P. Chandakkar, H. Zhao, C. d'Abramo, P. Davies and P. Marambaud (2011). Novel synthetic small-molecule activators of AMPK as enhancers of autophagy and amyloid-beta peptide degradation. FASEB J 25(1): 219-231.

235. Viswanathan M, Kim SK, Berdichevsky A, Guarente L (2005) A Role for *sir-2.1* Regulation of ER Stress Response Genes in Determining *C. elegans* Lifespan. Dev Cell 9:605-615.

236. Vogel K, Cabaniols JP, Roche PA (2000) Targeting of SNAP-25 to Membranes Is Mediated by Its Association with the Target SNARE Syntaxin. J Biol Chem 275:2959-2965.

237. Voisine C, Varma H, Walker N, Bates EA, Stockwell BR, Hart AC (2007) Identification of Potential Therapeutic Drugs for Huntington's Disease

Using *Caenorhabditis elegans*. PLoS One 2.

238. Waelter S, Scherzinger E, Hasenbank R, Nordhoff E, Lurz R, Goehler H, Gauss C, Sathasivam K, Bates GP, Lehrach H, Wanker EE (2001) The Huntingtin Interacting Protein HIP1 Is a Clathrin and Alpha-Adaptin-Binding Protein Involved in Receptor-Mediated Endocytosis. Hum Mol Genet 10:1807-1817.
239. Walker FO (2007) Huntington's Disease. The Lancet 369:218-228.
240. Washbourne P, Thompson PM, Carta M, Costa ET, Mathews JR, Lopez-Bendito G, Molnar Z, Becher MW, Valenzuela CF, Partridge LD, Wilson MC (2002) Genetic Ablation of the t-SNARE SNAP-25 Distinguishes Mechanisms of Neuroexocytosis. Nat Neurosci 5:19-26.
241. Weninger K, Bowen ME, Chu S, Brunger AT (2003) Single-Molecule Studies of SNARE Complex Assembly Reveal Parallel and Antiparallel Configurations. Proc Natl Acad Sci U S A 100:14800-14805.
242. Williams A, Jahreiss L, Sarkar S, Saiki S, Menzies FM, Ravikumar B, Rubinsztein DC (2006) Aggregate-Prone Proteins Are Cleared from the Cytosol by Autophagy: Therapeutic Implications. Curr Top Dev Biol 76:89-101.
243. Wilson MC, Mehta PP, Hess EJ (1996) Snap-25, Ensnared in Neurotransmission and Regulation of Behaviour. Biochem Soc Trans 24:670-676.
244. Wishart TM, Parson SH, Gillingwater TH (2006) Synaptic Vulnerability in Neurodegenerative Disease. J Neuropathol Exp Neurol 65:733-739.

245. Wolfe MS, Xia WM, Ostaszewski BL, Diehl TS, Kimberly WT, Selkoe DJ (1999) Two Transmembrane Aspartates in Presenilin-1 Required for Presenilin Endoproteolysis and Gamma-Secretase Activity. Nature 398:513-517.

246. Wong E, Cuervo AM (2010) Autophagy Gone Awry in Neurodegenerative Diseases. Nat Neurosci 13:805-811.

247. Wood JG, Rogina B, Lavu S, Howitz K, Helfand SL, Tatar M, Sinclair D (2004) Sirtuin Activators Mimic Caloric Restriction and Delay Ageing in Metazoans (Vol 430, Pg 686, 2004). Nature 431:107-107.

248. Wu Y, Cao Z, Klein WL, Luo Y (2010) Heat Shock Treatment Reduces Beta Amyloid Toxicity in Vivo by Diminishing Oligomers. Neurobiol Aging 31:1055-1058.

249. Wu Y, Wu Z, Butko P, Christen Y, Lambert MP, Klein WL, Link CD, Luo Y (2006) Amyloid-Beta-Induced Pathological Behaviors Are Suppressed by Ginkgo Biloba Extract EGb 761 and Ginkgolides in Transgenic *Caenorhabditis elegans*. J Neurosci 26:13102-13113.

250. Yamanaka K, Okubo Y, Suzaki T, Ogura T (2004) Analysis of the Two P97/VCP/Cdc48p Proteins of *Caenorhabditis elegans* and Their Suppression of Polyglutamine-Induced Protein Aggregation. J Struct Biol 146:242-250.

251. Yang J-S, Nam H-J, Seo M, Han SK, Choi Y, Nam HG, Lee S-J, Kim S (2011) Oasis: Online Application for the Survival Analysis of Lifespan Assays Performed in Aging Research. PLoS ONE 6:e23525.

252. Yang YB, Piao YJ (2003) Effects of Resveratrol on Secondary Damages after Acute Spinal Cord Injury in Rats. Acta Pharmacol Sin 24:703-710.

253. Ye K, Ji CB, Lu XW, Ni YH, Gao CL, Chen XH, Zhao YP, Gu GX, Guo XR (2010) Resveratrol Attenuates Radiation Damage in *Caenorhabditis elegans* by Preventing Oxidative Stress. J Radiat Res 51:473-479.

254. Zhang H, Kelley WL, Chamberlain LH, Burgoyne RD, Lang J (1999) Mutational Analysis of Cysteine-String Protein Function in Insulin Exocytosis. J Cell Sci 112 (Pt 9):1345-1351.

255. Zhang J (2006) Resveratrol Inhibits Insulin Responses in a Sirt1-Independent Pathway. Biochem J 397:519-527.

256. Zimprich A, Biskup S, Leitner P, Lichtner P, Farrer M, Lincoln S, Kachergus J, Hulihan M, Uitti RJ, Calne DB, Stoessl AJ, Pfeiffer RF, Patenge N, Carbajal IC, Vieregge P, Asmus F, Muller-Myhsok B, Dickson DW, Meitinger T, Strom TM, Wszolek ZK, Gasser T (2004) Mutations in LRRK2 Cause Autosomal-Dominant Parkinsonism with Pleomorphic Pathology. Neuron 44:601-607.

257. Zinsmaier KE, Bronk P (2001) Molecular Chaperones and the Regulation of Neurotransmitter Exocytosis. Biochem Pharmacol 62:1-11.

258. Zinsmaier KE, Eberle KK, Buchner E, Walter N, Benzer S (1994) Paralysis and Early Death in Cysteine String Protein Mutants of *Drosophila*. Science 263:977-980.

259. Zinsmaier KE, Hofbauer A, Heimbeck G, Pflugfelder GO, Buchner S, Buchner E (1990) A Cysteine-String Protein Is Expressed in Retina and

Brain of *Drosophila*. J Neurogenet 7:15-29.